Development of the high-speed video-oculographic system and its application to the study on the saccadic eye movements in mice

マウスにおける眼球運動測定装置の開発とサッケード研究への応用

Tomoya Sakatani

坂谷　智也

Department for Physiological Sciences, School of Life Science

The Graduate University for Advanced Studies (Sokendai)

総合研究大学院大学

生命科学研究科 生理科学専攻

Table of Contents

Abstracts

Due to the increasing use of transgenic and knockout mice in neuroscience research, it is urgently necessary to develop the technique for quantitative measurement of behaviors in mice. The video-oculography is often used to measure the eye movements of mice, but due to its limitation in temporal resolution, its use was limited to analysis of slow eye movements such as vestibuloocular reflex and optokinetic responses. As a result, rapid eye movements such as saccades have not been properly analyzed in mice as yet. To overcome such difficulties, I have newly developed a video-oculography system with high temporal resolution (240 Hz) by combining high speed CCD camera with image processing software written in LabVIEW run on IBM-PC. By this recording system, the dynamic characteristics of the rapid eye movements (saccades) in alert, head-fixed mice (C57BL/6 strain) were investigated.

Mice spontaneously made rapid eye movements in the dark at a frequency of 3.2 /min with mean amplitude of 9 degrees mainly in horizontal direction. The peak velocity of saccades increased almost linearly against the saccadic amplitude with slope of 54 / sec, whereas the saccadic duration saturated at the level of 60 msec against larger saccades.

These saccade-like rapid eye movements could be induced by the electrical stimulations of the intermediate and deep layers of the SC in a head-fixed condition. Suprathreshold current stimulus evoked mainly contraversive saccades having a roughly constant vector depending on the stimulus sites in the SC. The

amplitude and the direction of evoked saccades highly depended on the initial eye position in the orbit as well as on the stimulus sites in the SC, and evoked saccades were goal-directed in mice, suggesting that eye position signals might strongly affect the dynamics of saccades in this species. Though, most sites in the SC yielded contraversive characteristic saccades, from the antero-medial region, where the visual representation of the superficial layer shared the same location in the visual field with the opposite SC, ipsiversive saccades could be induced.

For further investigation of the mechanisms underlying saccades, especially molecular mechanisms of saccade generator circuitry, the dynamic characteristics of both the spontaneous and the electrically induced saccades were examined in mice lacking a GABA-synthesizing enzyme, glutamic acid decarboxylase (GAD) 65, and a functional role of the inhibitory neurotransmitter gamma-amino butyric acid (GABA) in the saccadic system was analyzed. The peak velocity of the saccadic eye movements was significantly higher and the amplitude of saccades tended to be smaller in GAD65 knockout mice than those in wild-type animals. Moreover, significant increase in fluctuations was observed in the eye position after the termination of saccades in the GAD65 knockout mice. Prolonged electrical stimulation of the SC often evoked oscillation-like eye movements after saccades in the mutant mice. Computer simulations based on the control system model with a negative feedback loop could attribute these experimental results to the increase in the efficacy of feedback loop in the saccade generator circuitry in the downstream of the SC in GAD65 knockout mice. These results support the hypothesis that the neural system underlying the saccade generation consists of a feedback loop, and

suggest that GABA plays an important role in stabilizing the saccade control system in the downstream of the SC.

The results presented in this study show that the newly developed video-oculographic system provides a powerful tool for analyzing dynamic characteristics of saccadic eye movements in mice. Furthermore, this study will provide a fundamental knowledge to study molecular basis of the oculomotor and, moreover, cognitive functions by using various lines of mutant mice.

General Introductions

The saccadic eye movement is a rapid shift of the eye position to capture an object in the visual environment and is a highly controlled motor system which has been intensively investigated especially in cats and primates (Wurtz and Goldberg, 1989, Moschovakis et al., 1996, Scudder et al., 2002)

Studying the saccadic eye movement is important not only because its control system is a good model to study the neural computation for accurate control of movements, but also because the saccadic eye movement can be a good behavioral indicator of psychological processes such as attention, motivation and decision making (Fischer and Weber, 1993, Kawagoe et al., 1998, Glimcher, 2003). Saccades can be also used for diagnosis of several neurological and psychiatric disorders such as Parkinson's disease, schizophrenia, attention deficit hyperactive disorder (ADHD) and Tourettes' syndrome (Fukushima et al., 1994, Vidailhet et al., 1994, Cairney et al., 2001, LeVasseur et al., 2001, Mostofsky et al., 2001, Crawford et al., 2002, Armstrong and Munoz, 2003, Munoz et al., 2003).

Recent advances in molecular genetic techniques in mice have contributed a lot to elucidating the physiological functions of various molecules in mammals. Under such trend of biomedical sciences, it is of urgent necessity to develop a model system that enables quantitative measurement of cognitive behaviors in mice. In this regard, if mice execute saccades and I can analyze them, it will bring us great opportunities to obtain insights into the molecular basis of the oculomotor system and, moreover, cognitive functions of the mammalian brain.

Although, brief observations of the rapid eye movements in mice have been reported (Mitchiner et al., 1976, Mangini et al., 1985, Grusser-Cornehls and Bohm, 1988), a systematic analysis of saccades has not been made in mice, despite their increasing use in studies of oculomotor control (Raymond, 1998). This is largely due to the technical difficulties in recording such rapid eye movements in small animals like mice.

To overcome such difficulties, I have newly developed a video-oculographic system with high temporal resolution (240 Hz) by combining high-speed CCD camera with the image processing software written in LabVIEW run on IBM-PC. The configuration of this new video-oculographic system, the technical methods used and their theoretical backgrounds are described in part 1.

By using this video-oculographic system, I firstly investigated the spontaneous saccade in mice quantitatively. Thus, dynamic characteristics of spontaneous saccades in mice were described in part 2. In next part 3, the functional importance of the superior colliculus in midbrain was examined to induce the saccade in mice, and its motor representation was described. Finally, the attempt was performed to investigate the molecular mechanisms of saccades by the combined use of gene-engineered mice and model simulation study in part 4.

Part 1

PC-based high-speed video-oculography for measuring rapid eye movements in mice

Introduction

The saccadic eye movement is a rapid shift of the eye position to capture an object in the visual environment and is a highly controlled motor system which has been intensively investigated especially in cats and primates (Wurtz and Goldberg, 1989, Moschovakis et al., 1996, Scudder et al., 2002)

Recent advances in molecular genetic techniques in mice have contributed a lot to elucidating the physiological functions of various molecules in mammals. Under such trend of biomedical sciences, it is of urgent necessity to develop a model system that enables quantitative measurement of cognitive behaviors in mice. In this regard, if mice execute saccades and we can analyze them, it will bring us great opportunities to obtain insights into the molecular basis of the oculomotor system and, moreover, cognitive functions of the mammalian brain.

The search coil technique, electro-oculography (EOG) and infrared video-oculography are major techniques for tracking eye positions in this species. The search coil technique has been widely used for measuring eye positions (Robinson, 1963, Fuchs and Robinson, 1966, Remmel, 1984), because of good temporal and spatial resolution. However, this technique may have disadvantage to be used in small animals because of technical difficulties in implanting coils. Actually it has been reported that the presence of the coil distorts performance of the eye movements in mice (Stahl et al., 2000) and in humans (Frens and van der Geest, 2002). EOG recordings also have several drawbacks to be used in mice since implantation of recording wires is time-taking, and the drifts and non-linearity

of recording signals are well-known problems. On the other hand, infrared video-oculography is a non-invasive technique for measuring eye movements and, therefore, the most popular method in rodents (Nagao, 1990) as well as in humans.

Several studies investigated slow reflex eye movements in mice, the vestibulo-ocular reflex or optokinetic response, by search coil technique (De Zeeuw et al., 1998), or by video-oculography (Katoh et al., 1998, Iwashita et al., 2001) or by combination of both techniques (Stahl et al., 2000, Stahl, 2002). For robust tracking of rapid eye movements in mice by using a video-oculography, there are at least three problems to overcome. First, previous video-oculography had low temporal resolution limited by the video frame rate (up to 60 Hz for NTSC video format), which is not sufficient to analyze rapid eye movements such as saccades. Second, because the commercially available video-oculographic systems are primarily developed for human subjects, the image processing software provided by the manufacturer is not necessarily appropriate for tracking eye positions in mice. In general, the video-oculographic system measures an eye position by detecting the pupil from a captured eye image. The fact that the pupil of the mouse becomes considerably enlarged in the darkness renders detection of the pupil center unreliable. Further, the acquired images are often unsuitable for image processing because of eyelid occlusions, shadows or corneal reflections. Zooming with macro lens also impairs the image quality. These factors make it difficult to detect the pupil image stably, which results in poor quality of eye position measurement. Thirdly, in humans or trained monkeys, the eye position signal was calibrated by making the subject to shift its gaze to targets of a known visual angle. However,

because of difficulties in training mice, estimation based on the anatomical structure of the eyeball is needed for calibrating the pupil displacement into the rotation angle of the eye.

In this part, I describe the configuration of the newly developed PC-based infrared video-oculographic system for on-line tracking of saccadic eye movements in the awake and head-fixed mouse, with high temporal resolution (240Hz). I present the image-processing procedure for robust pupil detection written in LabVIEW. I also present a new technique to convert the eye displacement in the 2-dimensional video plane to the rotation angle of the eye.

Materials and methods

Hardware setup

The system consists of a commercially available high-speed analog CCD camera (CS3720; TELI, Japan) and an image processing software written in LabVIEW (National Instruments, Texas, USA) run on an IBM-PC with an add-on video grabber board. The high-speed CCD camera has the ability to sample 4 times faster than the standard NTSC format (30Hz), 120 frames per second (512 x 512 pixels). By the partial scanning mode, this camera can acquire maximally 240 frames per second (480 x 240 pixels). In my system, size reduced images (240 x 100 pixels) were captured at a sampling rate of 240 Hz.

I captured an area of 5.0 x 2.1 mm with a macro lens (VZM200i, Edmund Industrial Optics, New Jersey, USA). The acquired video images were digitized at 256 gray level resolutions by an add-on video grabber board (PCI-IMAQ-1408, National Instruments, Texas, USA) and processed on an IBM PC-compatible computer with a Pentium4 1.4 GHz processor and 512 MB RAM. PCI-IMAQ-1408 is easily controlled by the LabVIEW application, and can be customized with its configuration to capture non-standard video images. In order to send output signals to other computers, which stored and analyzed data, a plug-in D/A converter (PCI-6711; National Instruments, Texas, USA) was used.

Animal preparation

C57BL/6J male mice with black eyes (n = 3, 22 g, 8 week-old, supplied by SLC,

Japan) were used for the test in this article. Mice were housed individually with a light-dark cycle of 12 hr light/ 12 hr dark for more than 7 days under standard laboratory conditions and with food and water ad libitum. All surgical procedures were carried out under isoflurane (Forane, Abbott, Illinois, USA) anesthesia. The position of the head was adjusted so that the height of the skull surface at bregma and lambda was the same. After an incision was made in the skin, a pedestal was attached to a mouse on the cranial bone with the dental resin (SUPER BOND, SUN MEDICAL, Japan) (Fig. 1-1A). The whiskers on the side of the camera were cut to allow optimum view of the eye. The animal was allowed to recover for at least 24 hr after the end of an operation before use for the experiment. Its head was fixed to the stereotaxic platform (SR-6N, Narishige, Japan) with a brass rod attached to a manipulator (SM-15, Narishige, Japan) and its body was loosely restrained on a rubber sheet (Fig. 1-1A, and 1-1B). The mouse was then left restraint in the experimental chamber to adapt to darkness for an additional 30 minutes before experimentation began. Its legs were hanged out of the sheet in the air and did not touch anything else (Fig. 1-1B).

Movements of the right eye were monitored with a CCD camera placed at an angle of 60 degree laterally from the midline and 30 degree down from the horizontal plane (Fig. 1-1C). Infrared light-emitting diodes (HSDL4230, Agilent Technologies, USA) attached to the camera illuminated the eye with wavelength of 880 nm. The background light of the environment was adjusted to 50 - 100 lux, so that the pupil size was adequate for image processing (the pupil diameter is usually adjusted to 0.5-1.5 mm).

All the experimental procedures were approved by the Animal Ethical Committee of the Okazaki National Institutes.

Image processing software

The software was all written in the graphical programming language LabVIEW and its add-on software package IMAQ Vision, a library of LabVIEW functions for image acquisition and processing. In this paper, '**vi**' means a name of LabVIEW IMAQ Vision function. All the image-processing procedures are shown in Fig. 2A. The video input signal was digitized into 256 gray level images (**IMAQ Grab Acquire.vi**) (Fig. 1-2Aa). An acquired image is transformed to a binary image by using a threshold operation (**IMAQ Threshold.vi**) (Fig. 1-2Ab). The image is then digital-filtered by '**IMAQ FillHole.vi**' to remove noise and inner holes due to corneal reflections (Fig. 1-2Ac). It is not necessary to do this step if the quality of an acquired image is good enough since this step is time consuming. The time length for operation depends on the size of the area to be processed.

If the whole area of an acquired image should be processed, it is too time-consuming to operate 240 images per second on-line with the system in its present form. In order to assure the real time processing, a partial region of the acquired image is extracted (**IMAQ Extract.vi**) for the following operation (Fig. 1-2B). The center of the partial image is determined based on both the position of the pupil center and the velocity of eye movements calculated from the previous frame. The range of the partial image is determined based on the pupil radius calculated from the previous frame. This step reduces the processing time at its

subsequent operation and improves noise resistance.

Next step, '**IMAQ Find Circular Edge.vi**' determines the pupil boundary (Fig. 1-2Ad). In order to reduce the searching time, '**IMAQ Find Circular Edge.vi**' starts to search the pupil boundary at a point of the 70 % distance (● in Fig. 1-2C) relative to the pupil radius from the center (★ in Fig. 1-2C) in the previous flame. This function also returns the center position of the fitted circle.

For robust pupil detection, the following procedure was performed. '**IMAQ Point Distances.vi**' calculates the distance between each peripheral point and the center, respectively (Fig. 1-3). I refer the data array of these distances as a radial-distance function (Fig 1-3A). If a peripheral point exists just on the circumference, the calculated value is almost constant and close to the pupil radius. However, this value falls out of the pupil radius, if the pupillary boundary is disrupted by a shadow, an eyelid occlusion, or a reflection. For instance, a shadow makes this value higher, while an occlusion or a reflection makes it lower. Note the radial-distance function is sinusoidal in most cases because of the fact that the shape of the pupillary boundary becomes ellipse at the eccentric eye position. Thus, using this feature, only points whose radial-distance is within a range of 1 s.d. are adopted for circular approximation (Fig. 1-3B, Fig. 1-2Ae). I named this procedure as "the interruption exclude algorithm", and its performance was assessed in the later section.

Using these edge points, '**IMAQ Fit Circle.vi**' executes circle fitting to calculate the center of the pupil and returns the position of the circle center and its radius (Fig. 1-2Af). Through the above procedures, the position of the pupil center

and the pupil size of individual video frames were obtained.

Conversion to angular eye positions

Because eye movements are rotational, we need to convert the eye displacement in the 2-dimensional video plane to the rotational angular eye position (Fig 1-4A). Based on the eyeball model that is constructed referring to the anatomical parameters (Remtulla and Hallett, 1985), I estimated the rotation center and rotation radius to calculate angular eye positions. The radius of eyeball in this model is 1.6 mm.

The reliability of this model depends on several assumptions. An eye can be modeled with two spheres corresponding to the eyeball and cornea. The eye rotates around the point centering the eyeball. In this study, I used the same strain, adult C57BL/6J mice, as Remtulla and Hallett (1985) investigated.

Figure 1-4B shows the eyeball model I used. Assuming that the rotation radius of the pupil is known, we can calculate the angular eye position (E_h and E_v in Fig. 1-4A) from the eye displacement in video coordinates using the following equations.

$$E_h = \arcsin\left(\frac{dx}{R_{effective}}\right), \quad E_v = \arcsin\left(\frac{dy}{R_{effective}}\right)$$

where dx and dy represent horizontal and vertical distances from the estimated rotation center to the pupil respectively, $R_{effective}$ is effective rotation radius.

To get the value of dx and dy, we must determine the position corresponding to the rotation center in the video image. I determined this point in the following

way based on the eyeball model. Infrared LEDs were equipped around the macro lens in an equally spaced manner, which was parallel to the video axis. Consequently, the intersecting point of the reflection on cornea is the center point of corneal surface approximated by a spherical model (Fig.1-5A). This center of cornea exists in front of the rotation center of the eyeball. I calculated the rotation center in the video coordinates using the cornea center and pupil center based on the following equation.

As shown in Figure 1-5B,

$$\mathbf{P_oR_o} : \mathbf{P_oC_o} = R_{effective} : R_{effective} - \varepsilon$$

Thus

$$x_o = (x_c - x_p)\ \frac{R_{effective}}{R_{effective} - \varepsilon} + x_p, \qquad y_o = (y_c - y_p)\ \frac{R_{effective}}{R_{effective} - \varepsilon} + y_p$$

where R_o (x_o, y_o) is rotation center, P_o (x_p, y_p) is pupil center and C_o (x_c, y_c) is cornea center position in the video plane. $R_{effective}$ is effective rotation radius described below in detail. ε is the distance between the center of the eyeball and the center of the cornea curvature. ε is 0.2 mm referred from the literature (Remtulla and Hallett, 1985).

As I measure the pupil center to track eye movements, turning-radius depends on the size of the pupil. Consequently, the smaller the pupillary size is, the longer the displacement of eye is in the video plane against a given rotating angle. This is especially problematic in mice, which frequently change the size of their pupil. To solve the problem described above, I converted the eye displacement to the angular eye position based on the eyeball model in which the pupillary size was taken into

consideration. In the model, an outer curvature of the lens was approximated by a circle (Fig. 1-4B). The effective turning-radius of the pupil could be calculated by solving the following equation on the assumption that iris contracts and dilutes along a curvature of the lens and that the lens does not change its structure.

$$R_{effective} = \sqrt{R_{lens}^{2} - R_{pupil}^{2}} - \delta$$

where $R_{effective}$ is the effective rotation radius, R_{lens} is the lens radius, R_{pupil} is the pupillary radius and δ is the distance between the center of the lens curvature and the center of the eyeball. $R_{effective}$ is 1.25 mm and δ is 0.1 mm referred from the literature (Remtulla and Hallett, 1985). Then angular eye position (E_h, E_v) can be obtained from the following equation.

$$E_h = \mathbf{arcsin}\left(\frac{x_p - x_o}{R_{effective}}\right),\ E_v = \mathbf{arcsin}\left(-\frac{y_p - y_o}{R_{effective}}\right)$$

Evaluations

An attempt was made to evaluate the image processing software. Using artificial eye images synthesized by the computer, I assessed the accuracy of the circular fitting method in calculating the center of the partially occluded pupils. And I mention the spatial and the temporal resolution of our recording system.

Image processing

Fig. 1-6 shows examples of pupil boundary detection and circular fitting under various situations. Successfully, the image processing software could detect the edge points just on the periphery of the pupil in the case of a reflection (Fig. 1-6Aa), a shadow (Fig. 1-6Ab), and an eyelid occlusion (Fig. 1-6Ac). Stable circle approximation can be made independent of the image condition. Note that spots of illumination and video noises are filled by '**IMAQ FillHole.vi**' operation (Fig. 1-6Ab left, 1-6Ac left).

Robustness of the pupil boundary detection

I next evaluated the robustness of the pupil detection using "the interruption excluding algorithm" shown in Figure 1-3 against the effect of eyelids and corneal reflections on the measurement accuracy, because such occlusion of the pupil boundary results in incorrect circular fitting. And I evaluated the improvement in the pupil detection accuracy using the interruption excluding algorithm compared with "the simple circular fitting", in which the pupil is fit without "the interruption

excluding algorithm". To simulate these situations, the portion of the artificial pupil image with a diameter of 50 pixels (corresponding to 1.0 mm of an actual pupil diameter) was occluded by a small circle (Fig. 1-6Ba) or a plane (Fig. 1-6Bb, Bc).

Against a small circle occlusion, which may be caused by a corneal reflection, the maximum error values were plotted as a function of the diameter of the spot. Within the range from 0 to 50 % spot diameter relative to the pupil diameter, it was turned out that the maximum error values were less than 2 pixels in simple circular fitting condition (× in Fig. 1-6Ba), and were less than approximately 1 pixel in case when the interruption excluding algorithm was used (● in Fig. 1-6Ba). Against a simple plane occlusion, which might be the case of an eyelid shadow (Fig. 1-6Bb) or an eyelid occlusion (Fig. 1-6Bc), the maximum error values were also plotted as a function of the percentage of a shadow or an occlusion against the pupil diameter, and were found to be less than approximately 3 pixels below 50 % hidden ratio (× in Fig. 1-6Bb and × in Fig. 1-6Bc) respectively, and to be less than approximately 1.5 pixels if the interruption excluding algorithm was used (● in Fig. 1-6Bb and ● in Fig. 1-6Bc). In Figure 1-6Bc, the maximum error value dropped above 20 % occlusion because the circular edge finding function (**IMAQ Find Circular Edge.vi**) started to search pupil boundary from the point at the 70 % of the pupil radius determined in the previous video frame (Fig. 1-2C), and did not return any edge points when the pupil was occluded over the 30 % of its radius. In the present setup, one pixel corresponded to approximately 1.2 degrees when the diameter of pupil was around 1 mm.

Rotation center

I evaluated the accuracy of the rotation center that the eye tracking software determined. Five acquired video images from a single animal in which the pupil oriented in different directions were used for evaluation (Fig. 1-7B). Figure 1-7A shows good accordance of the rotation centers calculated by the software based on the eyeball model. On the other hand, there is much dissociation between the cornea centers and the estimated rotation centers. This indicates the fact that the center of cornea curvature is not identical to the center of the eyeball and is consistent with the previous report that the rotation center exists at slightly behind the spherical center calculated from the reflections (Stahl et al., 2000).

Accuracy and delay of the system

I verified the accuracy of the circular fitting method against the pupil image at various eccentric eye positions. The pupil boundary is elliptical when the eye is in eccentric gaze positions (Fig. 1-8A). Measurement error of the eye position (Fig. 1-8C) and the pupil size (Fig. 1-8D) was calculated as a function of eccentricity against different pupil sizes (Fig. 1-8B), respectively. For the range of 30 degrees at eccentric eye position, the error value for eye position was less than approximately 1 degree, and the error value for pupil size was less than 0.2 mm^2.

The spatial and the temporal resolution of the recording system depend on the capability of the CCD camera. The spatial resolution is approximately 0.02 mm in both horizontal and vertical axes and the temporal resolution is 4.17 ms in the

present setup. This spatial resolution corresponds to approximately 1.2 degrees when the diameter of pupil is around 1 mm and the eye position is within 30 degrees from the rotation center.

Eye tracking

I used this high-speed video-oculographic system and recorded the voluntary rapid eye movements in head-fixed mice. As exemplified in Figure 1-9, the mouse made saccade-like rapid eye movements spontaneously in the dark. Figure 1-9 shows the eye position sampled at 240 Hz. As shown in Figure 1-9B, the trajectories of rapid eye movements were recorded accurately, allowing analysis of the dynamics of the eye movements (Fig. 1-9C). In the darkness, the pupillary size frequently changed from 1 to 2 mm^2 with contraction or dilation (Fig. 1-9A bottom).

Discussions and conclusions

Features of the system

I developed a PC-based high-speed video-oculographic system for on-line recording of the rapid eye movements, and described examples of its application in mice.

Our recording system has following important features.

(1) Present system enables online recording of eye movements at a sampling rate of 240 Hz, which is sufficient for analyzing saccades in a quantitative manner.

(2) This system can be built up at low cost. The image processing for eye tracking is operated by a PC, not by specific hardware devices.

(3) The image processing software for the pupil detection is written in LabVIEW allowing great flexibility, which is particularly important in the research laboratory.

(4) The system consists primarily of commercially available hardware. Thus, we can easily improve the hardware according to specific needs. Moreover we can easily configure different types of cameras with different analog video formats such as RS-170 or CCIR using the configuration software, which is supplied by the manufacturer with an image grabber board IMAQ PCI-1408, and by selecting the appropriate camera file. Present recording system can also use standard analog video camera instead of CS3720.

(5) Not only the eye position but also the pupil size can be recorded simultaneously. This provides the information about autonomic nervous system. Based on the sudden change of the pupillary size, I can detect the occurrence of eye blinks

and get rid of the data at that point. Moreover, it may be possible to use this system to detect eye blinks for the study of eye blink conditionings.

(6) Since the mice are restrained to stereotaxic platform in our setup, we can easily combine the eye movements monitoring in genetically engineered mice with the electrophysiological techniques such as electrical stimulation or recording of neural activities.

Further improvements

There are several possibilities left for further improvements. The present system has reduced spatial resolution due to the capability of the image grabber board. Because of low sensitivity to near-IR wavelength (approximately 15% relative to the peak sensitivity), CS3720 CCD camera required intensive infrared light source and the acquired images are noisy. The use of a more IR-sensitive CCD camera will result in ideal images for processing and reduces calculating time, allowing the use of a computer with lower processing power.

It should be noted that Windows2000 is not a real-time operating system. Thus, other applications run on the same computer can affect the performance of the image processing software, which would result in failure for the real-time eye tracking with a constant delay. As to the method for the pupil center detection, I used the circular fitting method and could obtain accurate estimations of the eye positions in the described setup. However it has been reported that ellipse fitting is more accurate because the pupil boundary is elliptical when the eye is in eccentric gaze positions (Matsuda and Nagami, 1998, Zhu et al., 1999). Hence, using

ellipse-fitting algorithm to detect the pupil boundary might improve the accuracy of estimation of the pupil center.

In addition, excluding the points associated with eyelids, shadows, and corneal reflections from the circle-fitting routine might provide more robust estimate of the pupil center based on the characteristics of boundary curvature (Zhu et al. 1999). However, our method is quite simple and can be done without the heuristic information.

Finally, it should be noted that this system could be applied not only to mice, but also to monkeys or human subjects. For clinical use, video oculography will be a potentially important tool to diagnose neurological disorders (Kubo et al., 1991, Funabiki et al., 1999). The method presented here can also be used to monitor saccadic eye movements in experiments of visual physiology during functional magnetic resonance imaging without causing artifacts in the MR images (Gitelman et al., 2000).

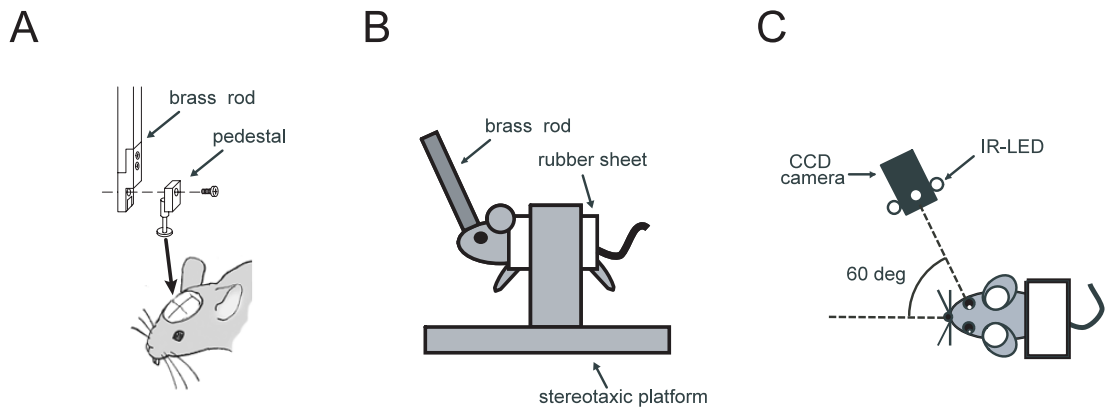

Figure 1-1
Schematic drawing of experimental setup.

(A) Mouse's head was fixed with a brass rod and a pedestal. The pedestal was attached to a mouse on the cranial bone with dental resin. (B) The mouse was restrained with a rubber jacket and suspended in a sound attenuated, dim lit box. (C) Movements of the right eye were recorded using a black and white analogue CCD camera (240Hz) at an angle of 60 degree from the body axis and 30 degree down from the earth, then analyzed and stored in the PC. Infrared light-emitting diodes attached to the camera illuminated the mouse eye with wavelength of 880 nm.

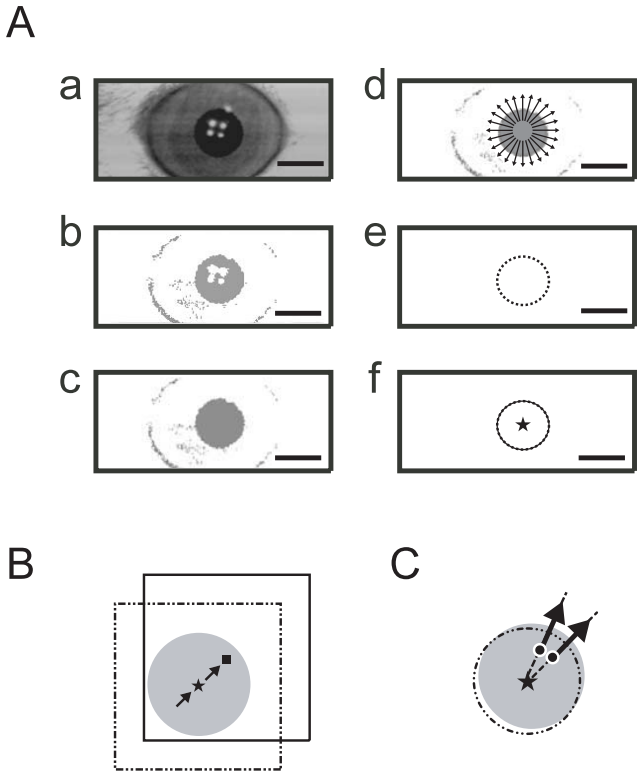

Figure 1-2
Image processing procedure for detecting the center of the pupil.

(A) An original grayscale image (a) was converted to a binary image by IMAQ Threshold.vi (b). Then within the region of interest, noise and reflections were removed by filtering operation (IMAQ FillHole.vi) (c). IMAQ Find Circular Edge.vi searched the points of pupil boundary (d, e). Finally, the center of the pupil (★) was obtained by IMAQ Fit Circle.vi (f). Scale bar, 1 mm. (B) The region of interest in the next frame (square) was partially extracted from the entire video image to reduce the processing time. The center of the partial region (■) was calculated from the previous video frame using the eye velocity (arrow) and the eye position (★). Dotted square indicates the region of interest in the current frame. (C) IMAQ Find Circular Edge.vi searched edge points radially from the pupil center (★) with 10-degree intervals. To reduce the searching time, this function started to detect edges from the point of 70 % distance (●) relative to the pupil radius.

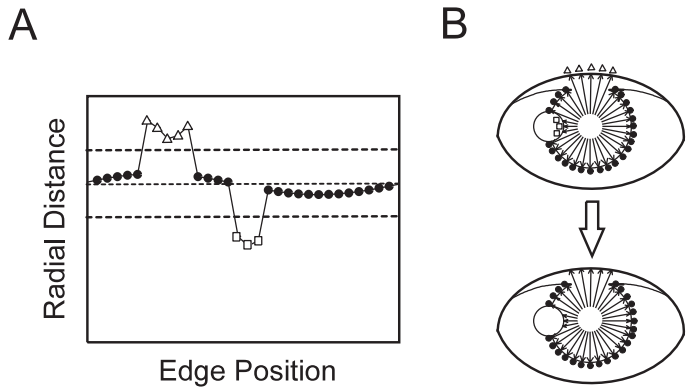

Figure 1-3
Edge points out of pupil boundary were excluded based on the interruption excluding algorithm.

(A) A schematic example of radial-distance function. Each value represents the distance between the edge point and the estimated center of the pupil. A shadow makes this value higher (△), while an occlusion or a reflection makes it lower (□). A broken line represents the value of pupil radius and dotted lines represent threshold values (pupil radius ± 1 s.d.) for exclusion. (B) Edge points, whose radial distance values are over or under the pupil radius beyond 1 s.d. ranges, are removed (□, △), and the remaining points (●) are used for circular fitting.

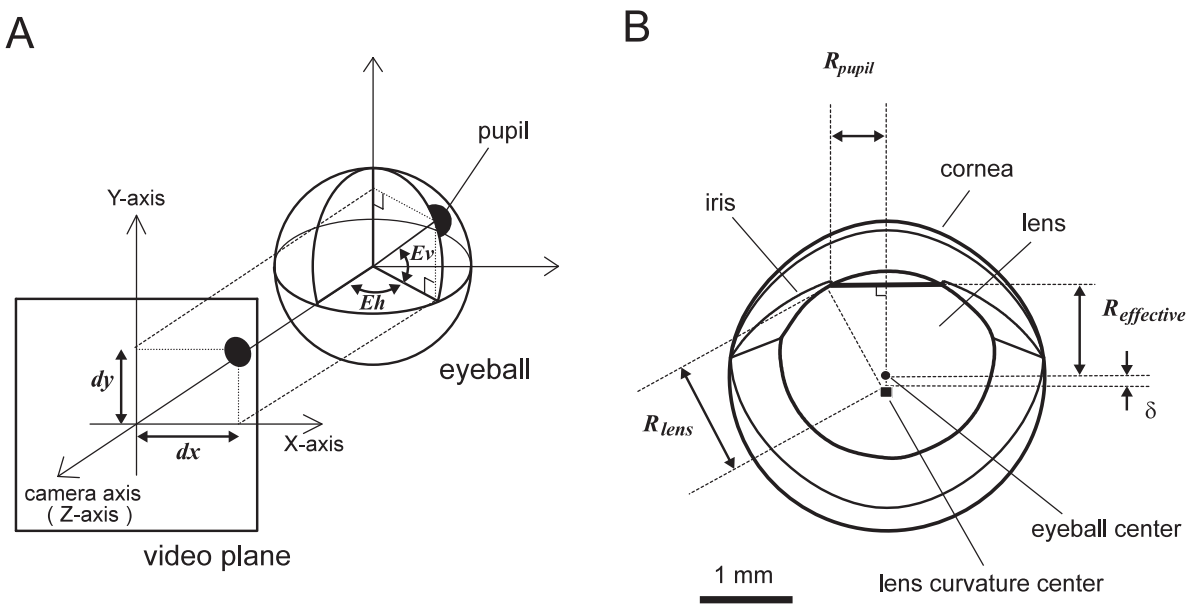

Figure 1-4
Eye displacement length was converted to the eye rotation angle based on an anatomical eyeball model.

(A) Angular eye position (***Eh***, ***Ev***) are represented by Cartesian coordinates (***dx***, ***dy***) in the video plane. ***dx*** is horizontal and ***dy*** is vertical displacement of the pupil center from the estimated rotation center in the video plane. (B) Anatomy of the eyeball in the mouse. The effective rotation radius ($R_{effective}$) is calculated from the pupil radius (R_{pupil}: obtained from a video image) and lens radius (R_{lens}: 1.25 mm). The radius of eye ball is 1.6 mm in the model. $\delta = 0.1$ mm.

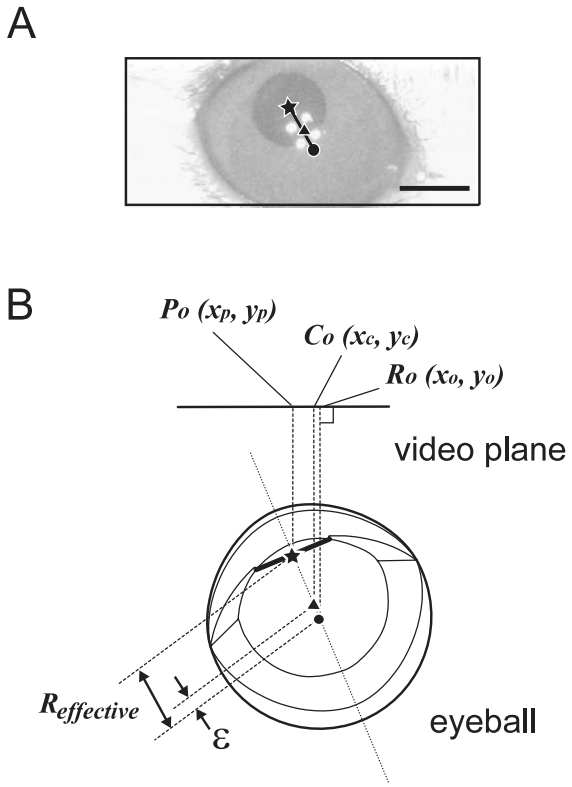

Figure 1-5
The rotation center was estimated in the video plane.

(A) An example of cornea reflections. ★, pupil center; ▲, reflection center (intersecting point of optical camera axis and corneal surface curvature); ●, estimated rotation center (the center of the eyeball). Scale bar, 1 mm. (B) Based on the distance between the pupil center and the reflection center, the rotation center is calculated in the video image. Note that the center of the eyeball (●) locates behind the center of the corneal surface curvature (▲). **Ro** (x_o, y_o), rotation center; **Po** (x_p, y_p), pupil center; **Co** (x_c, y_c) cornea reflection center; ε, a constant distance (0.2 mm) between the center of the eyeball and the center of the cornea curvature.

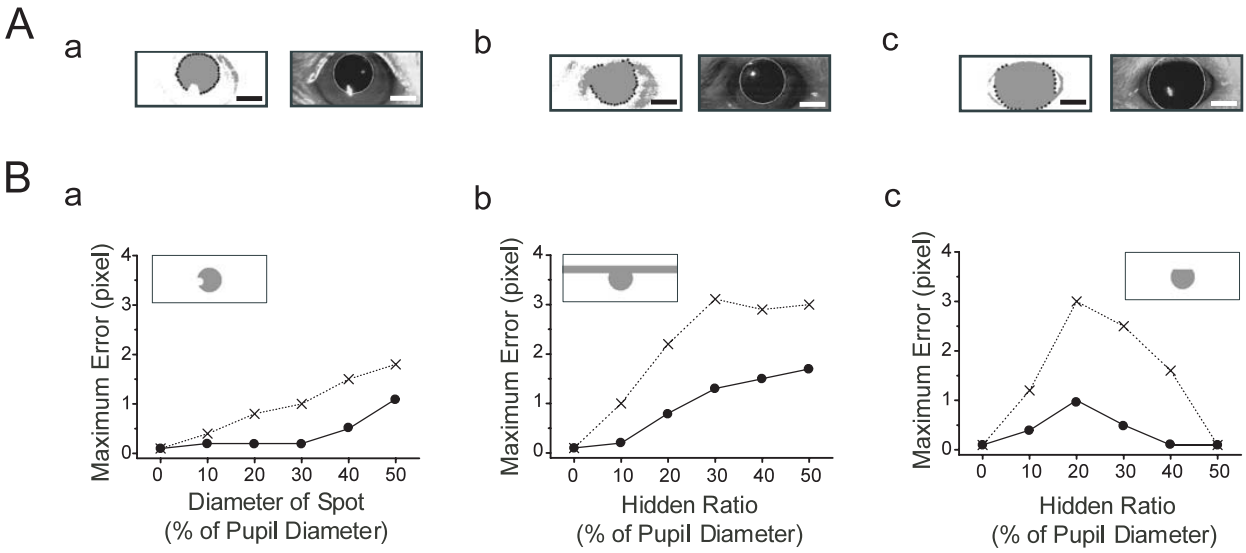

Figure 1-6
Examples of circular fitting with the interruptions of pupil boundary

(A) Examples of circular fitting with the interruptions of pupil boundary. Examples of the effects of the interruption excluding algorithm on detecting the pupil boundary were shown in the case of a reflection from the infrared light emitting diode illumination (a), an eyelid occlusion (b), or an occlusion of a shadow (c). Edge points other than pupil boundaries were removed (left panel), and the remaining points were used for circular fitting (right panel). Scale bar, 1 mm. (B) Error estimation in measuring eye positions with the interruptions of pupil boundary. Maximum error was plotted against a diameter of the reflection spot (a), a hidden ratio of a shadow (b), or a hidden ratio of eyelid occlusion (c), relative to the pupil diameter respectively. A computer synthesized pupil image with a diameter of 50 pixels was used for the evaluations. Solid line with closed circles indicates the results by “the interruption excluding algorithm”. Dotted line with crosses indicates the results by “the simple circular fitting”, in which the pupil is fit without “the interruption excluding algorithm”.

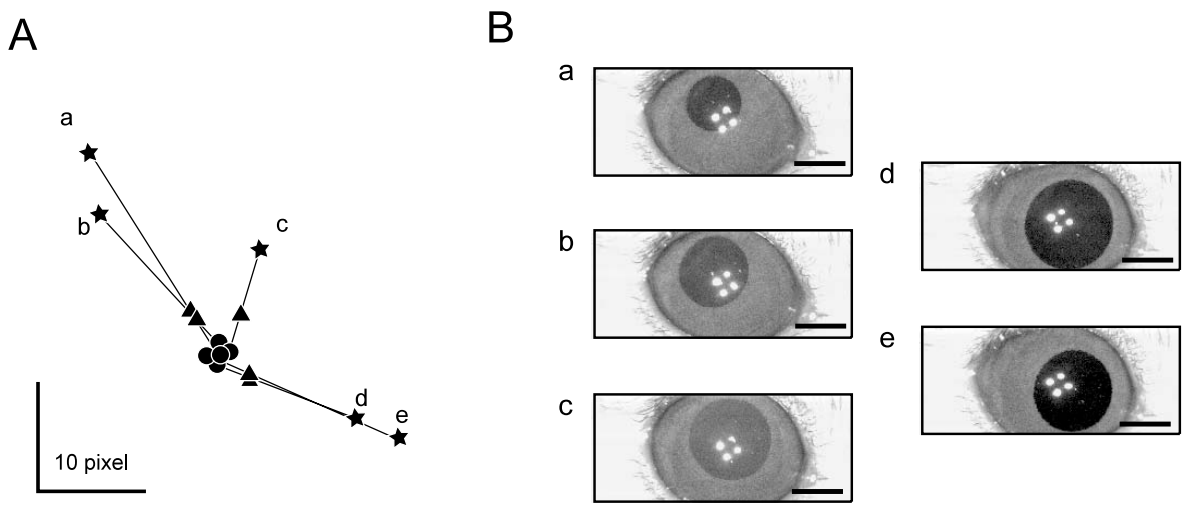

Figure 1-7
Estimated rotation center converged at a single point in the video plane.

(A) The rotation center of the eyeball was calculated for five individual eye images respectively. All estimated rotation center was plotted in the same plane. (★, pupil center; ▲, reflection center (intersecting point of optical camera axis and corneal surface curvature); ●, estimated rotation center). (B) Actual eye images used for estimating the rotation center. Each figure (a-e) corresponds to the identical data in A. Scale bar, 1 mm.

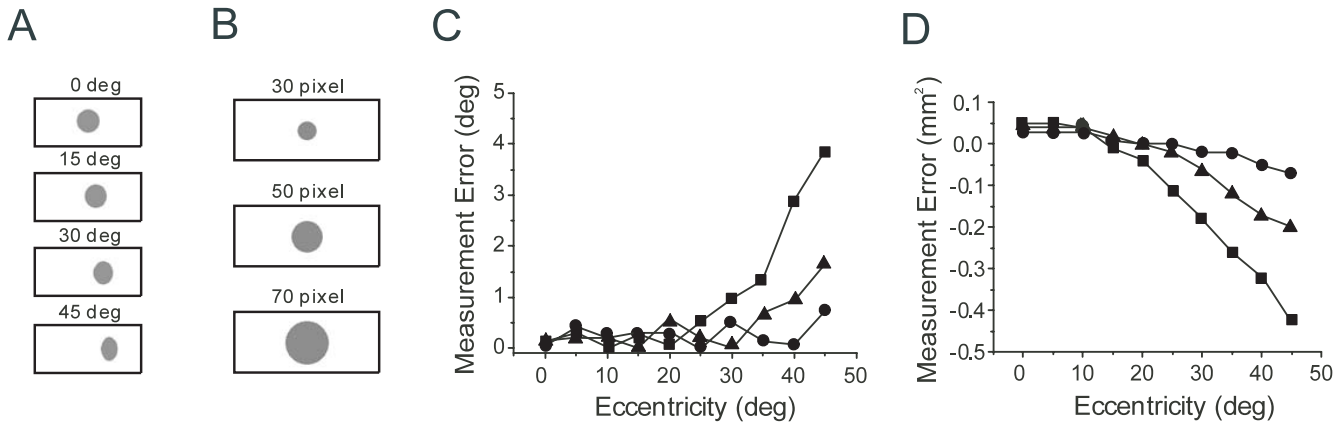

Figure 1-8
Error plot against the eccentricity of the eye position.

(A) Examples of the computer synthesized pupil image at different eye positions. Pupil boundary changes from circle to ellipse at eccentric eye positions. (B) Synthesized eye images with a different diameter of the pupil (30, 50, 70 pixels) were used for the error estimation. (C) Measurement error of the eye position. (D) Measurement error of the pupil size. Error values increased depending on both the eccentricity and the pupil size. (●,▲,■; diameter of the pupil, 30, 50, 70 pixels respectively.)

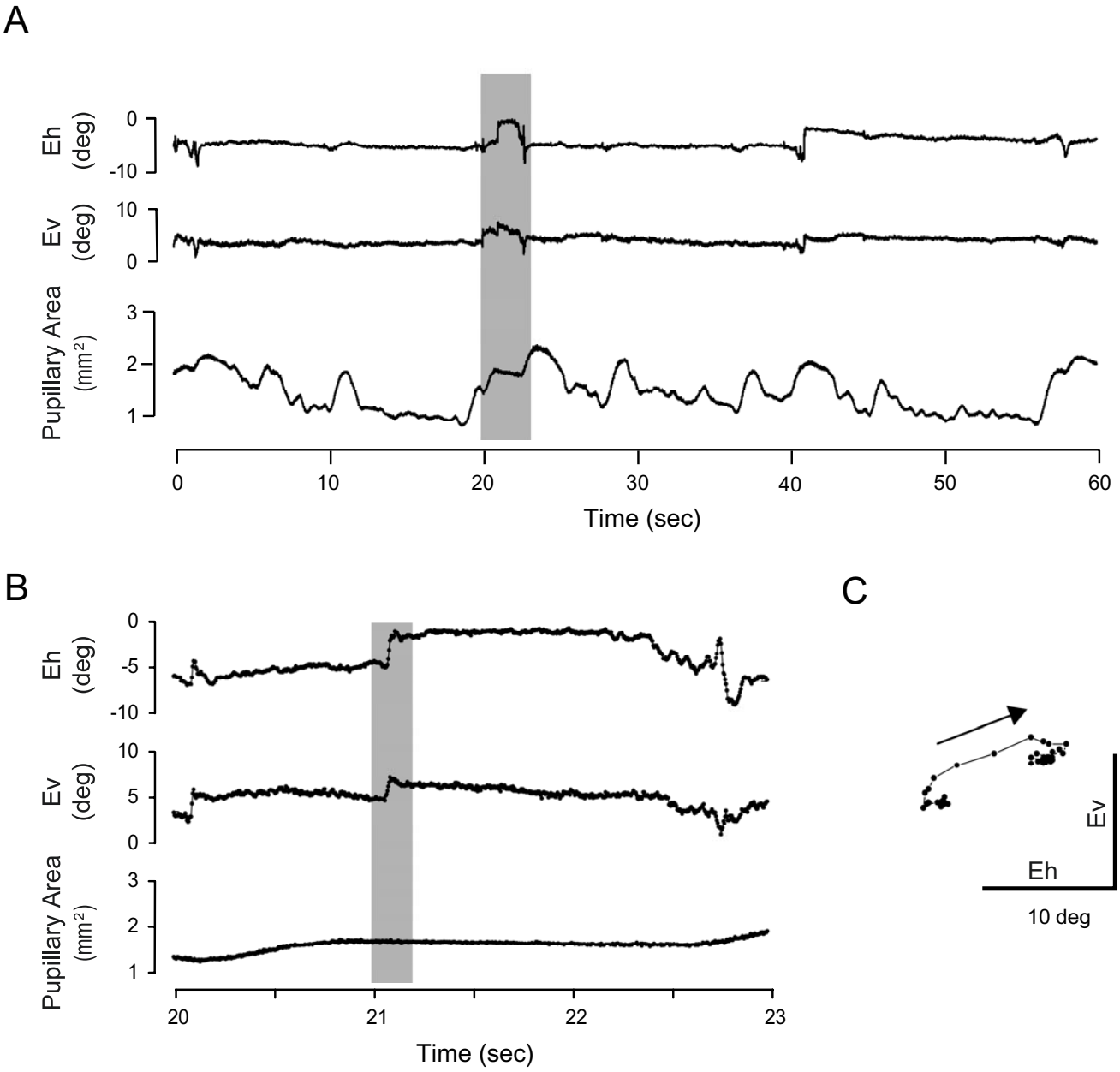

Figure 1-9
Examples of recorded eye positions and pupillary area.

(A) Horizontal (upper) and vertical (middle) eye positions during 60 second recording period. Shifts of eye positions were observed. The size of pupillary area changed frequently in darkness (bottom). (B) 3 second recording of eye positions and pupillary area corresponding to the shaded period in A. A rapid eye movement was observed. (C) Eye trajectory during 200 ms recording period corresponding to the shaded part in B. Arrow indicates the direction of a rapid eye movement. Eye positions during the rapid eye movement were accurately recorded at the sampling rate of 240 Hz.

Part 2

Dynamic characteristics of saccadic eye movements in C57Bl/6J mice

Introduction

The saccadic system is a suitable experimental system to study neuronal mechanisms to control the accurate movements for several reasons. First, eye movements can be measured easily and quantitatively. Second, the topographic organization of the oculomotor circuitry allows electrical stimulation in the brain to be used to elicit eye movements artificially. Finally, detailed studies on identified neurons of the oculomotor system can be performed *in vivo* during eye movements. Due to these facts, the neuronal circuitry that underlies the generation of saccades has been intensively investigated especially in monkeys and cats. Moreover, numerous theoretical models have been proposed for explaining the saccadic system, owing to the relative simplicity of the mechanical system to be controlled. Studying the saccadic eye movement would be expected to reveal the neural mechanisms underlying cognitive process in the brain as well as its accurate motor control. In primates, the combined electrophysiological and behavioral experiments using saccadic eye movements as a behavioral indicator have made a large contribution to our understanding of the cognitive functions of the brain such as anticipation, decision-making, attention and motivation (Fisher and Weber 1993; Glimcher and Sparks 1992; Gold and Shadlen 2000; Kawagoe et al. 1998; Kustov and Robinson 1996). In humans, studies of the executive control of saccades have been useful for assessing neurological dysfunction in schizophrenia (Fukushima et al 1990; Park and Holzman 1993; Crawford et al 1995), Parkinson's disease (Luek et al 1990; Vermersch et al 1994), and depression (Sweeney et al., 1998). Recent

advances in mouse molecular genetics offer a new approach to study the neural basis of behavior (Steele et al., 1998). However, previous studies on oculomotor system in mice have been made from the view of motor learning, and concentrated on the slow, reflexive eye movements such as the vestibulo-ocular reflex and the optokinetic reflex (Raymond, 1998). Studies concerned with the saccadic eye movements have usually used primates and carnivores as experimental animals. Because rodents have poor fovea in their retina, it has been believed that they are unlikely to use saccade for visual orientation.

Thus, there is little knowledge about saccadic eye movements in rodents with laterally located eyes and less distinct fovea, like mice. Although, the existence of saccadic eye movements has been reported in several literatures (Mitchiner et al., 1976, Balkema et al., 1984, Grusser-Cornehls and Bohm, 1988), no report has been made that described the quantitative measurement of saccadic eye movements in mice. One reason for this is that the lack of an adequate method for tracking rapid eye movements in this species. In part 1, I have developed the high-speed video-oculography for mice. In this part, using this system, I investigated the spontaneous saccade in mice in a quantitative manner.

Materials and methods

Surgical procedures

C57BL/6J male mice with black eyes (n=8, body weight 20-25g, 3 month-old, SLC Japan) were used. Male mice were housed individually with a light-dark cycle of 12 hr light/12 hr dark for more than a week under standard laboratory conditions with a 12-h day/night cycle with lights on at 08:00 and food and water ad libitum. All surgical procedures were done under 2 - 3.5 % isoflurane anesthesia (FORANE, ABBOTT). After an incision was made in the skin, a pedestal was attached to a mouse on the cranial bone with the dental resin. The animals were allowed to recover for 24 hours. All procedures were approved by the Animal Ethics Committed of the Okazaki National Institutes.

Eye movements recording

The mouse was left restraint in the experimental chamber to adapt to darkness for an additional 30 minutes before experimentation began. Its legs were hanged out of the sheet in the air and did not touch anything else. Its head was fixed to the stereotaxic platform (SR-6N, Narishige, Japan) with a brass rod attached to a manipulator (SM-15, Narishige, Japan) and its body was loosely restrained on a rubber sheet.

Spontaneous movements of the right eye were monitored during 30 minutes with a CCD camera placed at an angle of 60 degree laterally from the midline and 30 degree down from the horizontal plane (Fig. 2-1). Infrared light-emitting

diodes (HSDL4230, Agilent Technologies) attached to the camera illuminated the eye with wavelength of 880 nm. The background light of the environment was 50 - 100 lux.

Data analysis

Eye-movement data were analyzed and displayed off-line using custom-designed software. The amplitude, duration, peak velocity, and direction were digitally computed for each saccade. For quantitative analysis, instantaneous eye velocity was determined by differentiating the position signals. To calculate eye velocity, a two points central difference algorithm was used.

$$\dot{E}(i) = \big(E(i+1) - E(i-1)\big)/2dt,$$

where *dt*, the sampling interval, is 4.17 msec and *i* is the index for discrete time. $\dot{E}(i)$ is the eye velocity and $E(i)$ is the eye position at the time *i*, respectively. This differentiation algorithm had a cut off frequency of 60 Hz (-20 dB). Saccade duration was defined as the time duration which instantaneous eye velocities exceeded 100 deg/sec.

Results

Characteristics of the spontaneous saccade in mice

An example of eye movement recordings is shown in figure 2-2. Arrowheads indicate the occurrence of the saccadic eye movements (Fig. 2-2E). The mouse made rapid shifts of eye position spontaneously in the dimly illuminated box. Horizontal and vertical eye position signals were then differentiated to obtain an estimate of horizontal and vertical eye velocity, respectively (Fig. 2-2C, D). Mice could hardly hold the eye position at the end of saccades. In most cases, eyes drifted back slowly after the saccades toward the center of the orbit. Therefore, most saccades occurred from the center of the orbit (Fig. 2-3).

Frequency of the spontaneous saccadic eye movements

Mice made saccadic eye movements at a nearly constant rate (Fig. 2-4A) under the recording condition. In this mouse, saccades occurred at a frequency of 2.2 /min. Average spontaneous saccades in all subjects with a fixed head occurred at a frequency of 3.2 $\pm$0.9 /min (n=8) (Fig. 2-4B). Mice were almost unresponsive to the sound or visual stimuli.

Dominant direction of spontaneous saccades

Figure 2-5A shows direction distributions of spontaneous saccades in a single mouse. Horizontal saccades, especially in forward direction, were mostly observed (Fig. 2-5D). It should be noted that this coordinates largely depends on

the way in which the head of mice was fixed. In order to obtain the mean direction of the spontaneous saccades during the recording period, the direction of the addition of the unit vectors was calculated from the vector of individual saccades (Fig. 2-5Ab arrow).

Mean direction = $\tan^{-1}\left(\sum \sin\theta_i / \sum \cos\theta_i\right)$

,where θ_i is a direction of each saccade. I also determined the estimated horizontal axis from the direction distribution data. Because the horizontal direction was preferred direction, the 180 degrees rotational operation of the data ranging from 90 to 270 provided the unimodal distribution of an angular histogram. I obtained the median direction of the converted angular distribution as the estimated horizontal axis for each subject (Fig. 2-5Ab solid line). For all the subjects, the preferred direction of saccades was forward direction (Fig. 2-5B), and estimated horizontal axes were slightly downward (mean= -21.8 ± 7.3 degrees, n=8) in our experimental set-up (Fig. 2-5C).

Amplitude of spontaneous saccades and the oculomotor range

Figure 2-6A shows an example of the histogram of the saccadic amplitude during 30 min recording period with a threshold of 100 deg/sec. This mouse made saccades with mean amplitude of 9.0 ± 5.5 degrees. Although most spontaneous saccades were less than 10 degrees in amplitude, large saccades over 20 degrees were also observed. Distribution of mean amplitude for all the mice (n=8) is shown in figure 2-6B. Average value of the mean amplitude is 8.5 ± 2.0 degrees (n=8).

Figure 2-7 shows an example of the scatter plot of the end position of the

spontaneous saccades. This animal exhibited the 61.6 degrees deviation of the eye position in the orbit in the horizontal preferred direction and 38.1 degrees in the orthogonal direction. In all the subjects, the most eccentric excursion of the eye in the orbit was 33-98 degrees (mean= 57.3 ± 26.4 degrees) for the horizontal direction and 18-67 degrees (mean= 38.4 ± 15.6 degrees) for the vertical direction.

.

Main sequence relationship

Kinematics of saccadic eye movements can be defined on the basis of velocity-amplitude characteristics. Figure 2-8 shows velocity profiles of saccades with five different amplitudes in a single subject. The velocity profile of saccade with different amplitudes exhibited a characteristic appearance. The spontaneous saccades of mice exhibited approximately symmetrical and typical bell-shaped velocity profiles. Larger saccades tended to have dynamic overshoot; the eye went beyond its final position and returned very rapidly. The amplitude and the peak velocity of spontaneous saccades exhibited nearly linear correlation across the observed amplitude range of 2 to 35 degrees. Figure 2-9A shows an example of the relationship between amplitude and the peak velocity in a single subject. This relationship showed nearly linear correlation (correlation coefficient = 0.92) and could be well fitted to the linear regression line. Peak velocity increased almost linearly with a slope of 64.0 / sec, and Y-intersect was 68.5. Saccadic amplitude and peak-velocity were found to be linearly correlated in all eight subjects, with a mean slope of 54.2 ± 8.5 / sec (Fig. 2-9B). Correlation coefficients ranged from 0.82 to 0.96 (mean= 0.89 ± 0.05, n=8). There was little intersubject variability in

peak-velocity vs. amplitude relationship. The slope of the curve was much steeper in mice than in other mammals. It should be noted that saccades smaller than 2 degrees were not measured due to the limitation of the recording method.

Duration of saccades also increased with amplitude, although it was highly variable (Fig. 2-10A). Duration tended to be saturated for larger saccadic amplitude. Therefore, I used a nonlinear regression to fit the data with the following model. Saccadic amplitude and duration had a nonlinear relationship that was fit by an exponential equation (Fig. 2-10A). An exponential curve of the form:

$$D = K * \left(1 - e^{-A/tau}\right)$$

, where D = saccadic duration, A = saccadic amplitude, and K and L = constants returned by the curve-fitting program. I found that the model provided a good fit for the data. Correlation coefficient was 0.68 for the data in Figure 2-10A. Averaged correlation coefficient was 0.73 ± 0.08 for all subjects (Fig. 2-10B). The mean K value was 42.3 ± 4.2 msec and the mean tau values was 5.11 ± 1.27 / degree. In all subjects, most of the saccades ended within about 60 msec with a detection threshold of velocity at 100 deg/sec.

Discussions and conclusions

I successfully measured the saccadic eye movements in mice quantitatively in this study. And I indicated that the peak velocity of the saccadic eye movements increases linearly against its amplitude in mice, similar way to the other mammals such as human, monkey, and cat. Even though there is the same tendency among these mammals, mice have some differences in the following points. The peak velocity did not saturate at least in the range of observation. The peak velocity of saccades in mice increased almost linearly as a function of their amplitude with a slope of 54 /sec, which is much higher than those of other mammals; human: 20 /sec (Boghen et al., 1974), monkey: 40 /sec (Fuchs, 1967), cat: 10 /sec (Evinger and Fuchs, 1978), rabbit: 13 /sec (Collewijn, 1970), rat: 20-40 /sec (Fuller, 1985, Hikosaka and Sakamoto, 1987). On the other hands, the duration of saccadic eye movements saturated at 60 ms for saccades of over 15 degrees.

It was found that most of spontaneous saccadic eye movements were in horizontal directions. Not many but few vertical saccades were also observed. These results suggest the possibility that, although both horizontal and vertical saccade generator exists, horizontal eye movements are developed in particular in this lateral-eyed species.

I often found the tendency that the eye quickly returned to the primary position after the saccadic eye movements in a reflexive manner. Other cases were found in that the eye drifted back slowly to the center of orbit. Several explanations can be made for these results. It has been conceptually suggested that the eye position

signal is generated by the putative neuronal integrator, which integrates the velocity signal from the saccadic command generator. If this neuronal integrator is leaky in the mathematical sense, it is difficult to keep holding an eye position and likely to drift back to the primary eye position. It has been reported that in darkness it is also difficult to keep an eye stable and the eyes tend to drift. Because mice are nocturnal animal and have poor visual acuity (Dräger, 1975), they might be unable to control saccadic eye movements precisely.

Mice had an oculomotor deviation of about 60 degrees on average in the horizontal direction and of 40 degrees in the vertical direction. The observed maximum oculomotor range of 100 degrees in the horizontal direction in mice is larger than that in cats (50 degrees: Guitton et al., 1980) and in rabbits (30 degrees: Collewijn, 1970), and is close to the oculomotor range in humans (110 degrees: Guitton and Volle, 1987).

I observed that mice strain C57BL/6J rarely made saccadic eye movements. This result is consistent with the previous report observing the eye movements in the same strain (Mitchiner et al., 1976). They also reported that the strain difference exists in the frequency of spontaneous saccades in mice. Therefore, the results of present study may not apply to the characteristics of spontaneous saccades in all the strains of mice. However, since C57Bl/6 strain I used here is regarded as one of the standards in the field of neuroscience (Banbury Conference on genetic background in mice(1997)), my data would provide the basis for analyzing the neural and molecular mechanisms engaged in the control of saccadic eye movements using genetically engineered mice.

The fact that mice hardly responded to the auditory and visual stimuli might support the idea that the rapid shit of eyes is essentially not important in orienting behavior in this species. Because present experiments were carried out under an artificial condition in which mice were slightly restrained with the head fixed in the dim box, further study should be needed to elucidate the nature of saccadic eye movements in freely moving animals.

In conclusion, here I investigated the dynamic characteristics of the rapid eye movements (saccades) in alert, head-fixed mice (C57BL/6 strain) using the high-speed video-oculography. Spontaneous saccades could be observed in the darkness at the frequency of the several times per minute with mean amplitude of 10 degrees. Mice made rapid eye movements mainly in horizontal direction. The peak velocity of saccades increased almost linearly against the saccadic amplitude with a slope of 60 / sec, whereas the saccadic duration saturated at the level of 60 msec against larger saccades. This study provides the basis for analyzing the neural and molecular mechanisms engaged in the control of saccadic eye movements using genetically engineered mice.

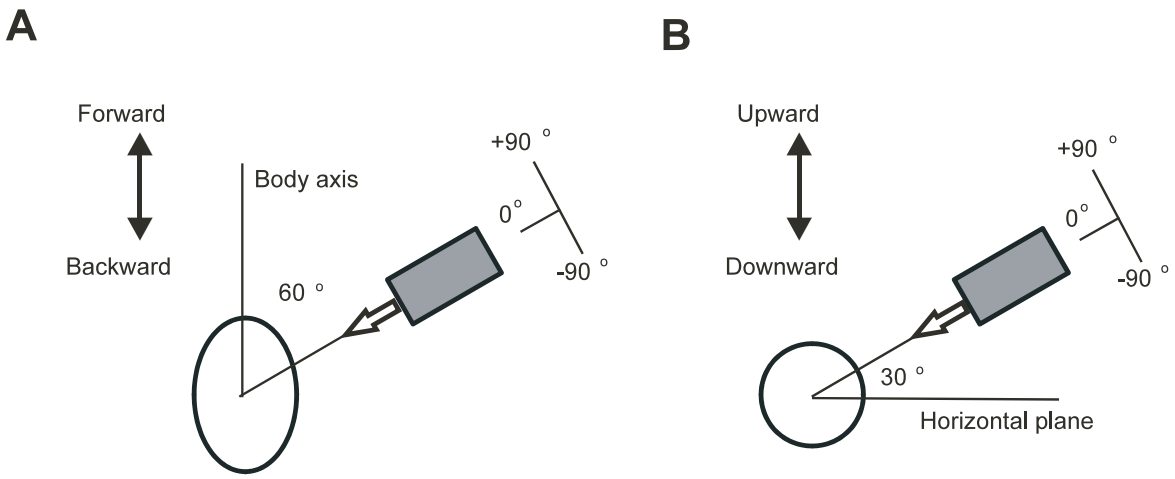

Figure 2-1
Arrangement of the camera for measuring eye movements.

Top-view (A), and back-view (B) diagram of video coordinate system. Optical axis of camera is shown as white arrow. The movements of right eye were monitored with a high-speed video camera. A CCD camera was set at an angle of 60 degrees right regarded to body axis and of 30 degrees down against horizontal plane

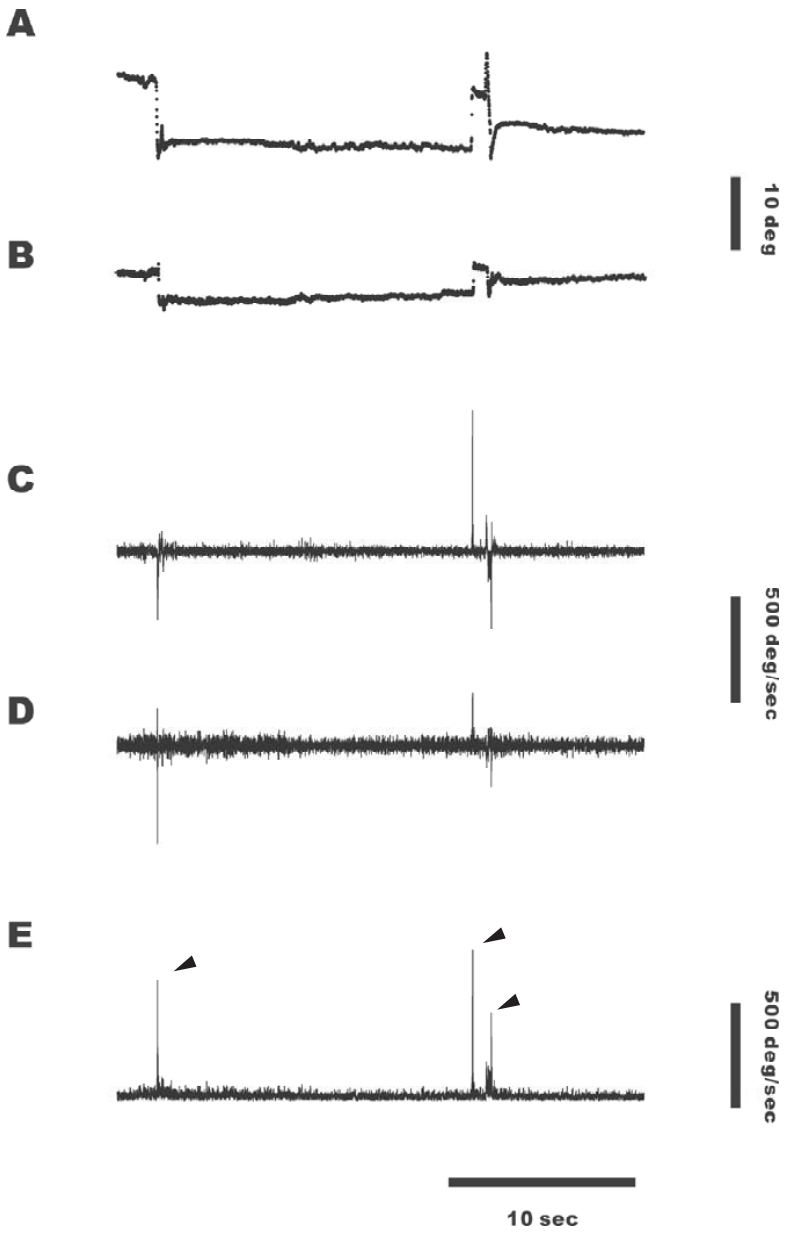

Figure 2-2
An example of recorded eye position and its velocity

Positive positions are to the forward and upwards. Horizontal (A) and vertical eye position (B). Horizontal (C) and vertical eye velocity (D). (E) absolute eye velocity calculated from horizontal and vertical eye velocity. Arrowheads indicate the occurrence of the spontaneous saccades.

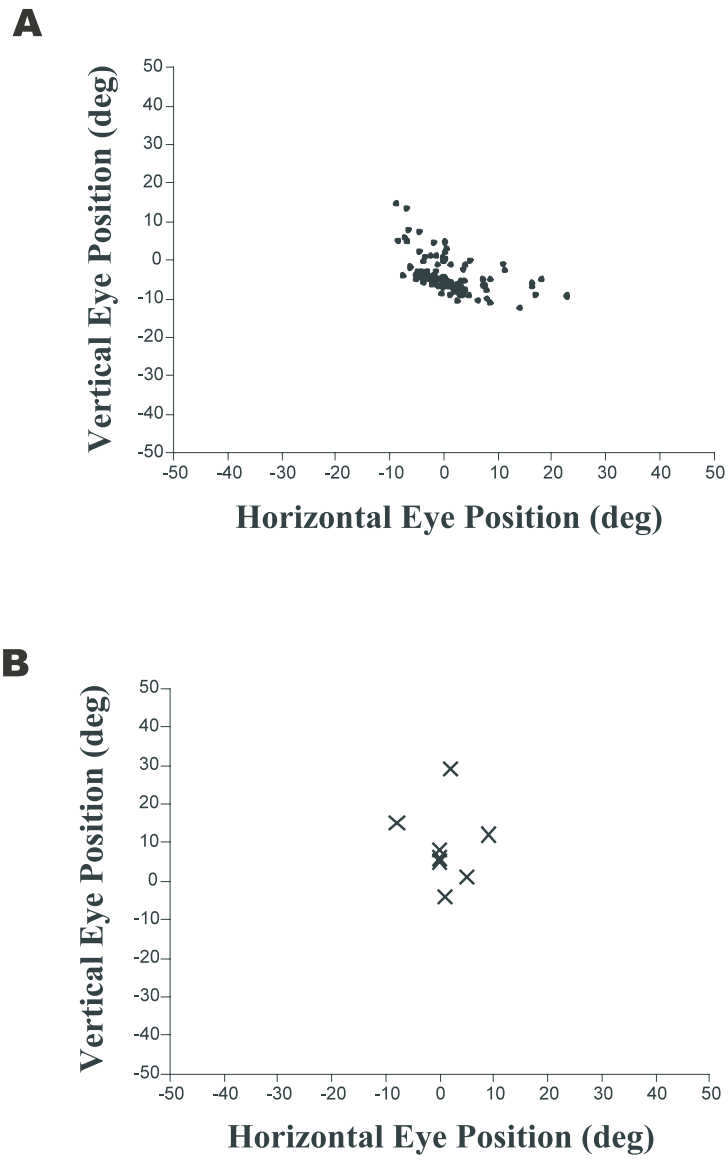

Figure 2-3
Distribution of the initial eye position

(A) An example of the scatter plot of the initial eye position of the spontaneous saccades. (B) Centroids of the scatter plot of the initial eye positions for each subject (n = 8).

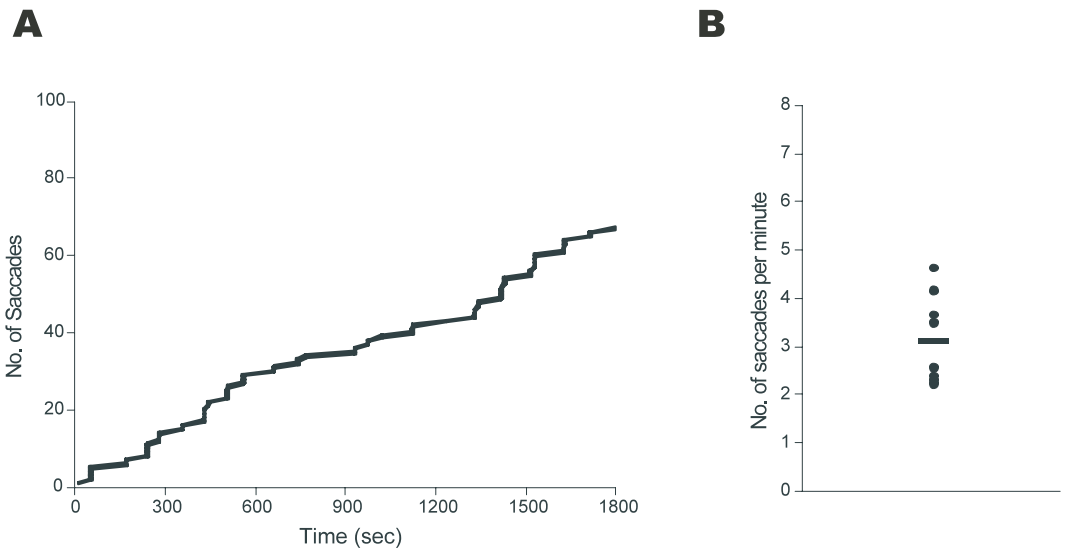

Figure 2-4
Frequency of rapid eye movements in mice

(A) Cumulative plot of the occurrence of the spontaneous saccades. (B) Distribution of the occurrence of spontaneous saccades for all subjects (n=8). Each plot indicates the data from an individual subject. (mean = 3.2 ±0.9 /min).

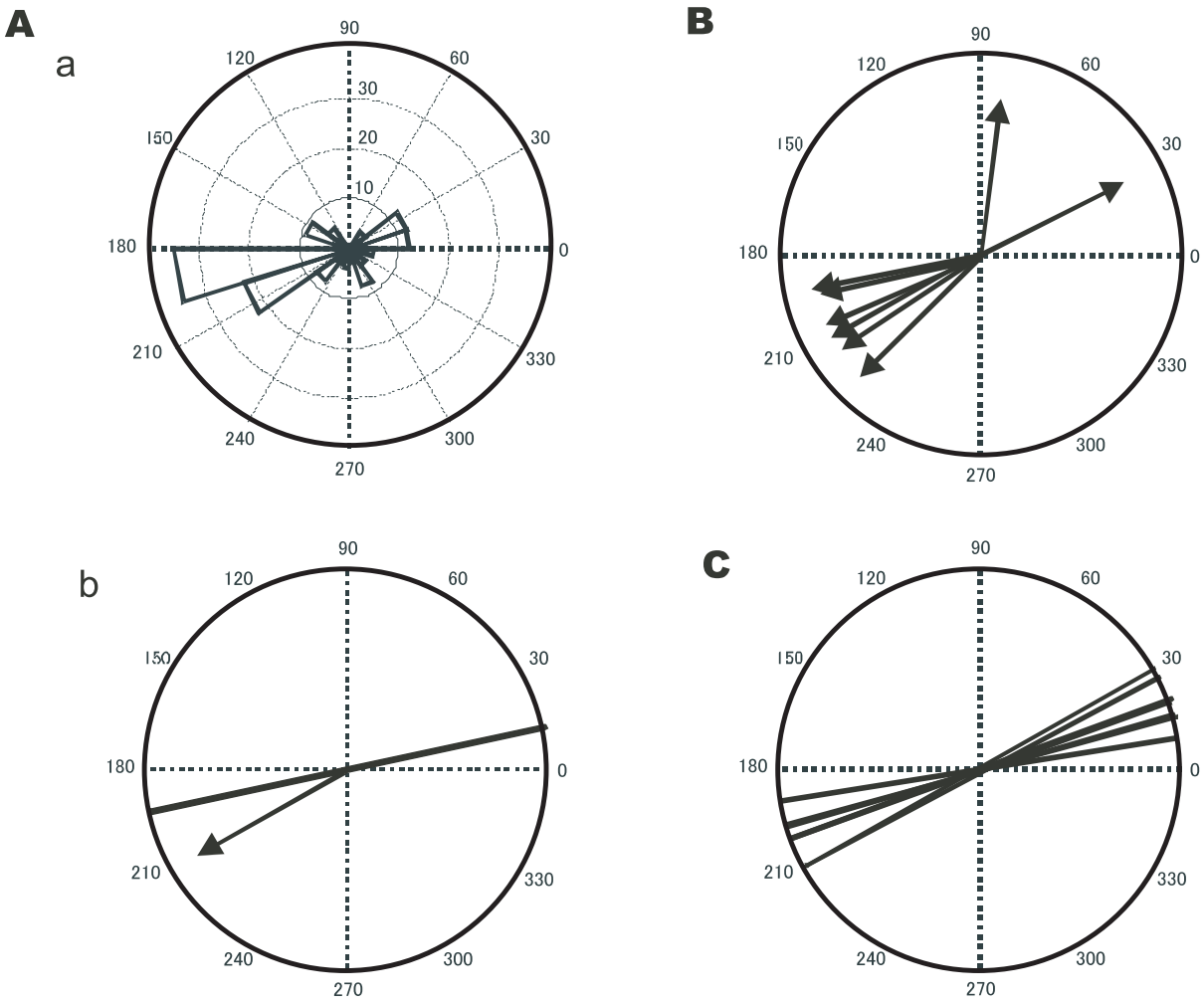

Figure 2-5
Preferred direction of the rapid eye movements in mice

(A) An example of the direction of spontaneous saccades during recording period (a), and its averaged direction (arrow line in b) and axis of symmetry (straight line in b). (B) Averaged direction and axis of symmetry. (C) Distribution for all subjects (n=8).

0, 90, 180 and 270 indicate backward, upward, forward, downward direction, respectively.

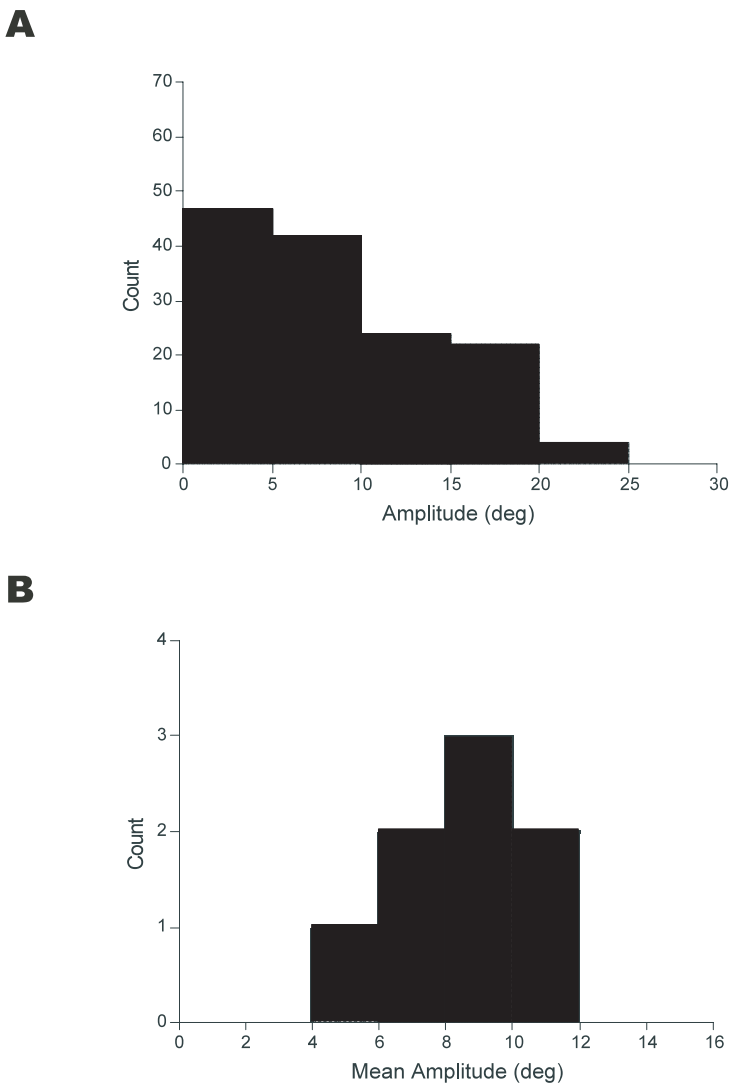

Figure 2-6
Distribution of amplitude of spontaneous saccades

(A) An example of the distribution of saccade amplitude from the entire data set during recording session in a single mouse. Mean= 9.0 ±5.5 degrees. (B) Mean amplitude distribution from the all subjects (n=8). Mean=8.5 ±2.0 degrees.

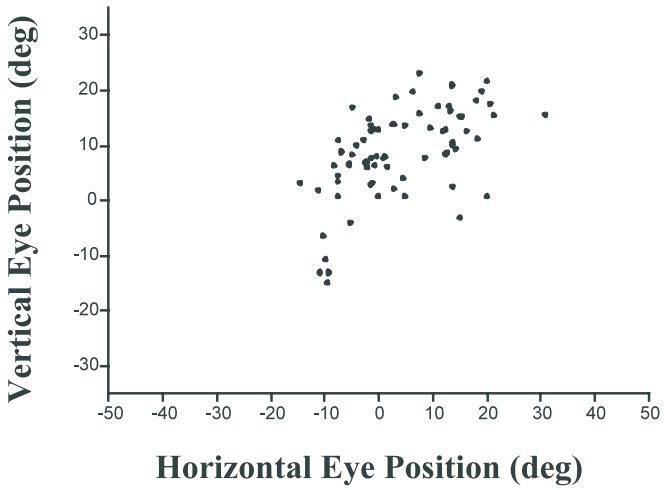

Figure 2-7
Motor range of the rapid eye movements

An example of the scatter plot of the end position of the spontaneous saccades. This animal exhibited the 61.6 degrees deviation of the eye position in the orbit in the preferred direction and 38.1 degrees in the orthogonal direction.

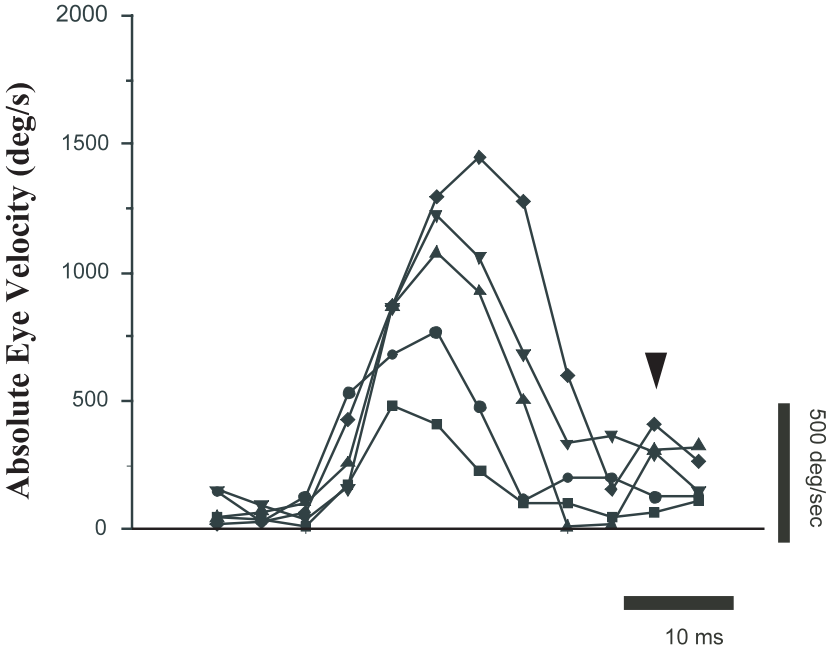

Figure 2-8
Velocity profile of the spontaneous saccades in mice

Examples of velocity profiles of saccadic eye movements of different size and velocity. Each velocity trace is aligned with the saccadic onset determined by velocity threshold above 100 degrees per second. Second peaks indicated by an arrowhead reflected the dynamic overshoot . The amplitude of spontaneous saccade is 5 (■), 10 (●), 15 (▲), 20 (▼), and 25 (◆) degrees, respectively.

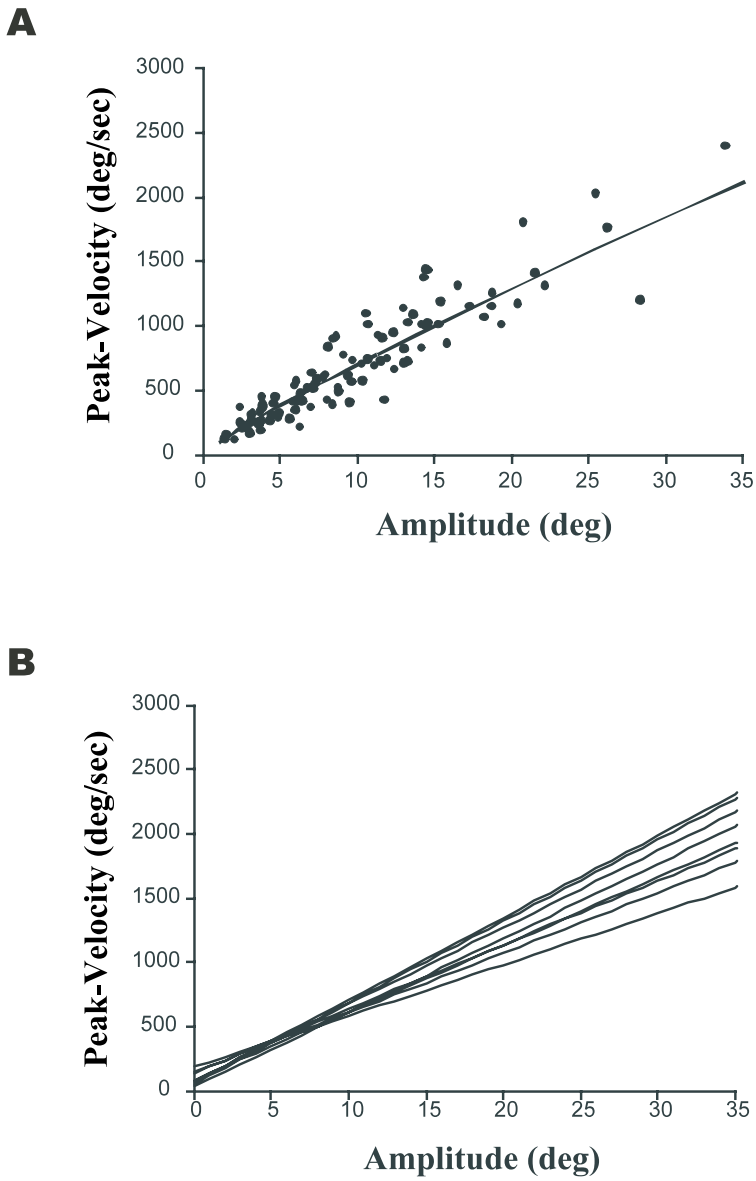

Figure 2-9
The relationship between peak-velocity and amplitude in spontaneous rapid eye movements

(A) An example of peak-velocity vs. saccade amplitude plot in one animal. The solid line indicates the linear regression line : y = 64.0 x + 68.5. Correlation coefficient was 0.92. (B) Regression lines for all subjects (n=8). Each solid line indicates the regression line from an individual subject. Mean slope is 54.2 ±8.5 / sec, correlation coefficients ranged from 0.82 to 0.96.

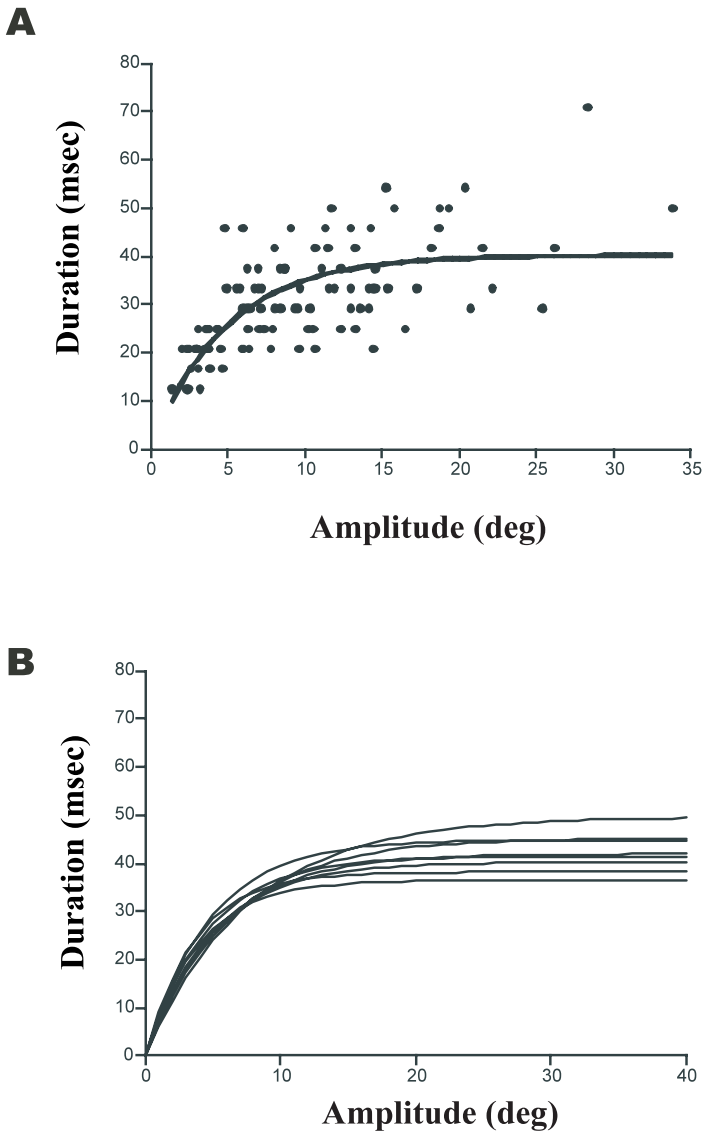

Figure 2-10
The relationship between duration and amplitude in spontaneous rapid eye movements

A) An example of duration vs. saccade amplitude plot in one animal. The solid line indicates the regression line. Correlation coefficient was 0.68. (B) Regression lines for all subjects (n=8). Each solid line indicates the regression line from an individual subject. For all subjects, most of the saccades ended within about 60 msec with a velocity threshold of 100 deg/sec.

Part 3

Quantitative study of the saccadic eye movements evoked by the electrical micro-stimulation of the superior colliculus in mice

Introduction

In the previous parts, I have established a high-speed video-oculography and found that mice spontaneously made saccade-like rapid eye in a head-fixed condition.

One of the questions I asked in this part is how the motor representation of the SC is coded in mice. This is mainly from the interests in comparative physiology. Functional roles of the SC in saccadic eye movements control are well studied in frontal-eye animals such as monkeys and cats. On the other hand, mice are lateral-eyed animals with poor vision and their visual representation on the superficial layer of the SC is different from that in frontal-eyed animals. In the antero-medial potion of mouse SC, the visual representation of the superficial layer share the same location in the visual field with the opposite SC (Dräger and Hubel, 1975). Therefore, this region represents the ipsilateral visual field in mice.

Electrical stimulation applied to the deeper collicular layers of the head-fixed monkey evokes contraversive saccadic eye movements whose amplitude and direction depend on the stimulation site and are independent of the initial eye position (Robinson, 1972, Schiller and Stryker, 1972). These studies revealed a two-dimensional, retinotopically coded motor map within the intermediate and deep layers of the SC: amplitude, from small to large, is represented from rostral to caudal while direction, from upward to downward is represented from medial to lateral across the SC. It has also been shown that units in the deep layers of the monkey SC discharge before saccades that are similar in direction and amplitude to those

evoked by electrical stimulation (Schiller and Stryker, 1972). A characteristic feature of the motor map is its correspondence with the sensory map of visual space represented in the overlying superficial layer (Schiller and Koerner, 1971, Schiller and Stryker, 1972). This topographic correspondence of the intermediate and deeper layers with the superficial layer has been believed to be important in sensory-motor transformation of the SC.

Similar studies carried out in head-fixed cats demonstrated different patterns of saccadic eye movements depending on the rostrocaudal extent of the stimulation site (Roucoux and Crommelinck, 1976, Guitton et al., 1980, Roucoux et al., 1980, McIlwain, 1986). Stimulation of the caudal pole of the colliculus evoked movements which brought the eyeballs to a given position in the orbit, while electrical stimulation of most loci in the SC evokes eye movements consistent with the topographic scheme. The direction of these 'goal-directed' movements would differ depending upon the starting position of the eyes despite the fact that the locus of stimulation remained constant (Hyde and Eliasson, 1957, Roucoux and Crommelinck, 1976, Guitton et al., 1980, McIlwain, 1986, McIlwain, 1990, Moschovakis et al., 1998).

In rats, previous studies on the electrical stimulation of the SC have mainly focused on the analysis of head and body movements under head-free condition and suggested that this structure mediates either orienting responses or defensive movements such as avoidance or flight (Sahibzada et al., 1986, Dean, 1995). Dean et al. (1989) proposed that the role of the SC varies markedly between species, and suggested that in animals such as rodents, with laterally placed eyes and with a

poorly developed central area in the retina, the SC generates head, rather than eye, movements towards a novel stimulus or to move away from it depending on stimulus characteristics. Thus, common recognition for the role of the SC in rodents has been that the SC controls head and body movements not the eye movements. Only one study concerned with the role of the SC in eye movements have made in rats and hamsters under head-fixed condition by McHaffie and Stein (1982), finding that saccadic eye movements could be evoked in topographically organized pattern in these species. There is no previous report on the motor representation of the saccadic eye movements in the intermediate and deeper layers of the SC in mice. In order to investigate the functional role of the SC in the generation of saccadic eye movements, I measured the characteristics of electrically induced rapid eye movements and evaluate their dependence on stimulus site and on their initial eye positions in the orbit.

Another question is how the saccadic control system responds to the prolonged electrical stimulation of the SC. In monkeys, it has been reported that long-lasting stimulus evoked staircase saccades consisted of successive several small saccades (Robinson, 1972, Stryker and Schiller, 1975, Breznen et al., 1996). These results have been understood as the reflection of underlying neuronal structures. Several theoretical studies proposed the control model with negative feedback loop and a neural integrator for the saccadic control system (see introduction in part 4 in detail).

In this part, to study the properties of the saccadic circuit and the motor

representations of SC in mice, sustained step responses of the saccadic control system were examined by using prolonged electrical stimulation of the SC.

Materials and methods

Subjects

Male C57BL/6J mice with pigmented eyes (25-30g, 10-12 weeks, CLEA Japan) were used. All surgical procedures were performed under isoflurane anesthesia (FORANE, ABBOTT). A pedestal was attached to a mouse on the cranial bone with the bone cement (SUPER BOND, SUN MEDICAL). Holes were drilled in the bone stereotaxically. After recovery from anesthesia, a mouse was loosely restrained with a rubber sheet and its head was fixed to the stereotaxic platform.

Electrical stimulations

Repetitive electrical stimuli were applied to the left SC with the tungsten monopolar electrode with a trunk diameter of 200 μm (impedance 0.8-1.2 MΩ at 1 kHz). An electrode approached the SC through the visual cortex in 0.25-mm steps. Each stimulation consisted of 100-800 ms trains of 300-Hz constant current cathodal pulses with duration of 0.2 ms (10~100 μA). In the mapping study, constant suprathreshold intensity of 1.25-1.5 x threshold was used. The threshold current was defined as the current required to evoke saccades in 50% of the trails. At the end of the experimental session, the animal was anesthetized and perfused with a 10% formalin solution through the heart. After equilibration with 20% sucrose solution, 50 μm frozen sections of the brain were prepared. The location of the electrode tracks was identified by placement of a small electrolytic lesion and reconstructed from Nissl-stained sections.

Eye movement recording

The movements of the right eye were monitored under awake, head-fixed condition with a high-speed CCD camera at a sampling rate of 240 frames/sec placed at an angle of 60 degree laterally from the midline and 30 degree down from the horizontal plane, approximately perpendicular to the optical axis of the eye (see Fig. 2-1).

Data Analysis

Eye-movement data were analyzed and displayed off line using custom designed software. For quantitative analysis, velocity was determined by differentiating the position signals (for more detail, see materials and methods in part 2). Saccade duration was defined as the time duration which instantaneous eye velocities exceeded above 100 deg/sec. The duration, amplitude, peak velocity and direction were extracted for each saccade. In the case of overlapping saccade, the individual movements were identified manually by searching for local minima in the velocity trace.

All procedures were carried out in accordance with accepted ethical principles for animal research and were approved by the Animal Ethics committee of the Institute for Physiological Sciences.

Results

Electrical stimulation of intermediate and deeper layers of the SC induced the rapid eye movements.

Electrical stimulation of the SC could induce the rapid eye movements in mice. These electrically induced rapid eye movements had threshold current, and had roughly constant amplitude against the different stimulations with suprathreshold current intensity (Fig. 3-2). Increasing the stimulus current beyond the threshold shortens the latency. Threshold current intensity inducing the rapid eye movements was examined at different depth in the SC, and it was found that thresholds were lower in the intermediate and deeper layers (Fig. 3-3). This indicates that the cell body or axon of projection neurons relating rapid eye movements exist in the intermediate and deeper layers of the SC.

Dynamic characteristics of electrically induced rapid eye movements

Velocity profiles of the electrically induced rapid eye movements showed bell-shaped curve, typical feature of the saccadic eye movement in other mammals (Fig. 3-4). Larger eye movements were often accompanied with the following overshoot of eye position, resulting in the second peak of velocity profile as shown in Fig.3-4. For the rapid eye movement with larger amplitude, the peak velocity had higher value. This relationship was clearly demonstrated for pooled data of all subjects in Fig. 3-5A. The relationship between the peak-velocity and the amplitude of rapid eye movements induced by electrical stimulations was almost

linear similar to the result of spontaneous saccades in part 2. The slope of the least-square regression line was 34.7. The duration of the evoked saccade saturated against large saccadic amplitude and these data could be successfully fitted to the saturating function with saturating value of 57 msec (Fig. 3-5B). These results indicate that electrically induced rapid eye movements have the fundamentally same characteristics in their dynamics as spontaneous saccades.

Motor map of the electrically induced rapid eye movements on the intermediate layer of the SC

Then, I examined the motor representation of the SC at the depth of the intermediate layer in a single animal. Trajectories of the eye movements evoked at different sites of a single mouse SC were represented in Fig. 3-6. In this figure, an ipsiversive saccade means saccade to forward direction, a contraversive means backward. From most sites in the SC, saccade-like rapid eye movements could be evoked in the contraversive direction. The amplitude of evoked rapid eye movements became larger when more posterior sites were stimulated, and smaller at more anterior sites, showing the similar motor representation to primates. Surprisingly, ipsiversive saccades could be induced from the antero-medial potion. In this region, the visual representation of the superficial layer shared the same location in the visual field with the opposite SC. Therefore, this region represents ipsilateral visual field. Thus, in mice, the SC codes both contraversive and ipsiversive saccades, probably, in agreement with the overlying retinotopy.

The vector of evoked saccades highly depended on the initial eye position

in the orbit as well as on stimulus sites, showing the similar result to cats. This dependence was shown obviously in Fig. 3-7. Figure 3-7 shows the time-course of horizontal eye movements evoked from different initial eye positions. There is a general tendency that the endpoints of saccades evoked from the same position in the SC converge at a specific point in the orbit. In other words, evoked saccades were goal-directed in this species. Thus, in some cases, the evoked saccade from the same sites resulted in the opposite direction depending on the initial eye position.

To illustrate the topography of sensitivity to initial position of saccades evoked from different collicular sites, the position sensitivity index was defined as the absolute value of slope of the least-squares regression line through the data plot of the horizontal component of saccadic amplitude against their initial eye positions in the orbit as shown in Fig. 3-8A. The absolute values of these slopes provide an index of the influence of initial position on saccadic amplitude, the steeper the slope the greater the sensitivity. Then, the degree of this position dependency was plotted on the surface of the SC as the position sensitivity index (Fig. 3-8B). Position sensitivity index becomes larger at those sites inducing larger amplitude of rapid eye movements.

Stimulation at a given collicular site produced saccadic components of different amplitudes, depending on the initial position of the eye. However, saccades evoked from different sites can be compared if the effects of initial position are kept constant by choosing a common starting point. Since a mouse normally initiates saccades from near the center of the orbit (Fig. 2-3), this initial

position was selected for study. Although the animals were not trained to fixate on a common point before the start of stimulation, the amplitudes of horizontal and vertical components evoked from the center of the orbit can be estimated from the linear regression of component amplitude on initial eye position (Fig. 3-8A). For example, the linear regression of Fig. 3-8A shows that saccades starting from an azimuth of 0 deg would have horizontal amplitudes of –26 deg. A horizontal vector having the amplitude of this intercept will be called the horizontal characteristic amplitude associated with that stimulus site. Similarly, the intercept of the regression of vertical amplitude on starting elevation with the horizontal midline of the oculomotor range estimates the vertical characteristic amplitude associated with a particular stimulus site. From these component characteristic amplitudes, characteristic vector and amplitude of saccade associated with a collicular site were determined. Figure 3-9 summarizes the collicular topography of the characteristic vectors and amplitudes.

Step response of the saccadic control system

In order to investigate the step response of saccadic system in mice, I applied prolonged electrical stimulations on the superior colliculus. Prolonged constant stimulation at the SC in monkey produces a periodic series of saccade-like movements. Thus the eyes move along in a ratchet-like fashion, a behavior that has been described as “staircase saccades” with intersaccadic interval of 50 to 250 msec (Robinson, 1972, Stryker and Schiller, 1975, Breznen et al., 1996). Figure 3-10 shows the results of prolonged stimulations. Prolonged suprathreshold

stimulus (800 msec) often evoked two or three successive saccades with a short interval of approximately less than 20 msec (Fig. 3-10A). However, unlike the staircase saccades in primates, longer stimulation period resulted in only maintaining the eye position and failed to induce additional saccades even within an oculomotor range (Fig. 3-10B). In general, beyond the constant period of approximately 100 msec, successive rapid eye movements could not be induced.

Rebound rapid eye movements after the end of electrical stimulation

In the anterior-medial regions, reversive saccades were observed in a reflexive manner. Figure 3-11 shows the time-course of the vertical eye movements evoked with different current strength, or different stimulus period. I call these rapid eye movements after the end of electrical stimulation as rebound saccades. These rebound saccades could be evoked by the lower current stimulus than the threshold current to evoke a normal saccade. This suggests rebound saccades are not simple motor reflex, but have some kind of underlying neural mechanisms. Rebound saccades had higher peak velocity than normal saccade (Fig. 3-12), and occurred within several ten milliseconds after the end of stimulation (Fig. 3-13). The latency of rebound saccades was relatively shorter than those of electrically induced rapid eye movements.

Discussions and conclusions

I demonstrated in this part that, in mice, the SC plays an important role in saccadic generation and its control, having basically similar dynamical characteristics to the other mammals. At the same time, I found the several unique features of saccadic system in mice.

Major species differences demonstrated in this study is the fact that ipsiversive saccades could be induced from the anterior-medial potion. The visual representation of the superficial layer upon this region shares the same location in the visual field with the opposite SC (Dräger and Hubel, 1975). Thus, this region represents ipsilateral visual field. Although the SC codes both contraversive and ipsiversive saccades in mice, the motor representation of the mouse SC would be probably in agreement with the overlying retinotopy, which is the same manner as the other mammals.

However, ipsiversive saccades cannot be explained completely by the theoretical model of the saccade control system previously proposed (Robinson, 1975, Zee et al., 1976, Lefevre and Galiana, 1992, van Opstal and Kappen, 1993, Arai et al., 1994, Massone, 1994, Moschovakis, 1994, Optican, 1995, Breznen and Gnadt, 1997, Gancarz and Grossberg, 1998), since those models were based on the unilateral brain structure. Thus I propose a new theoretical model to explain my results. Figure 3-14A shows hypothetical scheme of saccadic control system in mice having the output from the SC to both sides of the brain stem. The brain stem burst neurons obviously cannot express a negative firing rate and thus cannot

realize ipsiversive saccades unilaterally. In this hypothetical model, the saccadic command formed in the SC is conveyed to the brain stem bilaterally, and final outputs to eyes determined by the push-pull mechanisms between the neural activities of both sides. The strength of an output signal is dependent on both location of the colliculus and the eye position in the orbit. Using this model, the occurrence of ipsiversive saccades and position dependency of saccades can be explained. One possible neural structure required for this push-pull mechanism and for movements in the opposite direction would be cross-coupling from contralateral inhibitory burst neurons (Hikosaka and Kawakami, 1977). The push-pull mechanisms might be the corresponding neural mechanisms to the rebound saccades I observed. However, the most biologically realistic mechanism to account for this finding would so-called postinhibitory rebound. Many neurons do exhibit postinhibitory rebound where the sudden release of hyperpolarization produces a rebound activation of a few action potentials (Ito and Oshima, 1965). This push-pull mechanisms might also be related the recent report on the hyperpolarization in the frontal eye field (Seidemann et al., 2002) or the burst activation of the cerebellum at the timing of the termination of saccades (Dean, 1995, Thier et al., 2000).

Figure 3-14B shows a block diagram of the corresponding system in mice adapted from the generic model proposed in primates. In this model, a secondary negative feedback loop with longer delay is added to the generic model with a single feedback loop. In the step response study, prolonged stimulus could only evoked two or three successive saccades with a short interval, and beyond the

constant period of approximately 100 msec, successive rapid eye movements could not be induced. Therefore, I assumed that the secondary loop has longer delay of 100 msec conveying the neural signal relating the eye position in the orbit and that the local loop has short delay of less than 60 msec conveying the information relating the characteristic amplitude of saccade. In this block diagram, the local loop determines the dynamical characteristics of saccades and the modulation of the signal from the secondary loop results in the position dependency in mice. Assuming the neural structure corresponding to this model, higher peak velocity of saccade, short intervals of successive saccades and failure to induce staircase saccades can be attributed the shorter delay of these feedback loops.

As for the secondary loop with longer delay, I assume that the proprioceptive afferents from the eye muscles could be involved in this loop. Conceivably, they modify the gain of the internal feedback loop with short delay according to the position of the eye in the orbit. Eye muscle afferents are known to project to the cerebellar cortex in cats (Fuchs and Kornhuber, 1969, Baker et al., 1972). Degeneration of this area in humans is frequently associated with dysmetria (gross under- or overshoot) of goal directed saccades (Kornhuber, 1968). Taken together, this suggests that, if in fact the muscle afferents adjust the parameters of the local feedback loop to the different mechanics of the load occurring with different eye positions, this adjustment takes place at the level of the cerebellar cortex.

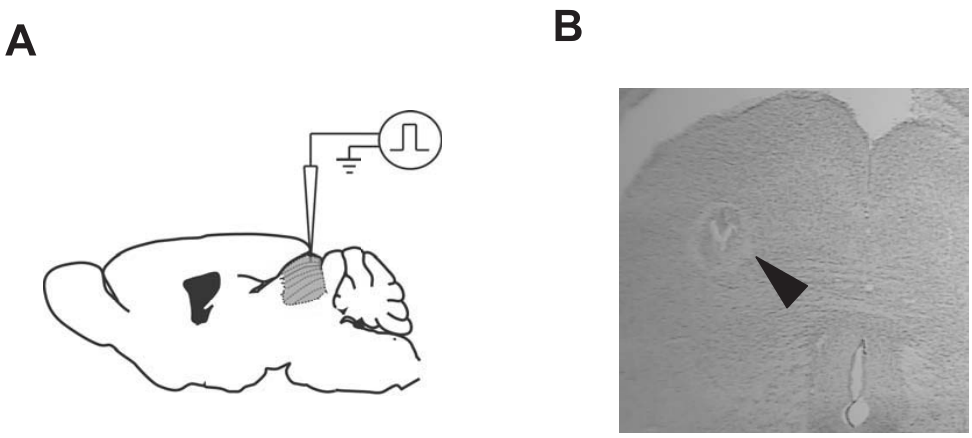

Figure 3-1
Electrical stimuli were applied to the SC

(A) Electrical stimuli were applied to the superior colliculus with a tungsten monopolar electrode. (B) The location of the stimulation was identified by placement of a small electrolytic lesion and reconstructed from histological sections.

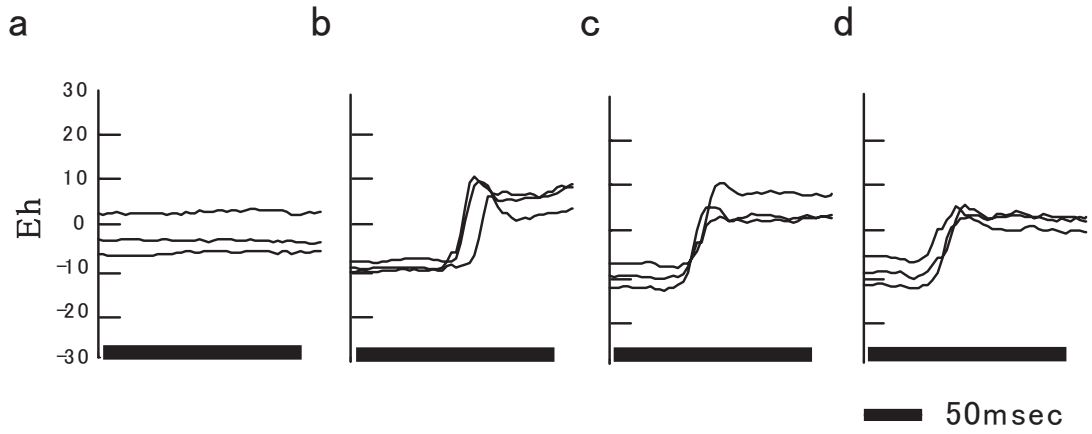

Figure 3-2
Horizontal eye position trace for different current strength

Electrically evoked rapid eye movements had threshold current. (a) 0.5 x, (b) 1.0 x, (c) 2.0 x, and (d) 3.0 x the threshold current, respectively (Threshold current = 10 μ A) . Boxes on the time axis indicate the onset and duration of stimulus trains. Electrically evoked saccades had threshold current and had roughly constant amplitude.

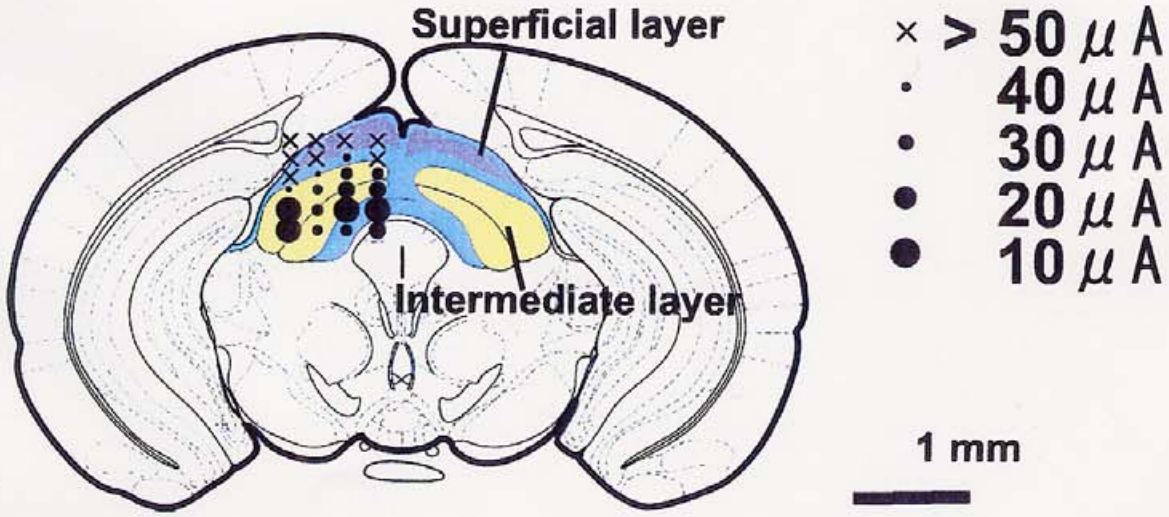

Figure 3-3
The threshold current at different depth

Threshold currents to induce the rapid eye movements in a single animal were represented on a coronal section of the SC. Thresholds were lower in the intermediate and deeper layers of the SC.

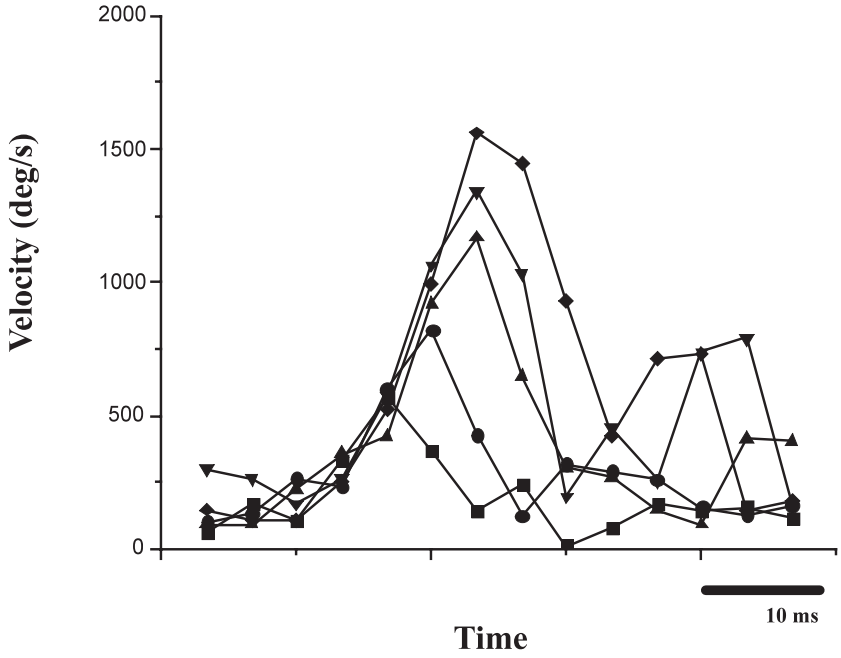

Figure 3-4
Velocity profile of the electrically-induced rapid eye movements

Velocity profile of the electrically-induced repid eye movements showed bell-shape velocity profiles similar to the spontaneous saccades. Each velocity trace is aligned with the saccadic onset determined by velocity threshold above 100 degrees per second. Second peak reflected saccadic overshoot. The amplitude of induce rapid eye movement is 5 (■), 10 (●), 15 (▲), 20 (▼), and 25 (◆) degrees, respectively.

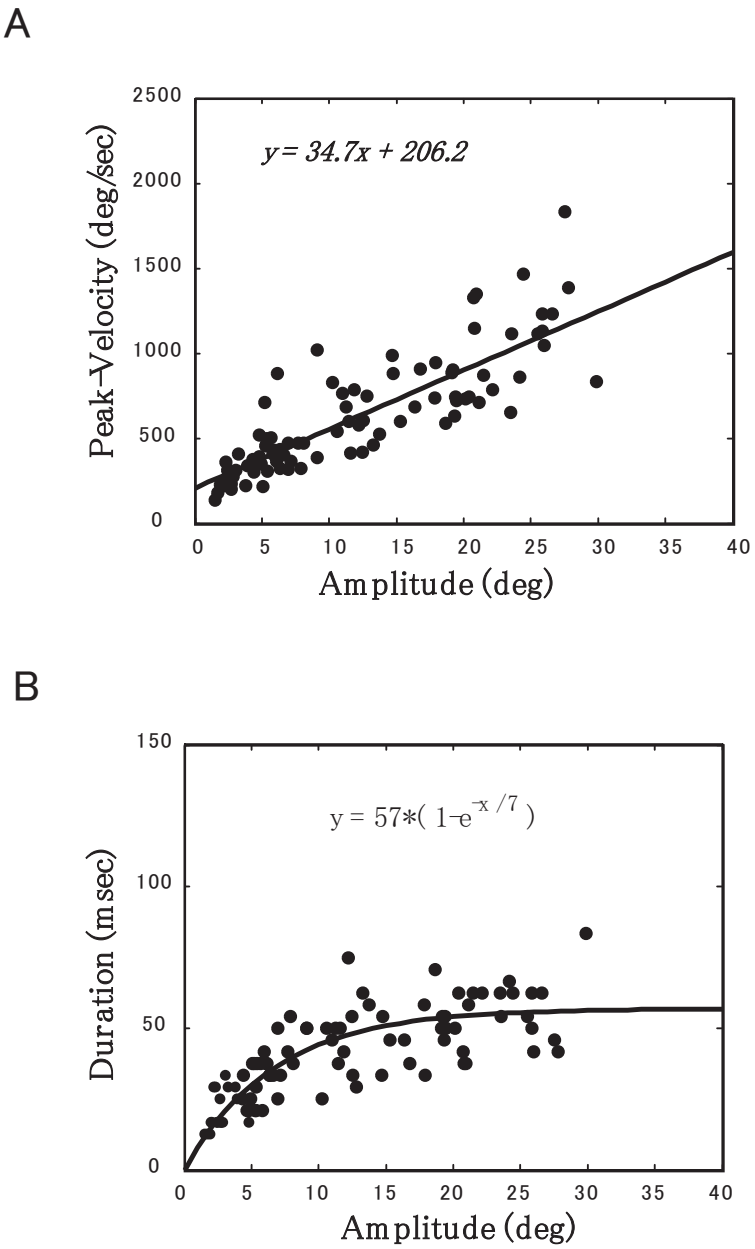

Figure 3-5
The main sequence relationship in electrically evoked rapid eye movements

(A) The peak-velocity vs. amplitude plot. The peak-velocity of the evoked saccade increased almost linearly against its amplitude. (B) The saccadic duration vs. amplitude plot. The duration of the evoked saccade saturated against large saccadic amplitude.

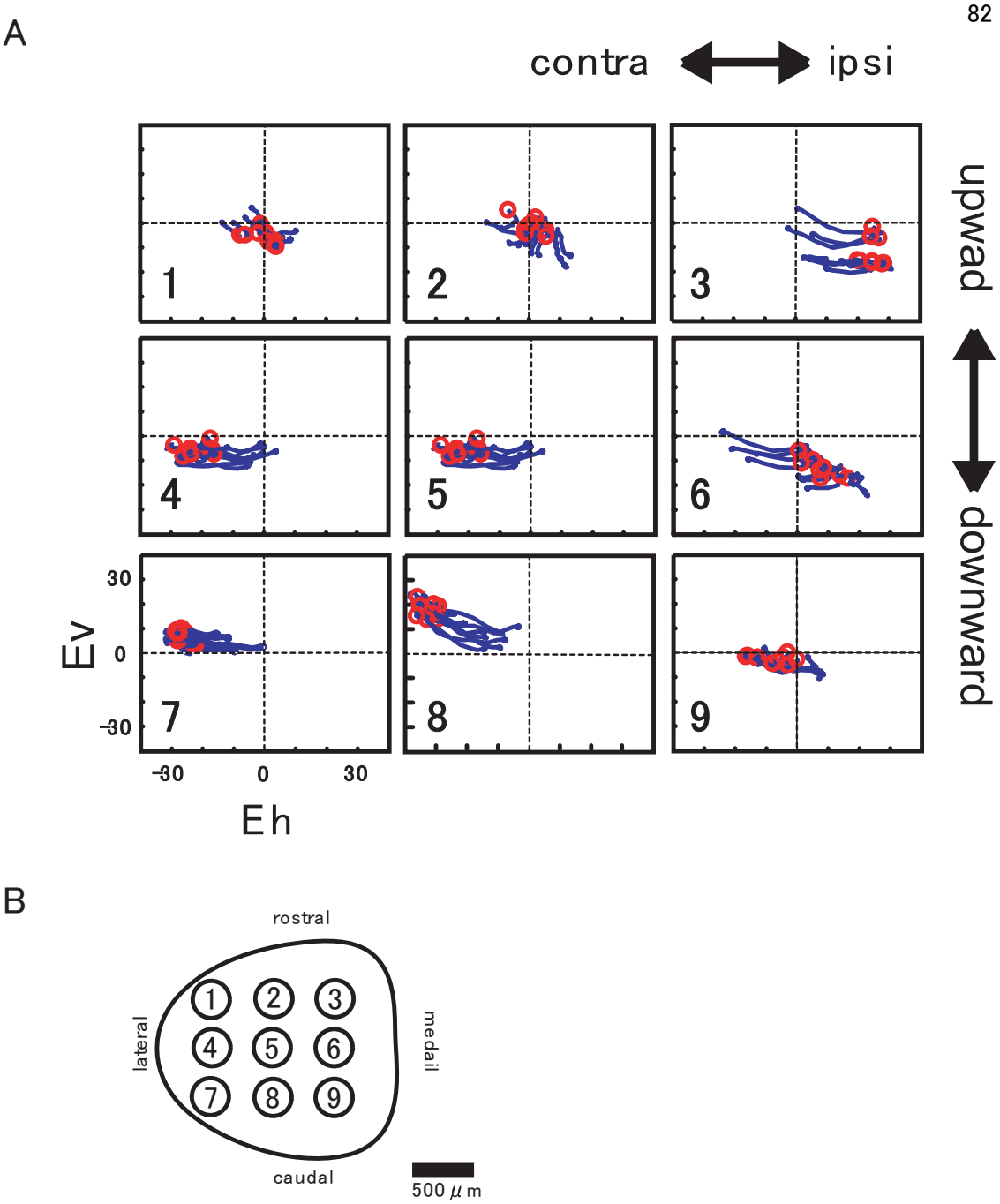

Figure 3-6

Trajectories of rapid eye movements evoked from different sites of a single mouse SC

(A) Examples of eye movements evoked at different sites of a single mouse SC. Red circles indicate initial eye positions. Circled letters indicate penetrations of the stimulating electrode on a dorsal view of the left SC (B), and the pattern of saccadic eye movements evoked by stimulating the deeper layers below these points are shown in the correspondingly identified figures (A1-9). Zero point indicates the center position of the eye orbit. It should be noted that, in mice, the SC code both contraversive and ipsiversive saccades.

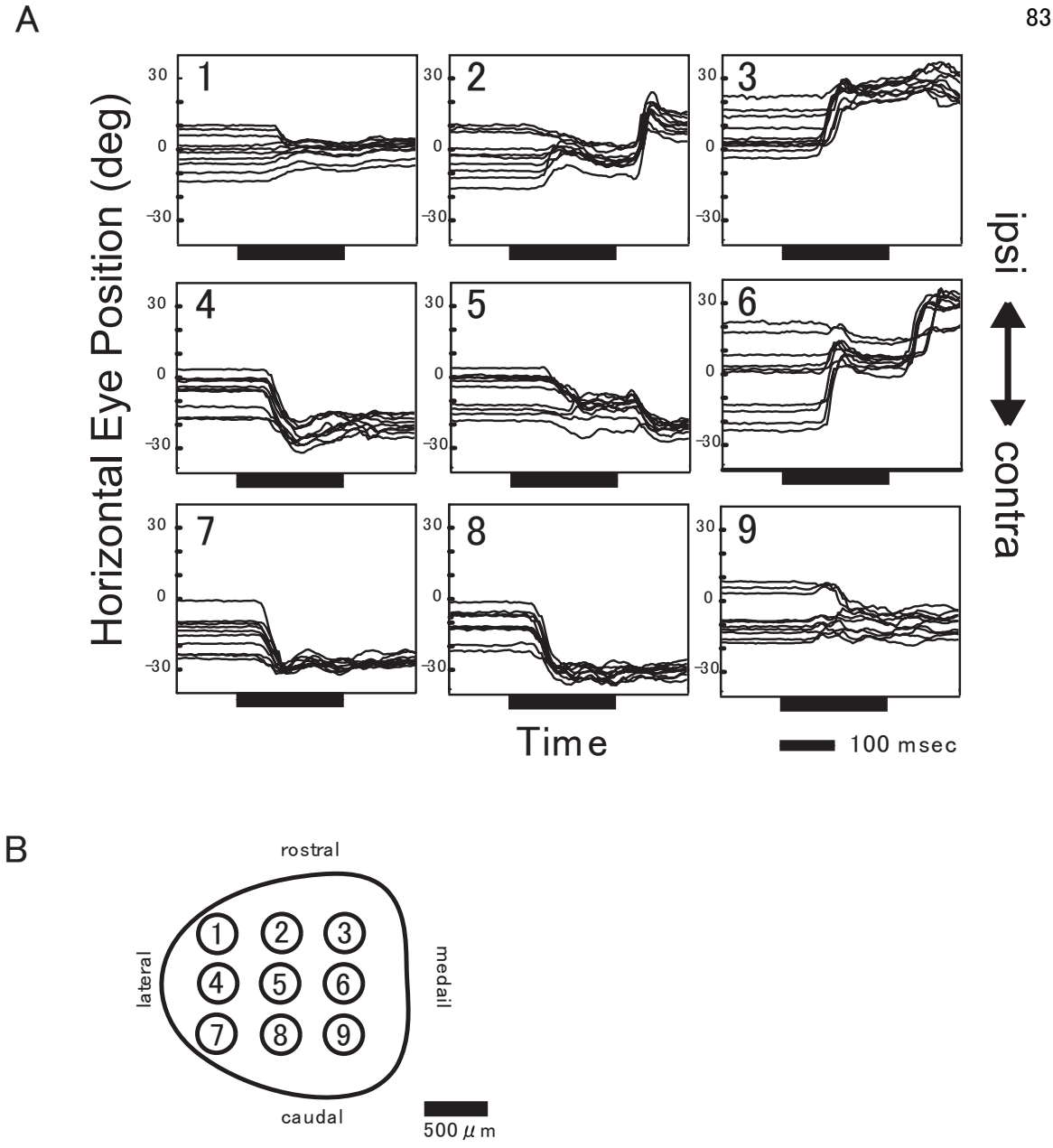

Figure 3-7
Time-course of rapid eye movements evoked from different initial eye positions

The vector of evoked saccades highly depended on the initial eye position in the orbit as well as on stimulus sites. There is a general tendency to converge at a specific position in the orbit. Evoked saccades were goal-directed. Boxes under the time axis indicate the onset and duration of stimulus trains. Circled letters indicate penetrations of the stimulating electrode on a dorsal view of the left SC (B), and the pattern of saccadic eye movements evoked by stimulating the deeper layers below these points are shown in the correspondingly identified figures (A 1-9).

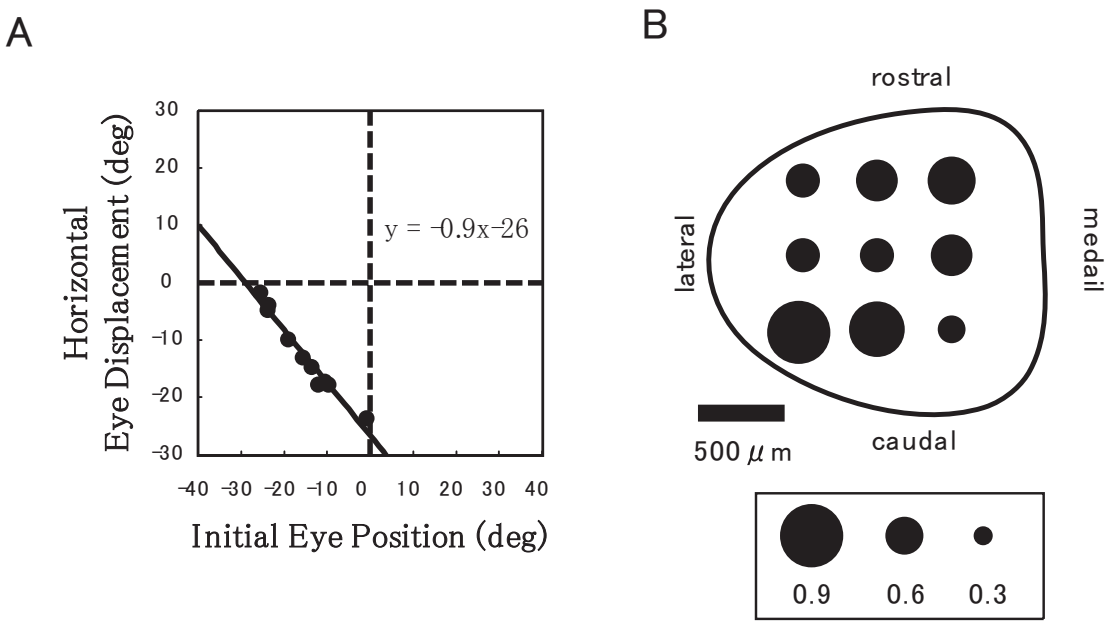

Figure 3-8

The directions and amplitudes of sacades evoked electrically from the mouse SC are strongly influenced by the initial position of the eye in the orbit.

(A) The solid line is the least-squares regression line through the data and obeys the equation displayed. The absolute values of these slopes provide an index of the influence of initial eye position on horizontal component of saccadic amplitude. (B) Position sensitivity index of horizontal components of evoked saccades. The value of position sensitivity index is represented by the scale of the circle.

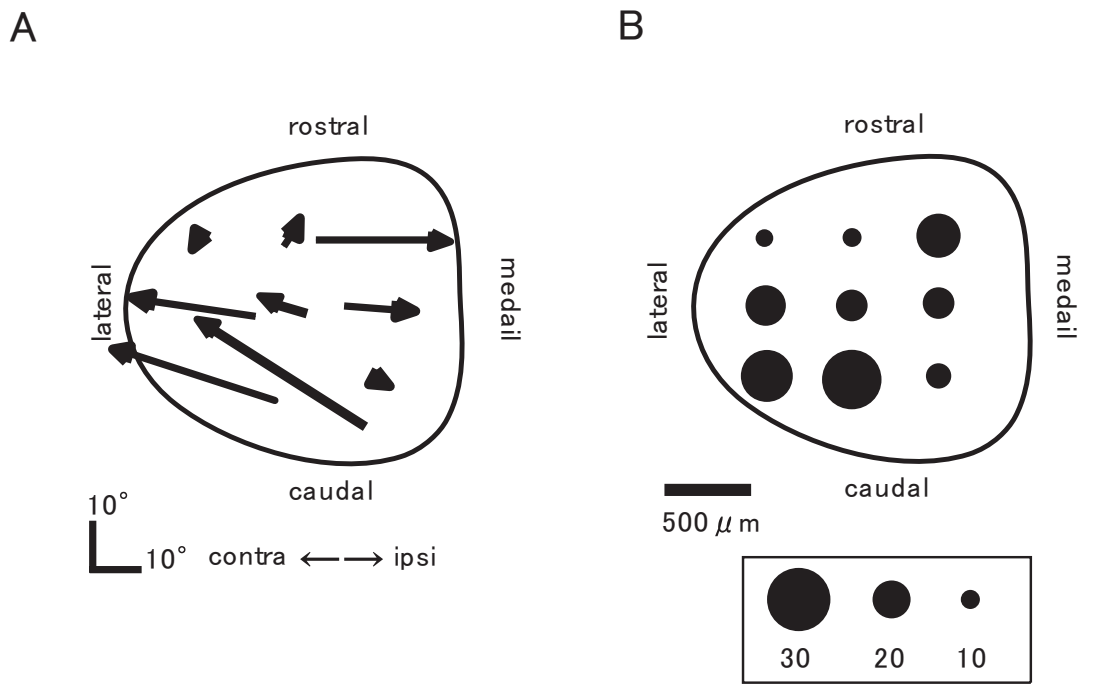

Figure 3-9
Representation of the characteristic vectors of evoked saccades in the left SC.

(A) Characteristic vector of the electrically-induced rapid eye movementsat at the different sites in the SC . Ipsiversive saccades were evoked from the antero-medial region where the ipsilateral visual field is represented. (B) Characteristic amplitude of the electrically-induced rapid eye movements. The scale of a circle represents the amplitude.

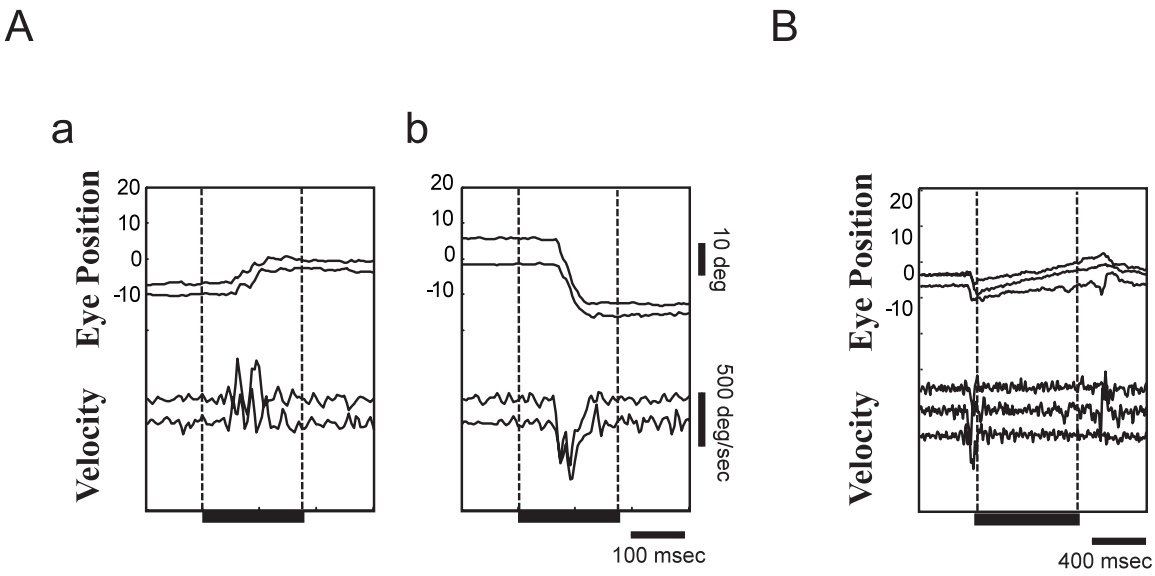

Figure 3-10
Step responses of the saccadic control system

(A) Staircase saccades evoked from rostral portion (a) and from caudal portion (b). Prolonged stimulus often evoked a staircase of two or three successive saccades. (B) Response to the long-lasting stimulation. Longer stimulation period (800 msec) resulted in only maintaining or drifting back the eye position and failed to induce additional saccades. Black under bar indicates the stimulation period.

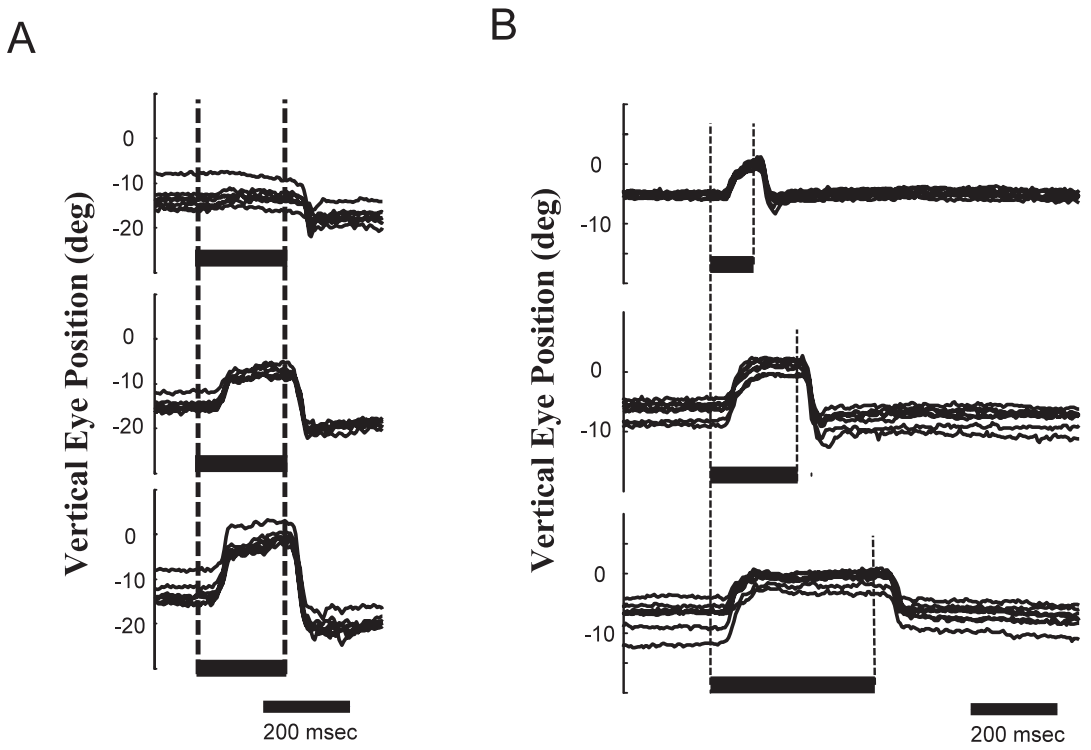

Figure 3-11
Rebound saccades evoked after the end of stimulation

In several regions, rebound saccades were observed in a reflexive manner. (A) Response to the different current intensities. Rebound saccades could be evoked by the lower current stimulus than the threshold current to evoke a normal saccade. (top) 0.5 x, (middle) 1.0 x, (bottom) 2.0 x threshold current, respectively (threshold current = 10 μ A) . (B) Response to the different stimulus durations. Rebound saccades occurred after the end of stimulation.

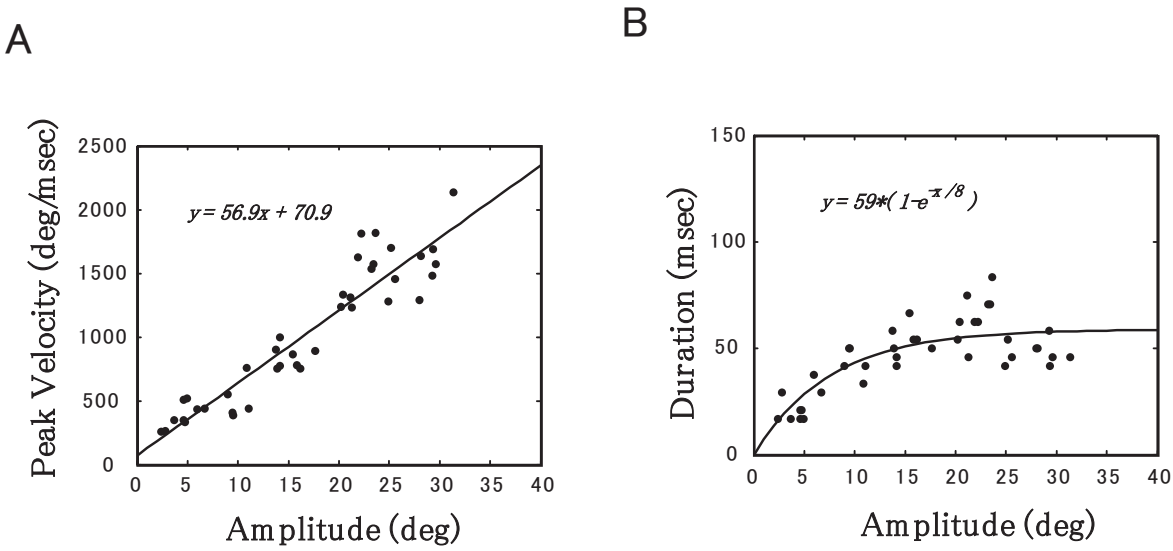

Figure 3-12
Main sequence relationship of the rebound saccades

(A) The peak-velocity vs. amplitude plot of rebound saccades. Rebound saccades had higher peak velocity than normal saccade. (B) The saccadic duration vs. amplitude plot of rebound saccades.

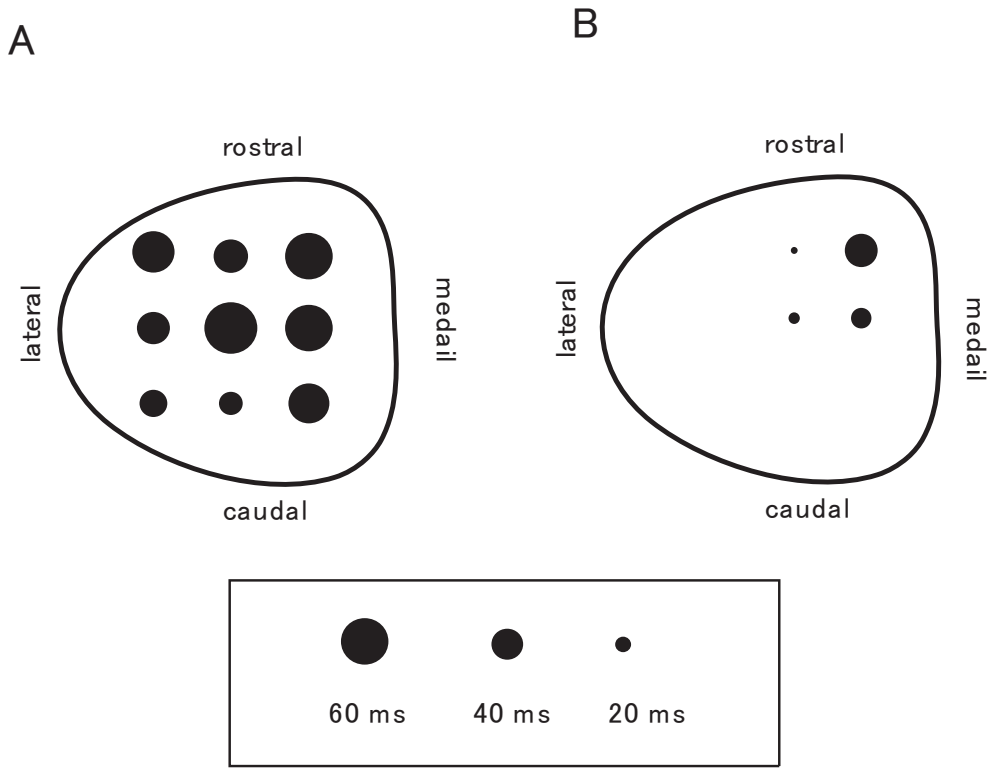

Figure 3-13
Latency of the induced saccade and the rebound saccade

Latency of the electrically-induced rapid eye movements (A) and of the rebound saccades (B) represented on the surface of the left SC..

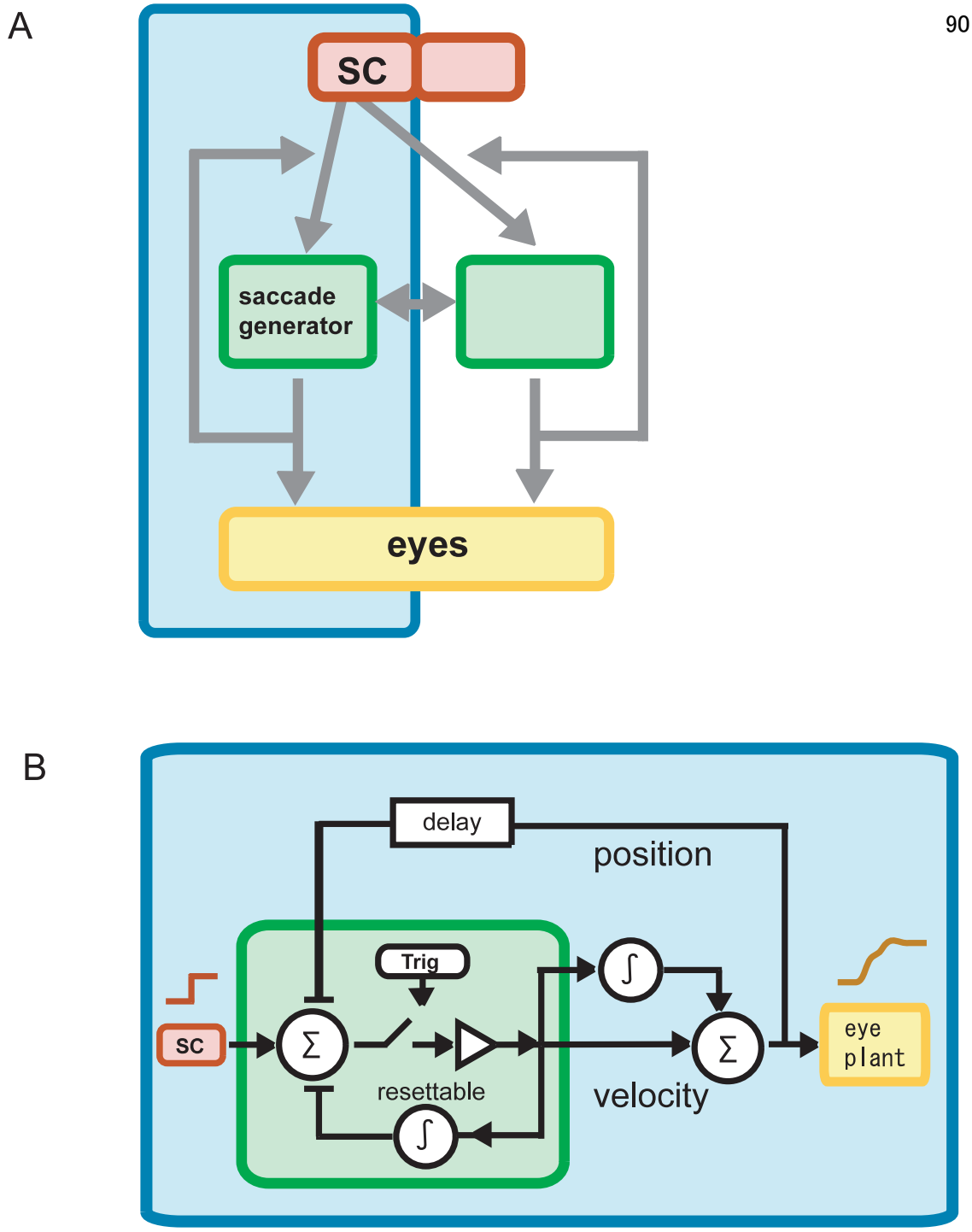

Figure 3-14
Hypothetical scheme of saccadic control system in mice

(A) Conceptual model. In this hypothetical model, the saccadic command formed in the SC is conveyed to the brain stem bilaterally. The strength of output signal is determined by both the collicular site and the eye position in the orbit. (B) Block diagram of the saccadic system in mice adapted from generic model in primates.

Part 4

Possible roles of GABA in the control of saccadic eye movements: A quantitative analysis of saccades evoked by the micro-stimulation of the superior colliculus in GAD65 knockout mice

Introduction

In part 1, I established a high-speed video-oculography for mice and found that mice made saccadic eye movements in a similar way to other mammals in part 2, and demonstrated in part 3 that saccadic eye movements can be evoked by electrical stimulation of the deeper layers of the superior colliculus (SC) in the mice under the head-fixed condition.

In contrast to a wealth of physiological and anatomical knowledge about saccadic system, little is known about their underlying molecular mechanisms. Here, in order to investigate the role of neurotransmitters underlying saccade generation, I studied the dynamical characteristics of both electrically evoked and spontaneous saccades in GAD65 knockout mice lacking one of GABA-synthesizing enzymes (Asada et al., 1996).

Gamma-aminobutyric acid (GABA) is a principal inhibitory neurotransmitter in the mammalian central nervous system (Obata, 1972) and is synthesized from glutamic acid by glutamic acid decarboxylase (GAD) in a specific population of nerve cells (GABAergic neurons). GABA has two isoform, GAD65 and GAD67, named for their molecular mass of 65 and 67 kDa, respectively, which are encoded by two independent genes (Erlander et al., 1991, Erlander and Tobin, 1991).

Whereas GAD67 is a cytosolic enzyme and distributed throughout the cell body, GAD65 is preferentially located in nerve termini, and is reversibly anchored to the membrane of synaptic vesicles (Christgau et al., 1991, Kaufman et al., 1991, Reetz et al., 1991, Christgau et al., 1992), suggesting that GAD65 may provide reserve

pools of GABA for regulation of inhibitory neurotransmission.

GAD67-deficient mice did not survive after birth because of cleft palate (Asada et al., 1997). GAD65 null mutants, on the other hand, are viable and show no detectable morphological change in the adult. However, they show a pronounced reduction of co-factor-induced GAD activity and an increased susceptibility to pentylenetetrazol- and picrotoxin-, as well as stress-induced seizure, indicating a loss of GABAergic inhibition (Asada et al., 1996, Kash et al., 1997). On the behavioral level, an increased anxiety-like behavior and insensitivity to the benzodiazepine diazepam have been reported in GAD65-/- mice (Kash et al., 1999). There is no evidence of tremor or movement disorder. The mice are not ataxic, as judged by performance on a Roto-Rod (Kash et al., 1997). GAD65 thus appears to be involved in GABA synthesis during the postnatal maturation of CNS circuitry, in contrast to GAD67, which is the predominant from during early development (Asada et al., 1997, Ji and Obata, 1999). The GABA deficit in adult GAD65-/- mice averaged 40-50% of wild type levels.

In this study, I examined both evoked saccades and spontaneous saccades, and compared those dynamics in GAD65-/- and wild-type mice, thus investigated the functional role of GABA in the saccadic system in terms of control systems theory. Since the first attempts to describe the oculomotor system in terms of control systems theory (Young, 1962), it has been recognized that the trajectory of saccadic eye movements cannot be controlled by a continuous visual feedback. Saccades are so fast that the relatively long latency of visual responses in the brain excludes the possibility that vision can supply dynamic feedback during the movements.

Thus either saccades are feedforward ballistic movements or there must be a short-latency "local" feedback mechanism (Robinson, 1975, Zee et al., 1976). It is now recognized that saccades are dynamically compensated during mid-flight experimental perturbations (Keller, 1977, Sparks and Mays, 1983, Keller and Edelman, 1994), thus providing that the movements are not ballistic.

Most current models of the saccadic control system assume that the movements are driven dynamically by a signal that compares the actual eye position with a desired eye position (Arai et al. 1994; Breznen and Gnadt 1997; Gancarz and Grossberg 1998; Lefèvre and Galiana 1992; Massone 1994; Moschovakis 1994; Optican 1995; van Opstal and Kappen 1993). In these models, saccades are produced by a pulse-step signal applied to the ocular motoneurons. The pulse is shaped by a local feedback loop that continuously feeds a burst generator with an estimate of the current motor error. The step of innervation then is obtained by integrating the pulse. Once the output equals the target position, the motor error disappears and the burst generator ceases firing thereby terminating the saccade. These models succeeded in generating realistic saccades, showing the well-known relationships among amplitude and peak velocity (the main sequence), characteristic of experimentally recorded saccades (Bahill et al., 1975, Baloh et al., 1975). A useful and standard input signal in terms of systems engineering analysis is the step input, an instantaneous change in input to a new and sustained level of activity. The step response reveals the system's reaction to a sudden change in input. This systems dynamics methodology is particularly useful for motor circuits, which generate machine-like outputs. One advantage of applying this concept to the

saccadic circuit is that it offers an experimental framework for challenging the closed-loop circuit for the characteristic system responses derived from systems control engineering.

Thus I applied prolonged electrical stimulation to the SC as the step input, and its response was examined. Then numerical simulation was performed with general feedback model to explain the results I observed and investigate the functional role of GABA as a control variable in the saccade control system. Because eye speed is well correlated with the firing rate of the brain stem burst neurons (Cullen and Guitton, 1997), the velocity profile of saccade is a good measure of the actual neuronal output of the saccadic control system. Therefore, if GABA produced by GAD65 plays an important role in the saccade control system, significant changes would be expected in the dynamic characteristics of the saccades.

Materials and methods

Subjects

GAD65(-/-) and wild-type mice of 3-4-month-old littermates were obtained by intercrossing between heterozygote. They were housed in groups of four to six under standard laboratory conditions with a 12-h day/night cycle with lights on at 8:00 h and food and water ad libitum. Using probes specific for the GAD65 genes (Asada et al., 1996), the genotypes were determined by polymerase chain reaction (PCR) from the tail tissue at the time of weaning during the 4^{th} to 5^{th} week after birth. Eleven GAD65(-/-) and 14 wild-type littermates were used in the examination of spontaneous saccades, 6 mutants and 6 wild-type animals were used in the examination of electrically induced saccades.

Eye movements recording

The movements of the right eye were monitored under awake, head-fixed condition with a high-speed CCD camera at a sampling rate of 240 frames/sec placed at an angle of 60 degree laterally from the midline and 30 degree down from the horizontal plane, approximately perpendicular to the optical axis of the eye.

Electrical stimulations

Repetitive electrical stimuli were applied to the superior colliculus through a tungsten monopolar electrode (FHC) with a trunk diameter of 200 μm (impedance; 1MΩ). Each stimulations consisted of 60 trains of 300-Hz (lasting for 200 ms)

constant current cathodal square wave pulses with duration of 0.2 ms (10~100 μA). For prolonged stimulation study, I used current pulses with 240 trains (lasting for 800 ms). At the end of the experimental session, the animal was anesthetized and perfused with a 10% formalin solution through the heart. After equilibration with 20% sucrose solution, 50 μ m frozen sections of the brain were prepared. The location of the electrode tracks was identified by placement of a small electrolytic lesion and reconstructed from Nissl-stained sections.

Data Analysis

Eye-movement data were analyzed and displayed off line using a custom designed software. For quantitative analysis, the eye velocity was determined by differentiating the position signals. Saccade duration was defined as the time duration which instantaneous eye velocities exceeded 100 deg/sec. All model simulation was done under Simulink/Matlab environment. Model parameters were tuned manually to match the slope of the main sequence curve to that of the experimental results with the fixed feedback strength, 1.0.

Results

Electrically induced saccades

Since the amplitude of these evoked saccades is highly dependent on its stimulation site upon the superior colliculus, I paid much attention to stimulate wide region of the SC along its anterior posterior axis in both wild type and knockout mice (Fig. 4-1).

Firstly, I compared the main-sequence relationship in wild-type mice and in knockout mice (Fig. 4-2Aa and 4-2Ab). Pooled data of all subjects were plotted and used for the statistical analysis. The slope of regression line was 47.5 ($r=0.84$) for wild-type mice and 58.8 ($r=0.67$) for knockout mice. The regression line of GAD65 knockout mice is significantly steeper than that of wild type (Fig. 4-2B). Namely, peak velocity of the evoked saccade in knockout mice increased compared with those in wild-type mice.

Interestingly, I found that saccades with larger amplitude could not be induced in the knockout mice (Fig. 4-2Ab). Distribution of amplitude was significantly different between knockout and wild-type animals (Fig. 4-4 $p<0.001$: F-test). Amplitude of evoked saccades was smaller in the GAD65 knockout mice (mean value 13.8 ± 8.6 wild-type, 9.3 ± 5.7 knockout).

Next, the stability of the system to the step input was analyzed by using prolonged electrical stimulation of the SC. Prolonged electrical stimulation resulted in inducing oscillation-like movements frequently after the end of saccades in the GAD65 knockout mice (Fig. 4-8B). These oscillation-like eye movements

were rarely observed in wild-type mice (Fig. 4-8A). Dominant frequency of observed oscillations was ranged from 10 to 20 Hz. This result indicates the instability of saccade control system in GAD65 knockout mice. For further evaluation of the amount of the instability of the saccade control system, I compared the fluctuation in the eye position after the end of evoked saccades. The fluctuation value was defined as the distance between the terminating position of the saccade and the eye position 25 msec after the end of saccades. These values of fluctuation were plotted against the amplitude of evoked saccades. Significant increase of fluctuations in eye position was observed after the termination of saccades in the GAD65 knockout mice ($p<0.01$: F-test) (Fig. 4-6), also confirming the instability of the saccade control system in GAD65 knockout mice.

Spontaneous saccades

As shown in figure 4-3, the relationship between peak-velocity and amplitude of spontaneous saccades was linear over the wide range of saccadic amplitude in both wild-type and knockout mice, and was well fitted with the linear regression line. The slope of regression line in knockout mice (69.3, $r=0.87$) was significantly higher than that in wild-type mice (62.2, $r=0.87$) ($p<0.01$, t-test).

Amplitude of spontaneous saccades tended to be smaller in knockout mice. The mean value of saccadic amplitude was not significantly different but the distribution of amplitude in knockout mice was significantly different from that in wild-type (Fig. 4-5, $p<0.05$, F-test).

As for the stability of saccade control system, a significant increase in

fluctuations in eye position after the termination of saccade was observed in knockout mice (Fig. 4-7). Deviation of the fluctuation values in knockout mice was significantly different from that in wild-type mice ($p<0.05$, F-test).

Basically, the same results were obtained from the examination of the spontaneous saccades as electrically induced saccades.

Model simulation

To explain the above experimental results from the aspect of control system, I performed computer simulation with a general negative feedback model. I changed the parameter for the feedback strength relatively in this theoretical model and assessed the effects on dynamical properties of saccades in a qualitative manner (Fig. 4-9A).

Based on this negative feedback model, higher feedback strength would be expected to result in higher peak velocity and smaller saccadic amplitude. On the other hand, lower feedback strength would be expected to bring the opposite effects (Fig. 4-9B and 4-9C). Thus, from this model simulation, both higher peak velocity and smaller amplitude of saccades in KO mice can be attributed to the increase in the feedback signal.

In this model, step input produces an instable output in case of higher feedback strength (Fig. 4-10). In an extreme case, an output of the system can result in an oscillation. Therefore, oscillatory eye movements can also be explained for the higher feedback efficacy and instability of saccadic system.

Discussions and conclusions

The peak velocity of the saccadic eye movements was significantly higher and the amplitude of saccades tended to be smaller in GAD65 knockout mice than those in wild-type animals. The increase in saccade peak velocity in GAD65 knockout mice is consistent with the fact that administration of diazepam, which enhances the amplitude of GABA-A IPSPs, reduces saccade velocity in human (Gentles and Thomas, 1971). Moreover, significant increase in fluctuations of eye positions was observed in eye position after the termination of saccades in the GAD 65 knockout mice. Prolonged electrical stimulation of the SC often evoked oscillation-like eye movements after saccades in mutant mice. All these observations can be attributed to the increase in the feedback efficacy and the instability of the saccade control system based on the theoretical model with a negative feedback loop in a qualitative manner.

Despite its simplicity, model simulation reasonably accounts for a number of experimental findings for the saccadic system. The ability of the model to explain the experimental results supports the validity of the theoretical assumption that an internal negative feedback controls the dynamic characteristics of saccades. Moreover, velocity outputs with negative values were observed in the case of oscillatory eye movements, suggesting the possibility of push-pull neuronal mechanisms between both hemispheres proposed in chapter 3, because output of a neuron itself cannot represent minus values.

As for the instability of the system, there are three parameters characterizing

the stability of the control system; input strength, feedback delay and feedback efficacy. An increase in input strength can lead not only the system instability, but also larger amplitude of saccades and no effects on the peak velocity vs. amplitude relationship, showing inconsistency with the experimental results. Longer feedback delay also results in system instability, but an expected increase in saccadic amplitude disagrees with the actual results. Thus, I attributed the instability of the saccade system in GAD65 knockout mice to the increased efficacy of the feedback loop.

Although the biological saccadic system is highly nonlinear, comparisons between experimentally derived data from the mice and the computational model have provided valuable insight into the saccade system. If GABA produced by GAD65 would be used as the negative signal in the feedback loop, one might expect that the efficacy of the feedback loop would decrease in GAD65 knockout mice. Consequently, the opposite conclusion described above leads to the idea that another inhibitory neurotransmitter (such as glycine) may be used as the negative signal in the feedback loop. The possibility of GABA produced by another synthetase GAD67 cannot be excluded, logically.

In order to increase the feedback efficacy, several neuronal mechanisms are considered. One mechanism is decreased inhibitory activities of the interneurons in the neural integrator. Theoretically, the negative feedback loop is expected to have neural integrator as shown in figure 4-10A. It has been known that, for a stable neural integration, interneurons are necessary to control the activity levels among the neural population (Cannon et al., 1983, Galiana and Outerbridge, 1984,

Arnold and Robinson, 1997). Another neuronal mechanism to increase the feedback efficacy is the neural modulation from the other neural structures such as cerebellum. Recent studies on the saccadic adaptation suggested the involvement of the cerebellum in gain controlling of saccades, suggesting the above possibility (Erlander and Tobin, 1991, Robinson, 1995, Raymond, 1998).

In conclusion, GABA produced by GAD65 plays an important role in termination of the saccade. This result can be attributed that GAD65 attenuates the feedback efficacy in the saccade control system (Fig. 4-11) based on the generic negative feedback model. This study shows that the interplay between hypothetical predictions of the models with experimental verification in vivo using mutant mice serves as a powerful technique for understanding the neurobiological basis of this motor behavior. Importantly, unlike traditional behavioral neurophysiology, this experimental strategy is not limited to the range of behaviors available by volitional activation and can reveal system properties not apparent during normal behavior. And one can 'reverse engineer' the internal workings of saccadic circuit by quantitative study of its system responses.

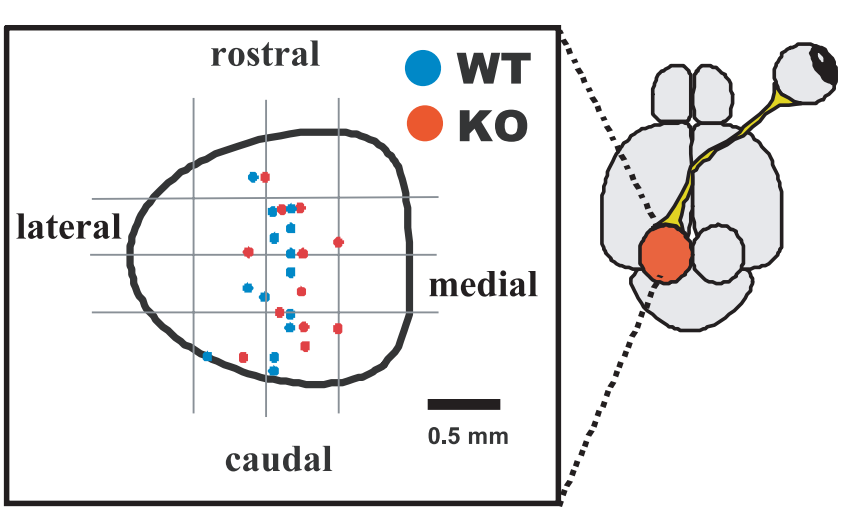

Figure 4-1
Stimulation sites on the surface of the SC

The locations of the electrode tracks were identified by placement of a small electrolytic lesion and reconstruction from Nissl-stained section. Each stimulation sites was represented on the surface on the left superior colliculus.

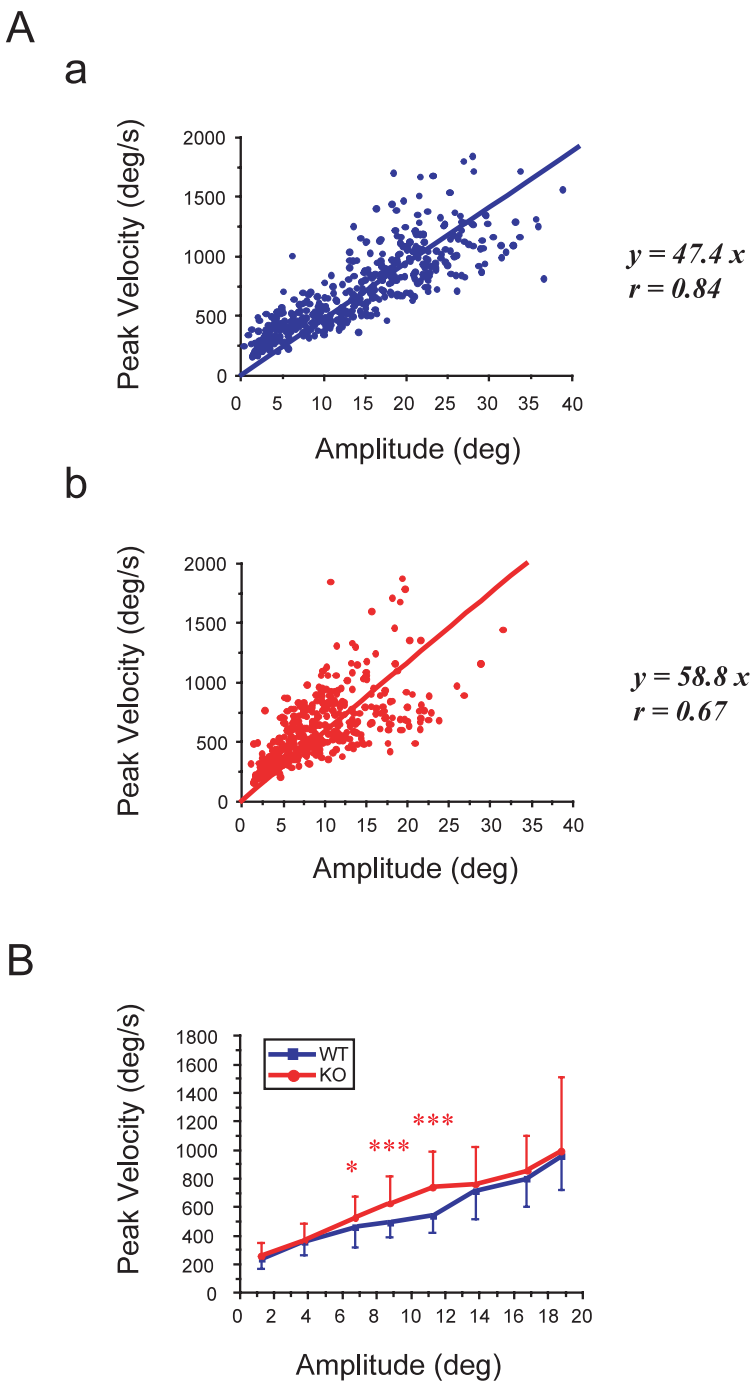

Figure 4-2
Peak-velocity vs. amplitude relationship of the electrically-induced saccadic eye movements

(A) Peak-velocity vs. amplitude relationship in wild-type mice (a) and in knockout mice (b). Solid line indicates the least-squares linear regression line. The slope of regression line was 47.5 (r=0.84) for wild-type mice and was58.8 (r=0.67) for knockout mice. (B) Peak velocity of the evoked saccade in knockout mice was significantly higher than those in wild-type mice. (* p <0.05, *** P<0.001; *t*-test)

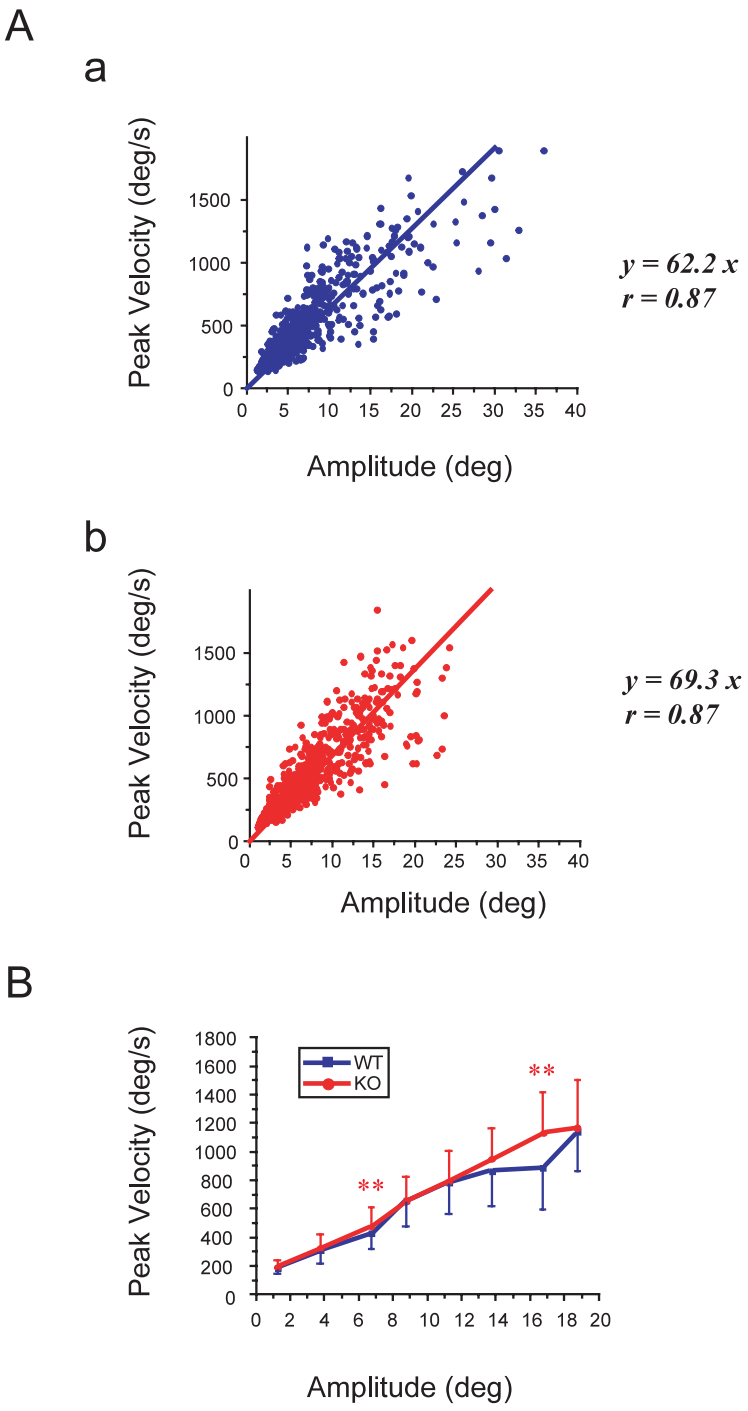

Figure 4-3
Peak-velocity vs amplitude relationship of the spontaneous saccadic eye movements

(A) Peak-velocity vs. amplitude relationship in wild-type mice (a) and in knockout mice (b). Solid line indicates the least-squares linear regression line. The slope of regression line was 62.2 (r=0.87) for wild-type mice and was69.3 (r=0.87) for knockout mice. (B) Peak velocity of the spontaneous saccade in knockout mice was significantly higher than those in wild-type mice. (** P<0.01; *t*-test)

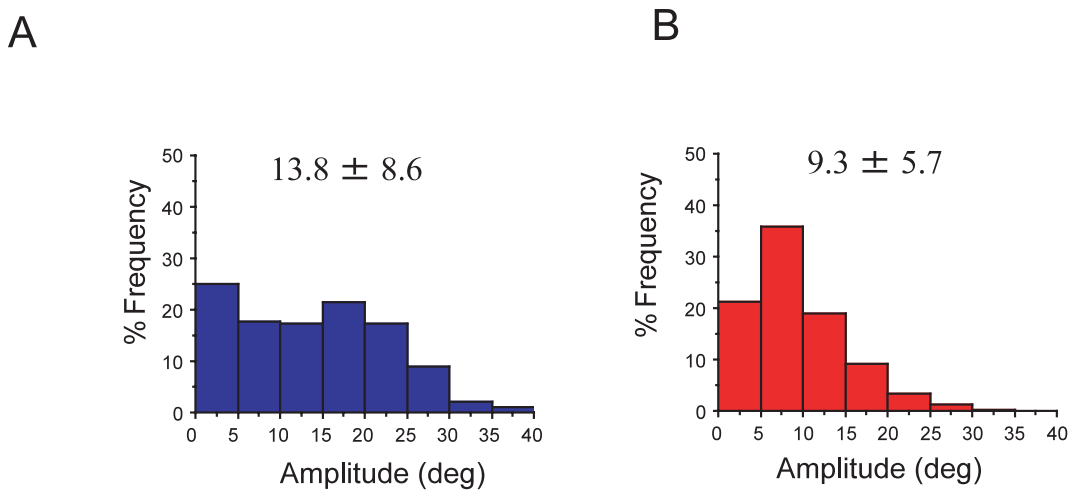

Figure 4-4
Amplitude distribution of the evoked saccades

Amplitude distribution of the evoked saccades in wild-type (A) and in knockout mice (B). Amplitude of evoked saccades tended to be smaller, and larger saccades could not be induced in GAD65 knockout mice. Distribution of amplitude was significantly different between knockout and wild-type animals ($p<0.001$: F-test).

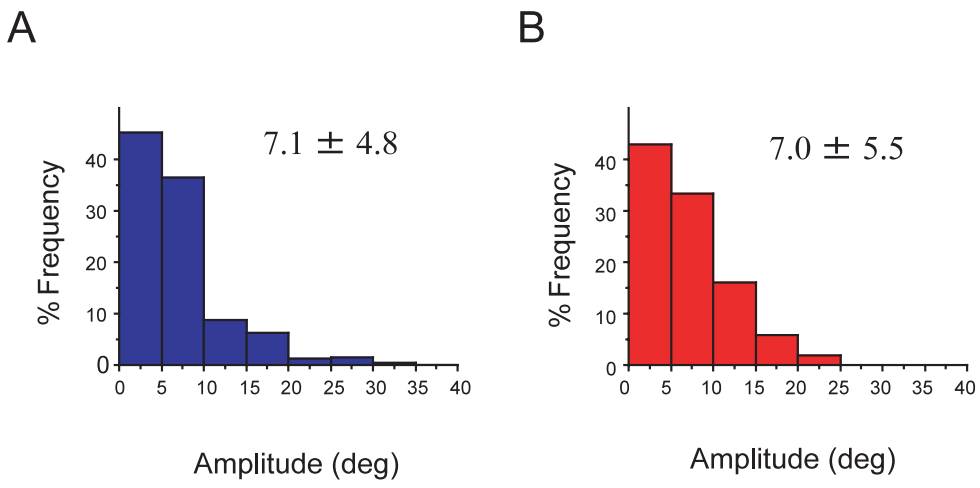

Figure 4-5
Amplitude distribution of the spontaneous saccades

Amplitude distribution of the spontaneous saccades in wild-type (A) and in knockout mice (B). Distribution of amplitude was significantly different between knockout and wild-type animals ($p<0.001$: F-test).

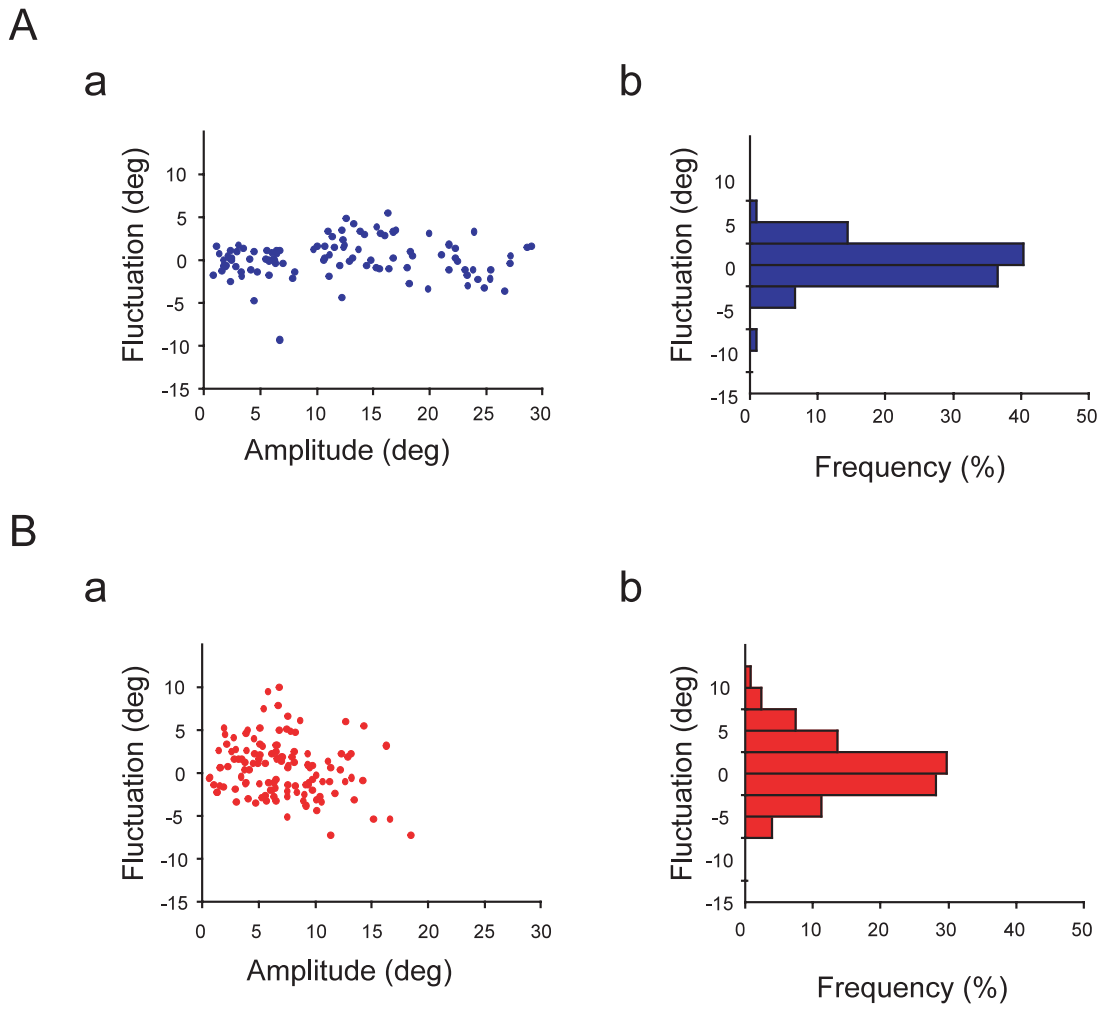

Figure 4-6
Fluctuation in the eye position after the end of evoked saccades

(A) Fluctuation values were plotter against the amplitude of evoked saccades in wild-type mice (a), and the frequency distribution histogram (b). (B) Fluctuation values were plotter against the amplitude of evoked saccades in knockout mice (a), and the frequency distribution histogram (b). Significant increase of fluctuations in eye position was observed after the termination of saccades in the GAD65 knockout mice ($p<0.01$: F-test).

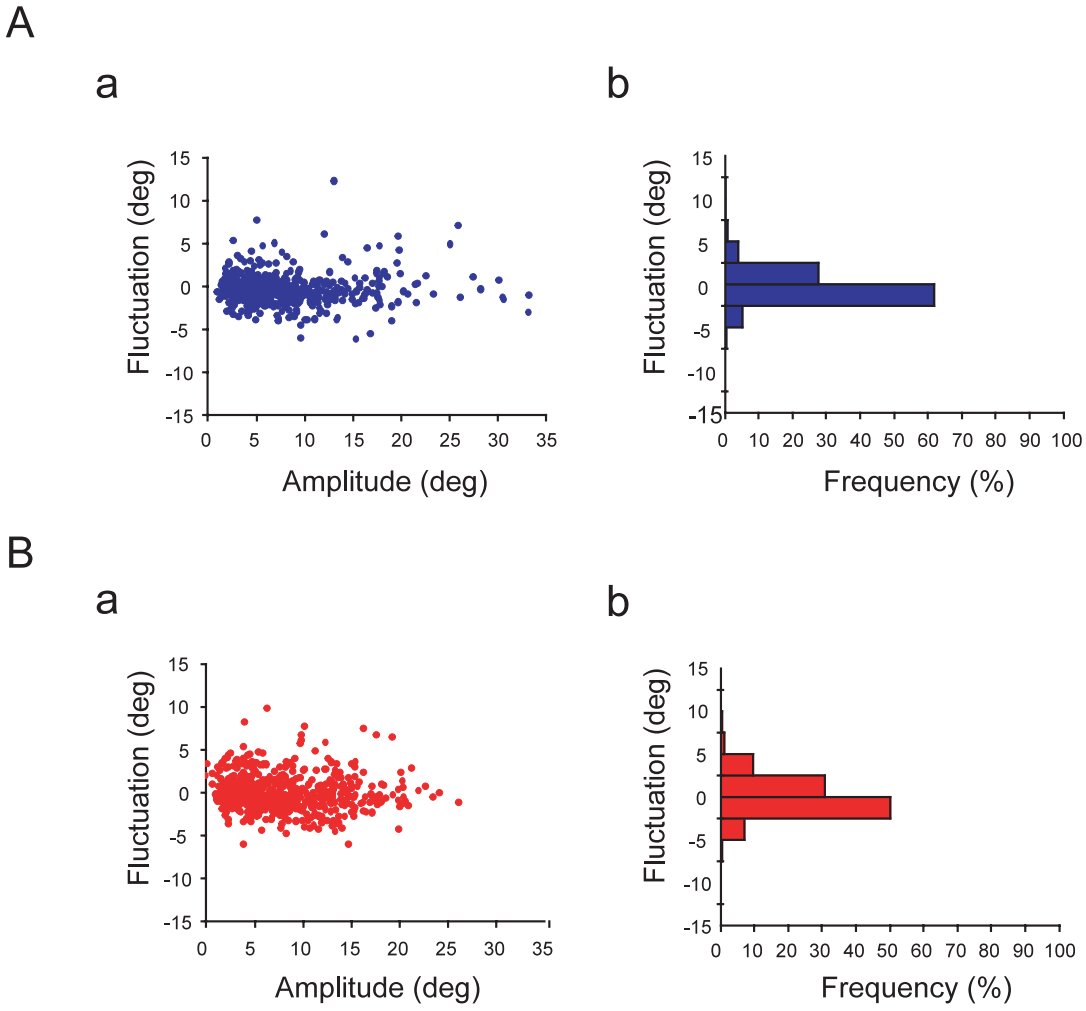

Figure 4-7
Fluctuation in the eye position after the spontaneous saccades

(A) Fluctuation values were plotter against the amplitude of spontaneous saccades in wild-type mice (a), and the frequency distribution histogram (b). (B) Fluctuation values were plotter against the amplitude of spontaneous saccades in knockout mice (a), and the frequency distribution histogram (b). Significant increase of fluctuations in eye position was observed after the termination of saccades in the GAD65 knockout mice ($p<0.01$: F-test).

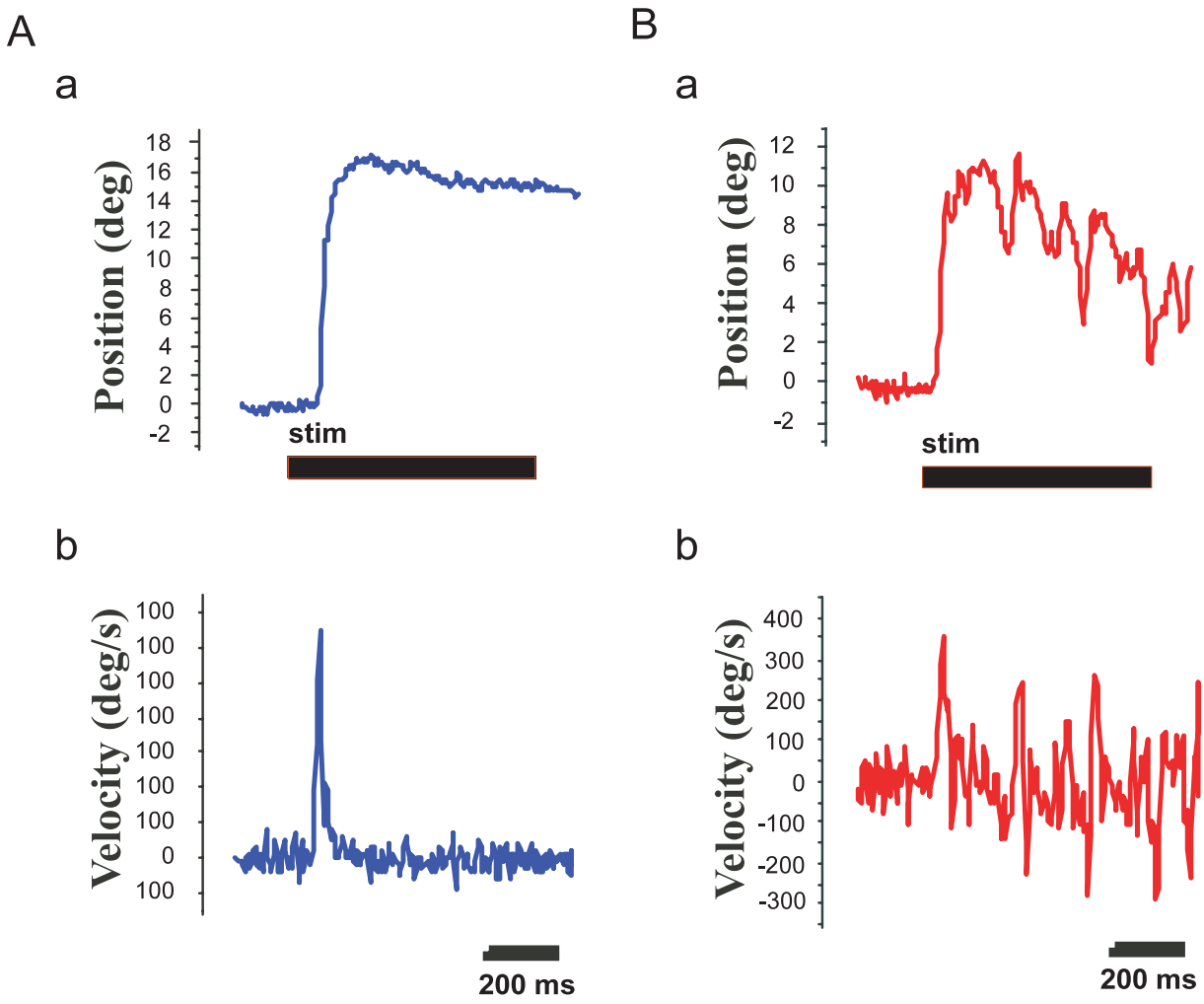

Figure 4-8
Oscillation-like eye movements in the GAD65 knockout mice

(A) Eye position trace (a) and its corresponding eye velocity (b) in response to prolonged electrical stimulation of the SC in wild-type mice. (B) Eye position trace (a) and its corresponding eye velocity (b) in knockoute mice. Prolonged electrical stimulation of the SC often evoked oscillation-like movements after the end of saccades in GAD65 knockout mice..

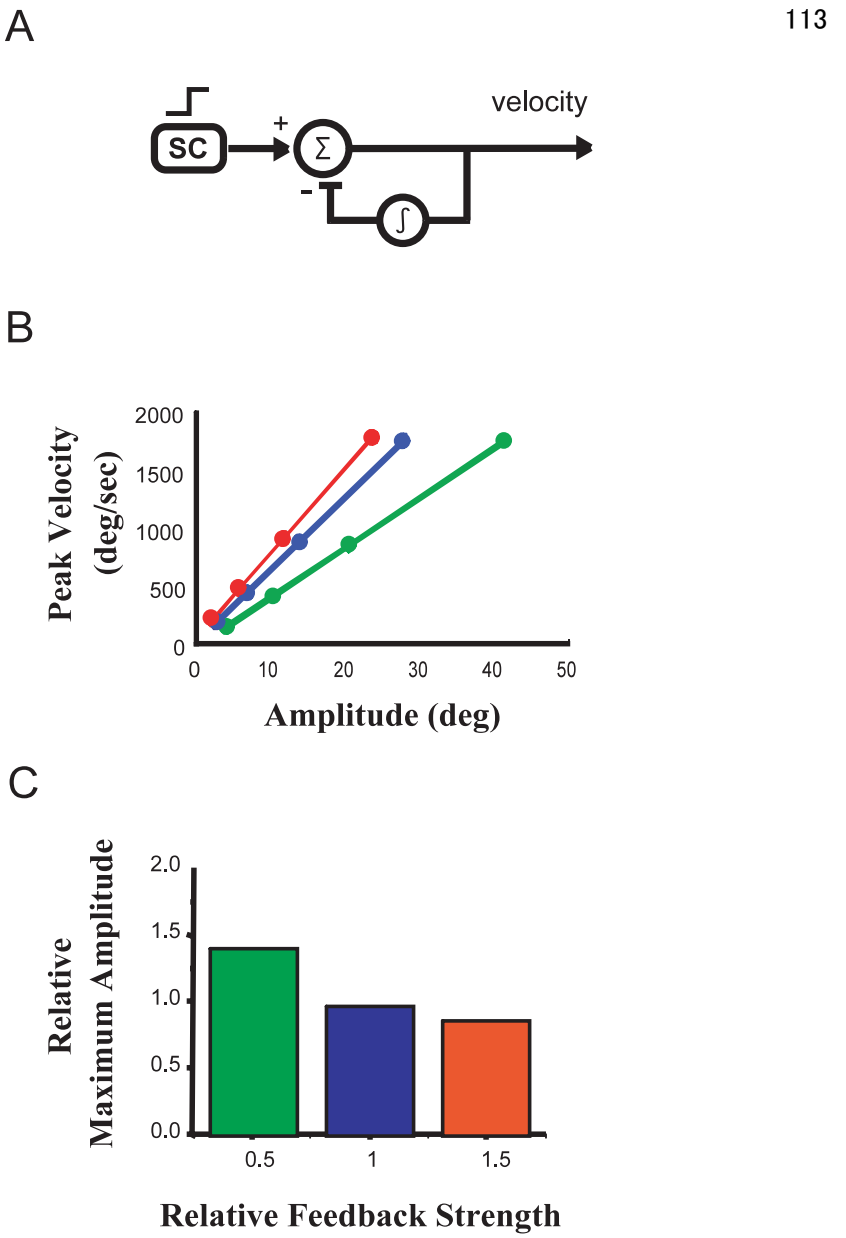

Figure 4-9
Model simulation based on generalized system with a negative feedback

(A) Block diagram of the control model used for the computer simulation. In this model, the parameter of feedback efficacy was changed relatively. (B) Peak-velocity vs. amplitude relationship under the different conditions in the feedback strength. The relative value of feedback strength is 0.5 (green), 1.0 (blue) and 1.5 (red), respectively. (C) Changes in the maximum amplitude of saccades under the different conditions in the feedback strength.

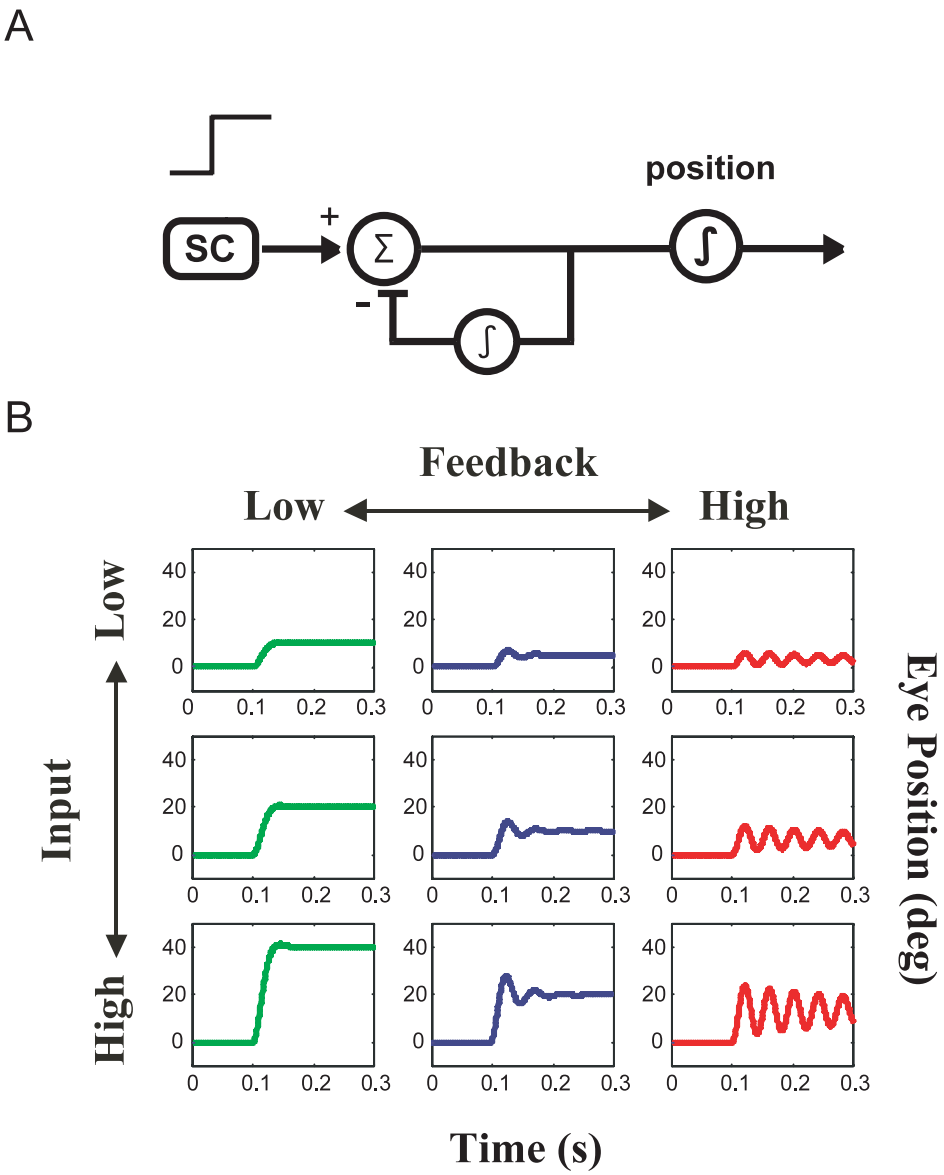

Figure 4-10
Effects of feedback strength on the eye position trace

(A) Block diagram of the control model used for the computer simulation. In this model, the parameter of feedback efficacy was changed relatively. (B) Eye position outputs under the different conditions in the feedback strength or in the input intensity. The relative value of feedback strength was 0.5 (green), 1.0 (blue) and 1.5 (red), respectively. The relative value of input intensity was 5 (top), 10 (middle), and 20 (bottom), respectively. Oscillatory eye movements in GAD65 knockout mice could be also explained by the increase in the feedback strength in the saccade control circuitry.

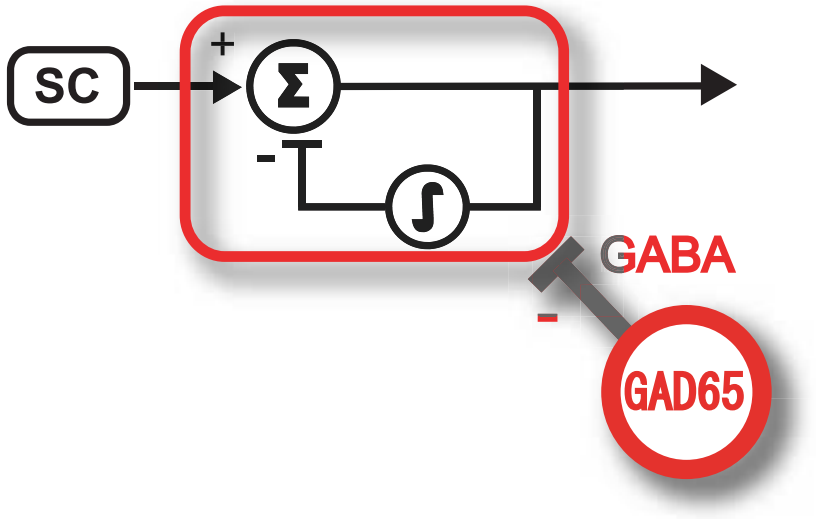

Figure 4-11
Proposed function of the GAD65 in the saccadic control system with negative feedback

Proposed function of the GAD65 in the saccadic control system with a negative feedback loop. GABA plays an important role in termination of the saccade, and possibly attenuates the feedback efficacy in the saccade control system.

General Conclusions

In this study, I have newly developed the video-oculographic system in order to record the rapid eye movements, and its applications to the study on the saccades in mice are described.

The newly developed video-oculographic system achieved high temporal resolution (240 Hz) by combining high speed CCD camera with image processing software written in LabVIEW run on IBM-PC. This software enables robust online calculation of rotation angle of the eye during rapid eye movements such as saccades in mice.

In part 2, by using this new system, I successfully measured the saccadic eye movements in mice quantitatively. Mice made rapid eye movements mainly in horizontal direction. The peak velocity of saccades increased almost linearly against the saccadic amplitude with slope of 54 / sec, whereas the saccadic duration saturated at the level of 60 msec against larger saccades.

In part 3, I found that the rapid eye movements dynamically similar to the spontaneous saccades could be induced by electrical stimulation of the SC in midbrain artificially. Most sites in the SC yielded contraversive characteristic saccades. However, from the anterior-medial region, where the visual representation of the superficial layer shared the same location in the visual field with the opposite SC, ipsiversive saccades could be induced. From rostral sites, small saccades were evoked, whereas from more caudal sites, larger saccades were evoked. The amplitude and direction of evoked saccades highly depended on the initial eye

position in the orbit as well as on stimulus sites in the SC, and evoked saccades were goal-directed in mice. These results suggest that eye position signals might strongly affect saccadic eye movements in mice.

In the last part, I showed an example of how to investigate the molecular mechanisms of saccades by the combined use of gene-engineered mice and model simulation. I investigated the dynamical characteristics of the saccades in GAD65 knockout mice, and found that the peak velocity of the saccade was significantly higher and the amplitude of saccades tended to be smaller in GAD65 knockout mice than those in wild type animals. I also found the significant increase of fluctuations in the eye position after the termination of saccades in the GAD65 knockout mice. Prolonged electrical stimulations of the SC often evoked oscillation-like eye movements in the mutant mice. Computer simulations based on the control system model with a negative feedback loop could attribute these experimental results to the increase in the efficacy of feedback signal in the saccade generator circuits in the downstream of the SC in GAD65 knockout mice.

In summary, the results presented in this study show that the newly developed video-oculographic system will provide a powerful tool for analyzing dynamic characteristics of saccadic eye movements in mice. I believe that the study described here will be a fundamental knowledge to study molecular basis of the oculomotor and, moreover, cognitive functions by using various lines of mutant mice.

Acknowledgements

I am deeply grateful to my supervisor, Professor Tadashi Isa at National Institute for Physiological Sciences, for instructing and encouraging me throughout my graduate school years.

I thank the collaborators of the study in part 4; Dr. Kunihiko Obata at National Institute for Physiological Sciences for kindly providing GAD65 knockout mice.

I thank the reviewers of the thesis; Profs. Hidehiko Komatsu, Tomoo Hrano and Ryuichi Shigemoto.

I thank all the members of Department of Integrative Physiology and Department of Developmental Physiology, National Institute for Physiological Sciences; Hiroshi Aizawa, Toshiaki Endo, Noriko Hirayama, Yuka Inoue, Kaoru Isa, Rikako Kato, Hideyuki Katsuta, Yasushi Kobayashi, Shuko Kumagai, Fengxia Lee, Masahiro Mori, Yosuke Morichika, Nikitin Nikolay, Yukio Nishimura, Yasuhiko Saito, Chika Sasaki, Kazuhiko Seki, Michi Seo, Nobuaki Takahashi, Sooksawate Thongchai, Masayuki Watanabe, Jun Yamamoto, Yoko Yamamoto, Tetsuji Yamashita, Masatoshi Yoshida (alphabetical order).

Finally, I would like to thank my parents, Shuji Sakatani and Chiyoko Sakatani for their spiritual and economical support thorough my graduate years.

References

Arai, K., Keller, E. L. and Edelman, J. A., 1994. Two-demensional neural network models of the primate saccadic system. Neural Networks. 7, 1115-1135.

Armstrong, I. T. and Munoz, D. P., 2003. Inhibitory control of eye movements during oculomotor countermanding in adults with attention-deficit hyperactivity disorder. Exp Brain Res. 152, 444-452.

Arnold, D. B. and Robinson, D. A., 1997. The oculomotor integrator: testing of a neural network model. Exp Brain Res. 113, 57-74.

Asada, H., Kawamura, Y., Maruyama, K., Kume, H., Ding, R., Ji, F. Y., Kanbara, N., Kuzume, H., Sanbo, M., Yagi, T. and Obata, K., 1996. Mice lacking the 65 kDa isoform of glutamic acid decarboxylase (GAD65) maintain normal levels of GAD67 and GABA in their brains but are susceptible to seizures. Biochem Biophys Res Commun. 229, 891-895.

Asada, H., Kawamura, Y., Maruyama, K., Kume, H., Ding, R. G., Kanbara, N., Kuzume, H., Sanbo, M., Yagi, T. and Obata, K., 1997. Cleft palate and decreased brain gamma-aminobutyric acid in mice lacking the 67-kDa isoform of glutamic acid decarboxylase. Proc Natl Acad Sci U S A. 94, 6496-6499.

Bahill, A. T., Clark, M. R. and Stark, L., 1975. Glissades - eye movements generated by mismatched components of saccadic motoneuronal control signal. Math Biosci. 26, 303-318.

Baker, R., Precht, W. and Llinas, R., 1972. Mossy and climbing fiber projections of extraocular muscle afferents to the cerebellum. Brain Res. 38, 440-445.

Balkema, G. W., Mangini, N. J., Pinto, L. H. and Vanable, J. W., Jr., 1984. Visually evoked eye movements in mouse mutants and inbred strains. A screening report. Invest Ophthalmol Vis Sci. 25, 795-800.

Baloh, R. W., Sills, A. W., Kumley, W. E. and Honrubia, V., 1975. Quantitative measurement of saccade amplitude, duration, and velocity. Neurology. 25, 1065-1070.

Banbury Conference on genetic background in mice., 1997. Mutant mice and neuroscience: recommendations concerning genetic background. Neuron. 19, 755-759.

Boghen, D., Troost, B. T., Daroff, R. B., Dell'Osso, L. F. and Birkett, J. E., 1974. Velocity characteristics of normal human saccades. Invest Ophthalmol. 13, 619-623.

Breznen, B. and Gnadt, J. W., 1997. Analysis of the step response of the saccadic feedback: computational models. Exp Brain Res. 117, 181-191.

Breznen, B., Lu, S. M. and Gnadt, J. W., 1996. Analysis of the step response of the saccadic feedback: system behavior. Exp Brain Res. 111, 337-344.

Cairney, S., Maruff, P., Vance, A., Barnett, R., Luk, E. and Currie, J., 2001. Contextual abnormalities of saccadic inhibition in children with attention deficit hyperactivity disorder. Exp Brain Res. 141, 507-518.

Cannon, S. C., Robinson, D. A. and Shamma, S., 1983. A proposed neural network for the integrator of the oculomotor system. Biol Cybern. 49, 127-136.

Christgau, S., Aanstoot, H. J., Schierbeck, H., Begley, K., Tullin, S., Hejnaes, K. and Baekkeskov, S., 1992. Membrane anchoring of the autoantigen GAD65 to microvesicles in pancreatic beta-cells by palmitoylation in the NH2-terminal

domain. J Cell Biol. 118, 309-320.

Christgau, S., Schierbeck, H., Aanstoot, H. J., Aagaard, L., Begley, K., Kofod, H., Hejnaes, K. and Baekkeskov, S., 1991. Pancreatic beta cells express two autoantigenic forms of glutamic acid decarboxylase, a 65-kDa hydrophilic form and a 64-kDa amphiphilic form which can be both membrane-bound and soluble. J Biol Chem. 266, 21257-21264.

Collewijn, H., 1970. The normal range of horizontal eye movements in the rabbit. Exp Neurol. 28, 132-143.

Crawford, T. J., Bennett, D., Lekwuwa, G., Shaunak, S. and Deakin, J. F., 2002. Cognition and the inhibitory control of saccades in schizophrenia and Parkinson's disease. Prog Brain Res. 140, 449-466.

Crommelinck, M. and Roucoux, A., 1976. Characteristics of cat's eye saccades in different states of alertness. Brain Res. 103, 574-578.

Cullen, K. E. and Guitton, D., 1997. Analysis of primate IBN spike trains using system identification techniques. I. Relationship To eye movement dynamics during head-fixed saccades. J Neurophysiol. 78, 3259-3282.

Dean, P., 1995. Modelling the role of the cerebellar fastigial nuclei in producing accurate saccades: the importance of burst timing. Neuroscience. 68, 1059-1077.

De Zeew, C.L., Hansel, C., Bian, F., Koekkoek, S.K., van Alphen, A. M., Linden, D.J., Oberdick, J., 1998. Expression of a protein kinase C inhibitor in Purkinje cells blocks cerebellar LTD and adaptation of the vestibulo-ocular reflex. Neuron 20, 495-508.

Dräger, U. C., 1975. Receptive fields of single cells and topography in mouse visual

cortex. J Comp Neurol. 160, 269-290.

Dräger, U. C. and Hubel, D. H., 1975. Responses to visual stimulation and relationship between visual, auditory, and somatosensory inputs in mouse superior colliculus. J Neurophysiol. 38, 690-713.

Erlander, M. G., Tillakaratne, N. J., Feldblum, S., Patel, N. and Tobin, A. J., 1991. Two genes encode distinct glutamate decarboxylases. Neuron. 7, 91-100.

Erlander, M. G. and Tobin, A. J., 1991. The structural and functional heterogeneity of glutamic acid decarboxylase: a review. Neurochem Res. 16, 215-226.

Evinger, C. and Fuchs, A. F., 1978. Saccadic, smooth pursuit, and optokinetic eye movements of the trained cat. J Physiol. 285, 209-229.

Fischer, B. and Weber, H., 1993. Express saccades and visual attention. Behav & Brain Sciences. 16, 553-567.

Frens, M. A. and van der Geest, J. N., 2002. Scleral search coils influence saccade dynamics. J Neurophysiol. 88, 692-698.

Fuchs, A. F., 1967. Saccadic and smooth pursuit eye movements in the monkey. J Physiol. 191, 609-631.

Fuchs, A. F. and Kornhuber, H. H., 1969. Extraocular muscle afferents to the cerebellum of the cat. J Physiol. 200, 713-722.

Fuchs, A. F. and Robinson, D. A., 1966. A method for measuring horizontal and vertical eye movement chronically in the monkey. J Appl Physiol. 21, 1068-1070.

Fukushima, J., Fukushima, K., Miyasaka, K. and Yamashita, I., 1994. Voluntary control of saccadic eye movement in patients with frontal cortical lesions and parkinsonian patients in comparison with that in schizophrenics. Biol

Psychiatry. 36, 21-30.

Fuller, J. H., 1985. Eye and head movements in the pigmented rat. Vision Res. 25, 1121-1128.

Funabiki, K., Naito, Y., Matsuda, K. and Honjo, I., 1999. A new vestibulo-ocular reflex recording system designed for routine vestibular clinical use. Acta Otolaryngol. 119, 413-419.

Galiana, H. L. and Outerbridge, J. S., 1984. A bilateral model for central neural pathways in vestibuloocular reflex. J Neurophysiol. 51, 210-241.

Gancarz, G. and Grossberg, S., 1998. A neural model of the saccade generator in the reticular formation. Neural Netw. 11, 1159-1174.

Gentles, W. and Thomas, E. L., 1971. Commentary. Effect of benzodiazepines upon saccadic eye movements in man. Clin Pharmacol Ther. 12, 563-574.

Gitelman, D. R., Parrish, T. B., LaBar, K. S. and Mesulam, M. M., 2000. Real-time monitoring of eye movements using infrared video-oculography during functional magnetic resonance imaging of the frontal eye fields. Neuroimage. 11, 58-65.

Glimcher, P. W., 2003. The neurobiology of visual-saccadic decision making. Annu Rev Neurosci. 26, 133-179.

Grusser-Cornehls, U. and Bohm, P., 1988. Horizontal optokinetic ocular nystagmus in wildtype (B6CBA+/+) and weaver mutant mice. Exp Brain Res. 72, 29-36.

Guitton, D., Crommelinck, M. and Roucoux, A., 1980. Stimulation of the superior colliculus in the alert cat. I. Eye movements and neck EMG activity evoked when the head is restrained. Exp Brain Res. 39, 63-73.

Guitton, D. and Volle, M., 1987. Gaze control in humans: eye-head coordination during orienting movements to targets within and beyond the oculomotor range. J Neurophysiol. 58, 427-459.

Hikosaka, O. and Kawakami, T., 1977. Inhibitory reticular neurons related to the quick phase of vestibular nystagmus--their location and projection. Exp Brain Res. 27, 377-386.

Hikosaka, O. and Sakamoto, M., 1987. Dynamic characteristics of saccadic eye movements in the albino rat. Neurosci Res. 4, 304-308.

Hyde, J. E. and Eliasson, S. G., 1957. Brainsten-induced eye movements in cats. J Comp Neurol. 108, 139-172.

Ito, M. and Oshima, T., 1965. Electrical behaviour of the motoneurone membrane during intracellularly applied current steps. J Physiol. 180, 607-635.

Iwashita, M., Kanai, R., Funabiki, K., Matsuda, K. and Hirano, T., 2001. Dynamic properties, interactions and adaptive modifications of vestibulo-ocular reflex and optokinetic response in mice. Neurosci Res. 39, 299-311.

Ji, F. and Obata, K., 1999. Development of the GABA system in organotypic culture of hippocampal and cerebellar slices from a 67-kDa isoform of glutamic acid decarboxylase (GAD67)-deficient mice. Neurosci Res. 33, 233-237.

Kash, S. F., Johnson, R. S., Tecott, L. H., Noebels, J. L., Mayfield, R. D., Hanahan, D. and Baekkeskov, S., 1997. Epilepsy in mice deficient in the 65-kDa isoform of glutamic acid decarboxylase. Proc Natl Acad Sci U S A. 94, 14060-14065.

Kash, S. F., Tecott, L. H., Hodge, C. and Baekkeskov, S., 1999. Increased anxiety and altered responses to anxiolytics in mice deficient in the 65-kDa isoform of

glutamic acid decarboxylase. Proc Natl Acad Sci U S A. 96, 1698-1703.

Katoh, A., Kitazawa, H., Itohara, S. and Nagao, S., 1998. Dynamic characteristics and adaptability of mouse vestibulo-ocular and optokinetic response eye movements and the role of the flocculo-olivary system revealed by chemical lesions. Proc Natl Acad Sci U S A. 95, 7705-7710.

Kaufman, D. L., Houser, C. R. and Tobin, A. J., 1991. Two forms of the gamma-aminobutyric acid synthetic enzyme glutamate decarboxylase have distinct intraneuronal distributions and cofactor interactions. J Neurochem. 56, 720-723.

Kawagoe, R., Takikawa, Y. and Hikosaka, O., 1998. Expectation of reward modulates cognitive signals in the basal ganglia. Nat Neurosci. 1, 411-416.

Keller, E. L., 1977. Control of saccadic eye movements by midline brain stem neurons. Elsevier-North Holland, Amsterdam.

Keller, E. L. and Edelman, J. A., 1994. Use of interrupted saccade paradigm to study spatial and temporal dynamics of saccadic burst cells in superior colliculus in monkey. J Neurophysiol. 72, 2754-2770.

Kornhuber, H. H., 1968. Neurologie des Kleinhirns. Zentralbl Ges Neurol Psychiartr. 191, 13.

Kubo, T., Saika, T., Sakata, Y., Morita, Y., Matsunaga, T. and Kasahara, T., 1991. Analysis of saccadic eye movements using an infrared video system in human subjects. Acta Otolaryngol Suppl. 481, 382-387.

Lefèvre, P. and Galiana, H. L., 1992. Dynamic feedback to the superior colliculus in a neural network model of the gaze control system. Neural Networks. 5, 871-890.

LeVasseur, A. L., Flanagan, J. R., Riopelle, R. J. and Munoz, D. P., 2001. Control of volitional and reflexive saccades in Tourette's syndrome. Brain. 124, 2045-2058.

Mangini, N. J., Vanable, J. W., Jr., Williams, M. A. and Pinto, L. H., 1985. The optokinetic nystagmus and ocular pigmentation of hypopigmented mouse mutants. J Comp Neurol. 241, 191-209.

Massone, L. L., 1994. A neural-network system for control of eye movements: basic mechanisms. Biol Cybern. 71, 293-305.

Matsuda, K. and Nagami, T., 1998. All purpose measurement system of the eye positions. Proceedings of the 12th Symposium on Biological and Physiological Engineering, 173-176.

McIlwain, J. T., 1986. Effects of eye position on saccades evoked electrically from superior colliculus of alert cats. J Neurophysiol. 55, 97-112.

McIlwain, J. T., 1990. Topography of eye-position sensitivity of saccades evoked electrically from the cat's superior colliculus. Vis Neurosci. 4, 289-298.

Mitchiner, J. C., Pinto, L. H. and Vanable, J. W., Jr., 1976. Visually evoked eye movements in the mouse (Mus musculus). Vision Res. 16, 1169-1171.

Moschovakis, A. K., 1994. Neural network simulations of the primate oculomotor system. I. The vertical saccadic burst generator. Biol Cybern. 70, 291-302.

Moschovakis, A. K., Dalezios, Y., Petit, J. and Grantyn, A. A., 1998. New mechanism that accounts for position sensitivity of saccades evoked in response to stimulation of superior colliculus. J Neurophysiol. 80, 3373-3379.

Moschovakis, A. K., Scudder, C. A. and Highstein, S. M., 1996. The microscopic anatomy and physiology of the mammalian saccadic system. Prog Neurobiol. 50, 133-254.

Mostofsky, S. H., Lasker, A. G., Cutting, L. E., Denckla, M. B. and Zee, D. S., 2001. Oculomotor abnormalities in attention deficit hyperactivity disorder: a preliminary study. Neurology. 57, 423-430.

Munoz, D. P., Armstrong, I. T., Hampton, K. A. and Moore, K. D., 2003. Altered control of visual fixation and saccadic eye movements in attention-deficit hyperactivity disorder. J Neurophysiol. 90, 503-514.

Nagao, S., 1990. A non-invasive method for real-time eye position recording with an infrared TV-camera. Neurosci Res. 8, 210-213.

Obata, K., 1972. The inhibitory action of -aminobutyric acid, a probable synaptic transmitter. Int Rev Neurobiol. 15, 167-187.

Optican, L. M., 1995. A field theory of saccade generation: temporal-to-spatial transform in the superior colliculus. Vision Res. 35, 3313-3320.

Raymond, J. L., 1998. Learning in the oculomotor system: from molecules to behavior. Curr Opin Neurobiol. 8, 770-776.

Reetz, A., Solimena, M., Matteoli, M., Folli, F., Takei, K. and De Camilli, P., 1991. GABA and pancreatic beta-cells: colocalization of glutamic acid decarboxylase (GAD) and GABA with synaptic-like microvesicles suggests their role in GABA storage and secretion. Embo J. 10, 1275-1284.

Remmel, R. S., 1984. An inexpensive eye movement monitor using the scleral search coil technique. IEEE Trans Biomed Eng. 31, 388-390.

Remtulla, S. and Hallett, P. E., 1985. A schematic eye for the mouse, and comparisons with the rat. Vision Res. 25, 21-31.

Robinson, D. A., 1963. A method of measuring eye-movement using a scleral search coil

in a magnetic field. IEEE Trans Bio-Med Electron. 10, 137-145.

Robinson, D. A., 1972. Eye movements evoked by collicular stimulation in the alert monkey. Vision Res. 12, 1795-1808.

Robinson, D. A., 1975. Oculomotor control signals. Pergamon, Oxford.

Robinson, F. R., 1995. Role of the cerebellum in movement control and adaptation. Curr Opin Neurobiol. 5, 755-762.

Roucoux, A. and Crommelinck, M., 1976. Eye movements evoked by superior colliculus stimulation in the alert cat. Brain Res. 106, 349-363.

Roucoux, A., Guitton, D. and Crommelinck, M., 1980. Stimulation of the superior colliculus in the alert cat. II. Eye and head movements evoked when the head is unrestrained. Exp Brain Res. 39, 75-85.

Sahibzada, N., Dean, P. and Redgrave, P., 1986. Movements resembling orientation or avoidance elicited by electrical stimulation of the superior colliculus in rats. J Neurosci. 6, 723-733.

Schiller, P. H. and Koerner, F., 1971. Discharge characteristics of single units in superior colliculus of the alert rhesus monkey. J Neurophysiol. 34, 920-936.

Schiller, P. H. and Stryker, M., 1972. Single-unit recording and stimulation in superior colliculus of the alert rhesus monkey. J Neurophysiol. 35, 915-924.

Scudder, C. A., Kaneko, C. S. and Fuchs, A. F., 2002. The brainstem burst generator for saccadic eye movements: a modern synthesis. Exp Brain Res. 142, 439-462.

Seidemann, E., Arieli, A., Grinvald, A. and Slovin, H., 2002. Dynamics of depolarization and hyperpolarization in the frontal cortex and saccade goal. Science. 295, 862-865.

Sparks, D. L. and Mays, L. E., 1983. Spatial localization of saccade targets. I. Compensation for stimulation-induced perturbations in eye position. J Neurophysiol. 49, 45-63.

Stahl, J. S., 2002. Calcium channelopathy mutants and their role in ocular motor research. Ann N Y Acad Sci. 956, 64-74.

Stahl, J. S., van Alphen, A. M. and De Zeeuw, C. I., 2000. A comparison of video and magnetic search coil recordings of mouse eye movements. J Neurosci Methods. 99, 101-110.

Steele, P. M., Medina, J. F., Nores, W. L. and Mauk, M. D., 1998. Using genetic mutations to study the neural basis of behavior. Cell. 95, 879-882.

Stryker, M. P. and Schiller, P. H., 1975. Eye and head movements evoked by electrical stimulation of monkey superior colliculus. Exp Brain Res. 23, 103-112.

Sweeney, J. A., Strojwas, M. H., Mann, J. J. and Thase, M. E., 1998. Prefrontal and cerebellar abnormalities in major depression: evidence from oculomotor studies. Biol Psychiatry. 43, 584-594.

Thier, P., Dicke, P. W., Haas, R. and Barash, S., 2000. Encoding of movement time by populations of cerebellar Purkinje cells. Nature. 405, 72-76.

van Opstal, A. J. and Kappen, H., 1993. A two-dimensional ensemble coding model for spatial-temporal transformation of saccades in monkey superior colliculus. Network. 4, 19-38.

Vidailhet, M., Rivaud, S., Gouider-Khouja, N., Pillon, B., Bonnet, A. M., Gaymard, B., Agid, Y. and Pierrot-Deseilligny, C., 1994. Eye movements in parkinsonian syndromes. Ann Neurol. 35, 420-426.

Wurtz, R. and Goldberg, M., 1989. The neurobiology of saccadic eye movements. Elsevier, New York.

Young, L. R., 1962. A sampled data model for eye tracking movements. In: Dept. of Aeronautics and Astronautics). Cambridge, MA.

Zee, D. S., Optican, L. M., Cook, J. D., Robinson, D. A. and Engel, W. K., 1976. Slow saccades in spinocerebellar degeneration. Arch Neurol. 33, 243-251.

Zhu, D., Moore, S. T. and Raphan, T., 1999. Robust pupil center detection using a curvature algorithm. Comput Methods Programs Biomed. 59, 145-157.